AD-A082 198 COLD REGIONS RESEARCH AND ENGINEERING LAB HANOVER NH F/G 11/4
ASPHALT CONCRETE FOR COLD REGIONS, A COMPARATIVE LABORATORY STU--ETC(U)
JAN 80 B J DEMPSEY, J INGERSOLL, T C JOHNSON
UNCLASSIFIED CRREL-80-5 NL

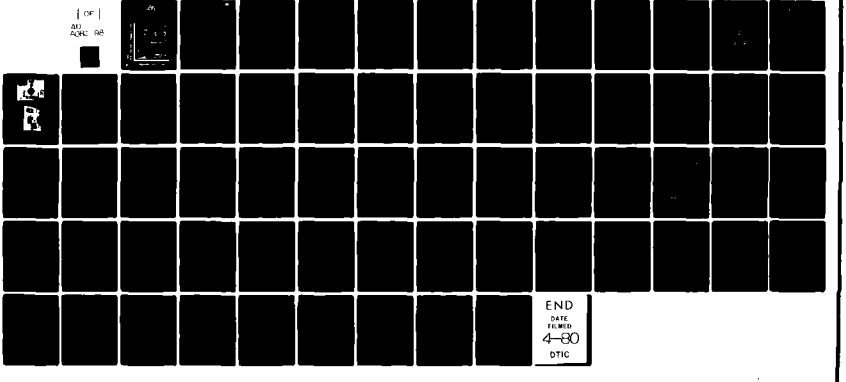

CRREL LEVEL II

AD A082193

12

Asphalt concrete for cold regions

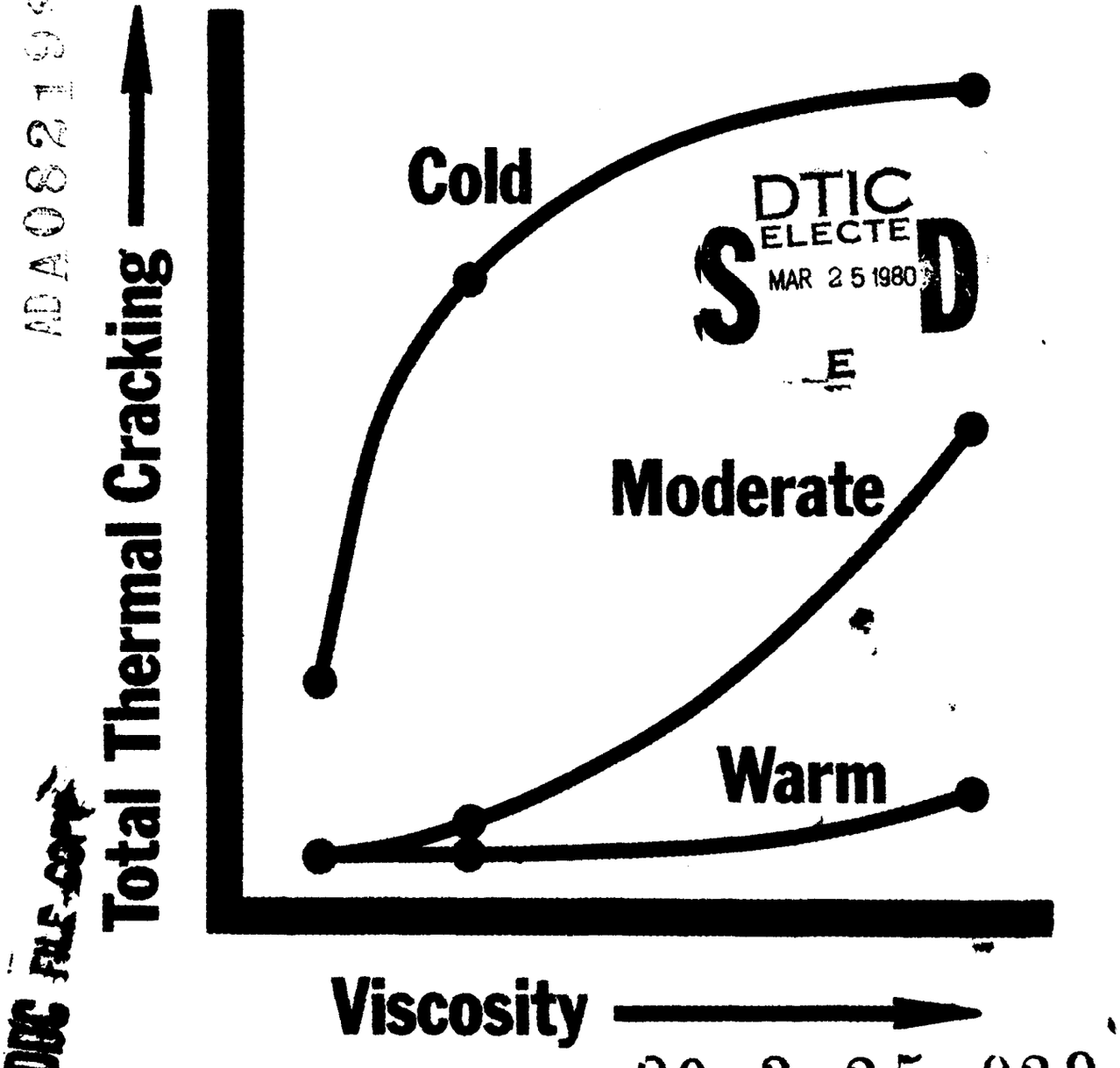

80 3 25 029

CRREL Report 80-5

Asphalt concrete for cold regions

A comparative laboratory study and analysis of mixtures containing soft and hard grades of asphalt cement

B.J. Dempsey, J. Ingersoll, T.C. Johnson and M.Y. Shahin

January 1980

Prepared for
DIRECTORATE OF MILITARY PROGRAMS
OFFICE, CHIEF OF ENGINEERS
By
UNITED STATES ARMY
CORPS OF ENGINEERS
COLD REGIONS RESEARCH AND ENGINEERING LABORATORY
HANOVER, NEW HAMPSHIRE, U.S.A.

Unclassified
SECURITY CLASSIFICATION OF THIS PAGE (When Data Entered)

REPORT DOCUMENTATION PAGE

READ INSTRUCTIONS BEFORE COMPLETING FORM

1. REPORT NUMBER: CRREL Report 80-5
2. GOVT ACCESSION NO.
3. RECIPIENT'S CATALOG NUMBER

4. TITLE (and Subtitle): ASPHALT CONCRETE FOR COLD REGIONS
A Comparative Laboratory Study and Analysis of Mixtures Containing Soft and Hard Grades of Asphalt Cement
5. TYPE OF REPORT & PERIOD COVERED
6. PERFORMING ORG. REPORT NUMBER

7. AUTHOR(s): B.J. Dempsey, J. Ingersoll, T.C. Johnson, M.Y. Shahin
8. CONTRACT OR GRANT NUMBER(s)

9. PERFORMING ORGANIZATION NAME AND ADDRESS
U.S. Army Cold Regions Research and Engineering Laboratory
Hanover, New Hampshire 03755
10. PROGRAM ELEMENT, PROJECT, TASK AREA & WORK UNIT NUMBERS
DA Project 4K078012AAM1
Work Unit 004, Task 00

11. CONTROLLING OFFICE NAME AND ADDRESS
Directorate of Military Programs
Office, Chief of Engineers
Washington, D.C. 20314
12. REPORT DATE
Jan[illegible]80
13. NUMBER OF PAGES
55

14. MONITORING AGENCY NAME & ADDRESS (if different from Controlling Office)
15. SECURITY CLASS. (of this report)
Unclassified
15a. DECLASSIFICATION/DOWNGRADING SCHEDULE

16. DISTRIBUTION STATEMENT (of this Report)
Approved for public release; distribution unlimited.

17. DISTRIBUTION STATEMENT (of the abstract entered in Block 20, if different from Report)

18. SUPPLEMENTARY NOTES
CRREL-80-5

19. KEY WORDS (Continue on reverse side if necessary and identify by block number)
Asphalt cement mixtures
Asphalt concrete tests
Catalytic cracking
Pavements
Traffic cracking and rutting

20. ABSTRACT (Continue on reverse side if necessary and identify by block number)
Pavements containing soft asphalt cement have been shown in the past to be less susceptible to low-temperature contraction cracking, but more susceptible to traffic-load-associated distress in warm weather, than pavements with harder asphalt cements. This research comprised laboratory testing to determine the properties of asphalt-aggregate mixtures containing three grades of asphalt cements, and analyses to project the performance of pavements containing each of the asphalts, in resisting thermally induced distress and traffic-associated distress. From the results it is concluded that only the softest asphalt cement tested (AC 2.5) would perform satisfactorily in a cold climatic zone. The moderately soft (AC 5) and moderately hard (AC 20) asphalt cements showed little susceptibility to thermal cracking in a moderate and a warm climatic zone, respectively. The AC 2.5 and AC 5 asphalts are not recommended for use

DD FORM 1 JAN 73 1473 EDITION OF 1 NOV 65 IS OBSOLETE

Unclassified
SECURITY CLASSIFICATION OF THIS PAGE (When Data Entered)

0271[illegible]

20. Abstract (cont'd)

in warm climates, however, owing to increased susceptibility to rutting under traffic.

PREFACE

This report was prepared by Dr. B.J. Dempsey, Associate Professor, Department of Civil Engineering, University of Illinois; J. Ingersoll, Civil Engineering Technician, and T.C. Johnson, Research Civil Engineer, Experimental Engineering Division, U.S. Army Cold Regions Research and Engineering Laboratory; and Dr. M.Y. Shahin, Research Engineer, U.S. Army Construction Engineering Research Laboratory.

The study was funded under DA Project 4K078012AAM1, *Operations and Maintenance, Army*; Task 00, *Facilities Investigations and Studies Program*; Work Unit 004, *Stiffness and Fracture Strength of Asphalt-Aggregate Mixtures Designed to Minimize Low Temperature Cracking*.

The technical content of the report was reviewed by E.J. Chamberlain and W.F. Quinn of CRREL.

CONTENTS

ILLUSTRATIONS

TABLES

ASPHALT CONCRETE FOR COLD REGIONS
A comparative laboratory study and analysis of mixtures containing soft and hard grades of asphalt cement

B.J. Dempsey, J. Ingersoll, T.C. Johnson and M.Y. Shahin

INTRODUCTION

Research setting

Low-temperature transverse contraction cracking is one of the most prevalent distress modes affecting asphalt roads in frost areas and is widely recognized as a significant adverse factor in pavement serviceability.[1] Thermal cracking also affects airfield bituminous pavements in cold regions, and the U.S. Army Corps of Engineers has reported extensive low-temperature transverse and longitudinal cracking at bases constructed for the U.S. Air Force in the northern states.[2, 3, 4] Adverse transverse cracking of asphalt pavements also has been reported in southern states[1], and the development of such cracking in the absence of severely low temperatures is attributed to daily temperature cycles that cause thermal fatigue failures.[5]

Several approaches have been developed for designing asphalt pavements with reduced propensity for thermal cracking, based on the stiffness values and other properties of the asphalt cement or of the asphalt-aggregate mixture, in relation to climatic conditions at the site.[6] The U.S. Army Corps of Engineers, upon adopting viscosity grading of asphalt cements for pavement construction, revised the basis for selecting appropriate grades and for specifying test properties of asphalt cement for pavements in the cold regions.[7] The revised criteria require that asphalt used in the cold regions be of a relatively soft grade and of low temperature-susceptibility. The temperature-susceptibility is determined by the relative values of the kinematic viscosity at 135°C and the penetration at 25°C. These values define the penetration-viscosity (pen-vis) number (PVN) according to a method developed by McLeod,[8] based on extensive experience with pavements in Canada.

Upon adoption by the Corps of Engineers of criteria for selection of asphalt cement of low temperature-susceptibility, the U.S. Army Cold Regions Research and Engineering Laboratory (CRREL) began laboratory research investigations of the properties of mixtures containing such asphalts, pertinent to their use in roads and airfields in cold regions. It was considered particularly important to investigate those properties that would elucidate the possible advantages of soft asphalt cements in reducing the incidence of thermal cracking and the possible disadvantages of inferior performance under traffic.

One of the earliest paving projects on which the new specifications were applied was the overlay of the runway at Thule Air Base, Greenland, for which asphalt cement of grade AC2.5, with a PVN of about -0.5, was used. Accordingly, the laboratory testing performed by CRREL for the present research project included mixtures made with that same asphalt cement, seeking indications of advantages and disadvantages of the material used at Thule, as well as research results of general application to cold regions paving problems.

Objectives

The primary purpose of the investigation was to determine the properties of asphalt-aggregate mixtures made with three grades of asphalt cement, ranging from very soft to moderately hard and, based on the measured properties, to project the performance of such mixtures in resisting thermally-induced distress (cracking) and traffic-associated distress (cracking and rutting). The laboratory testing included conventional physical property tests on the three asphalt cements and two aggregates, Marshall mix design tests, indirect tension (Brazil or diametral load) tests to failure on the mixtures, and repeated-load indirect tension tests to determine the resilient modulus of the mixtures.

The analysis of the data, and of the projected performance of each mixture in an airfield pavement

Table 1. Asphalt properties.

Test property	Asphalt viscosity grade AC 2.5	AC 5	AC 20
Penetration at 25°C	268	172	71
Softening point, °C	38.9	41.0	47.2
Specific gravity	1.034	1.054	1.023
Viscosity at 60 °C, Pa·s (poises)	26.9 (269.3)	48.2 (482.1)	211.3 (2113.2)
Viscosity at 135°C, mm^2/s (= centistokes)	157.3	199.0	389.9
Thin film oven test			
Penetration of residue at 25°C, mm x 10^{-1}	132	92	45
% Original penetration	49	54	63
% Weight loss	0.07	0.29	0.13
Penetration-Viscosity Number (PVN)	-0.49	-0.73	-0.63

section, included the following:

A. Comparison of Marshal stability, flow, unit weight, percentage of air voids, and percentage of voids filled with asphalt for all mix designs at their optimum asphalt content as determined by the Marshall test.

B. Comparison of Brazil test data, including tensile strength, tensile strain at failure, and vertical deformation at failure, of all mix designs at various temperatures.

C. Comparison of modulus of resilience for all mix designs at various test temperatures.

D. Correlation of Marshall stability, indirect tensile strength, and modulus of resilience for all mix designs.

E. Comparison of the asphalt-aggregate mixtures' susceptibility to temperature cracking over a 10-year period, by use of the thermal computer program developed by Shahin[5] as follows:

1. Prediction of the stiffness history for each mix design at depths of 0, 50.8, and 127 mm (0, 2, and 5 in.); loading time of 3600 s.; and three climatic conditions with low, average, and high temperatures.
2. Prediction of the amount of thermal cracking for each mix design at depths of 0, 50.8, and 127 mm (0, 2, and 5 in.); loading time of 3600 s.; and three climatic conditions with low, average, and high temperatures.

F. Comparison of the various asphalt-aggregate mixtures' susceptibility to traffic-load-associated distress in a typical airport pavement. Making use of a layered elastic system analysis, the study included an evaluation of rutting and fatigue distress occurring in pavements incorporating each mixture.

MATERIALS, MIXTURE DESIGNS, AND TESTS

Materials

Tests were performed on mixtures prepared from three asphalt cements and two aggregates. The asphalt cements had a wide range in viscosity and other properties (Table 1). The AC 2.5 was obtained from Petrofina in Montreal, Canada, and is the same asphalt used in pavement overlay construction at Thule Air Base, Greenland, in 1977. The AC 5 was obtained from Husky Oil Company, Cody, Wyoming, while the AC 20 was obtained from Pike Industries, Inc., Lebanon, New Hampshire.

The first aggregate was also obtained from the Pike plant; the coarse aggregate was a highly angular, crushed quarry stone from Lebanon, New Hampshire, while the sand was obtained by processing material from a gravel pit in Norwich, Vermont. Previous tests on aggregates from this source showed a Los Angeles abrasion value of about 42. The second aggregate was obtained from a plant in Tilton, New Hampshire. Both the coarse aggregate and the sand of the latter were produced by crushing and processing material from a gravel pit at the plant site, and individual particles ranged from rounded to angular. Previous Los Angeles abrasion tests on aggregates from the same pit showed a loss of about 32%. Figure 1 shows gradation curves for both the Pike and Tilton aggregates, while photographs of both aggregates are shown in Figures 2 and 3. The Pike aggregate had an apparent specific gravity of 2.79, while the Tilton aggregate had an apparent specific gravity of 2.75.

Mixture design tests

The proportioning of nine separate asphalt-aggregate mixtures was determined by the Marshall method.[9]

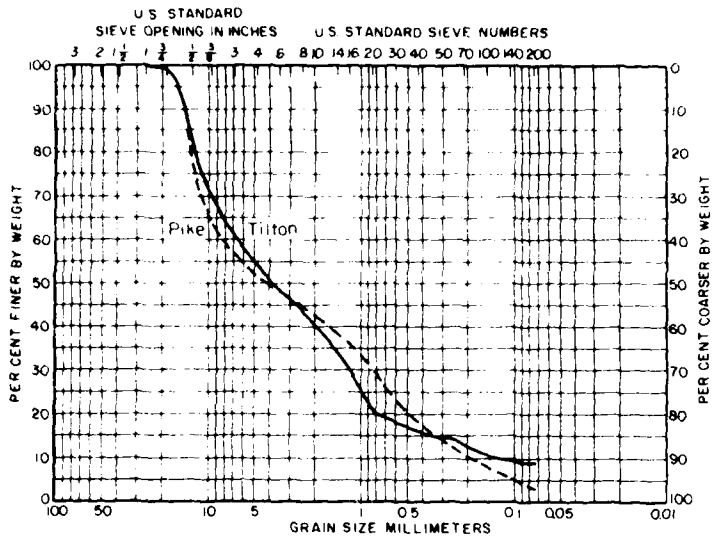

Figure 1. Gradation curves for Pike and Tilton aggregates.

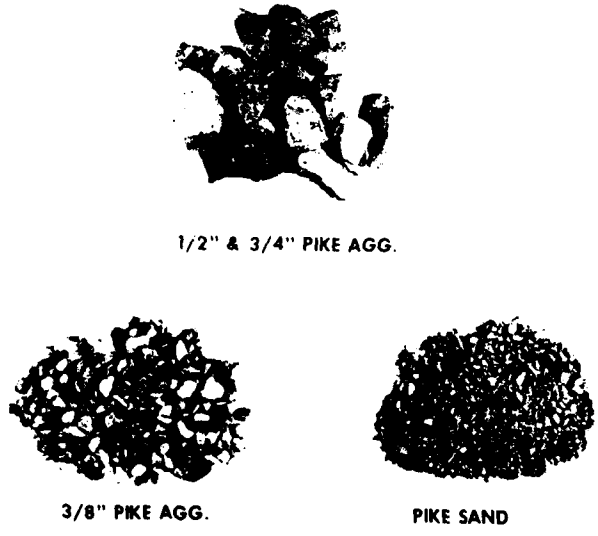

Figure 2. Pike aggregate.

Mixes with Pike aggregates were designed at 50 and 75 blows for each of the three asphalts, for a total of six mixes. A mix was designed, at 75 blows, for each of the asphalts with Tilton aggregates; constraints of time and resources made it necessary to forego preparing and testing a 50-blow mix.

For each mix design the following factors were determined: optimum asphalt content, Marshall stability, flow, air voids, voids filled with asphalt, and unit weight of the mixture. Complete mix design data are given in Appendix A, and a summary of mix properties at optimum asphalt content is given in Table 2. The optimum asphalt content was determined by averaging the asphalt content at (1) peak stability, (2) 5% air voids, and (3) 70% voids filled for mixes at 50 blows and 60% voids filled for mixes at 75 blows. A summary of these data is given in Appendix A.

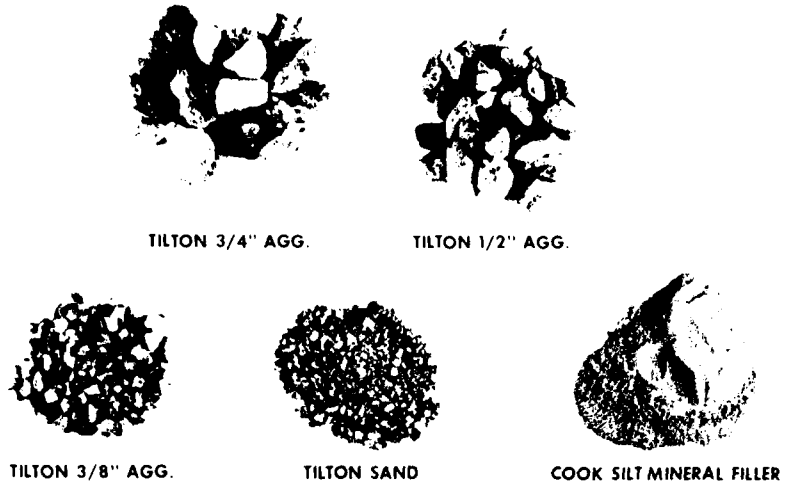

Figure 3. Tilton aggregate.

Table 2. Summary of Marshall mix design data at optimum asphalt content.

Aggregate	Compaction blows	Asphalt grade	Asphalt content (% by wt. of aggr.)	Marshall stability, kN (lb)	Flow mm (0.01 in.)	Air voids, (%)	Voids filled with Asphalt, (%)	Unit weight (Mg/m³) (pcf)
Pike	50	2.5	5.2	6.49 (1460)	2.8 (11.0)	4.7	72	2.46 (153.7)
		5	4.6	10.54 (2370)	2.7 (10.6)	5.2	66	2.46 (153.5)
		20	4.8	9.16 (2060)	2.8 (11.2)	5.3	68	2.44 (152.6)
	75	2.5	4.7	8.72 (1960)	2.5 (9.8)	5.8	64	2.44 (152.3)
		5.0	4.6	8.90 (2000)	2.4 (9.3)	6.2	63	2.48 (155.0)
		20	4.1	14.68 (3300)	2.6 (10.4)	5.5	64	2.46 (153.5)
Tilton	75	2.5	5.3	6.85 (1540)	3.2 (12.6)	5.5	67	2.39 (149.0)
		5	4.4	9.79 (2200)	2.8 (11.2)	6.3	62	2.42 (150.8)
		20	4.3	11.39 (2560)	2.8 (11.1)	6.0	62	2.42 (150.8)

Brazil test

The Brazil test was conducted on specimens representing each of the six mix designs compacted at 75 blows (Table 2). Other variables were rates of loading and temperature. A nominal rate of loading of 0.83 mm/s (1.97 in./min) was used for tests at the higher temperatures at which the principal pavement distress would be caused by traffic loading; this rate was considered to be the minimum at which the results would have significance for traffic loading.[10] A nominal loading rate of 0.03 mm/s (0.08 in./min) was used for tests at temperatures at which thermal cracking would be the principal distress mode; this is only slightly higher than the rate used by Christison et al.[11], who considered that rate effects on fracture strength under similar conditions are minimized.

The Brazil test, also called the indirect tensile or diametral load test, provided three outputs: (1) indirect tensile strength, (2) total tensile strain at failure, and (3) total vertical deformation at failure of the specimen.

The Brazil test was conducted using equipment (Fig. 4) similar to that described by Gonzalez et al.[10] A

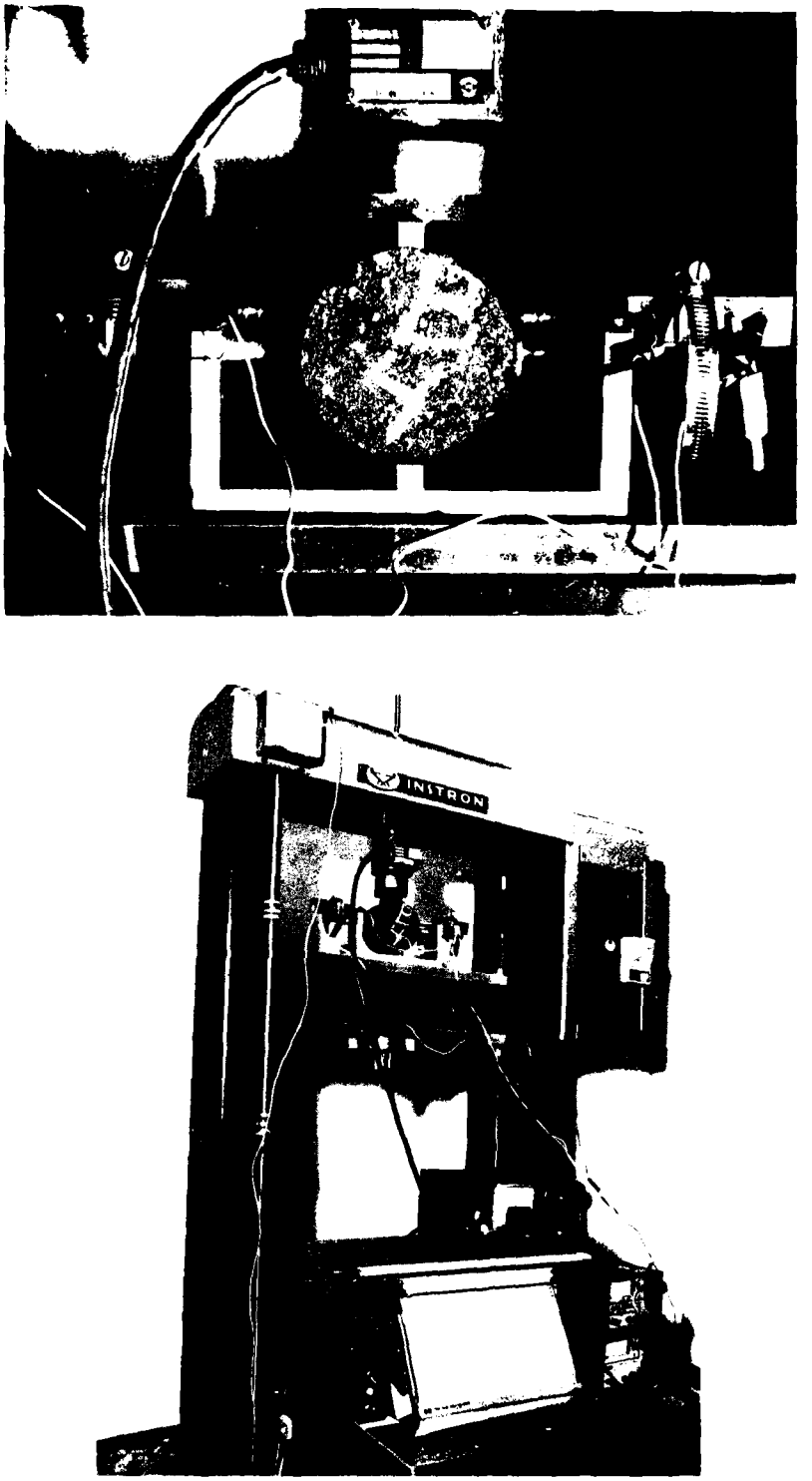

Figure 4. Brazil test equipment.

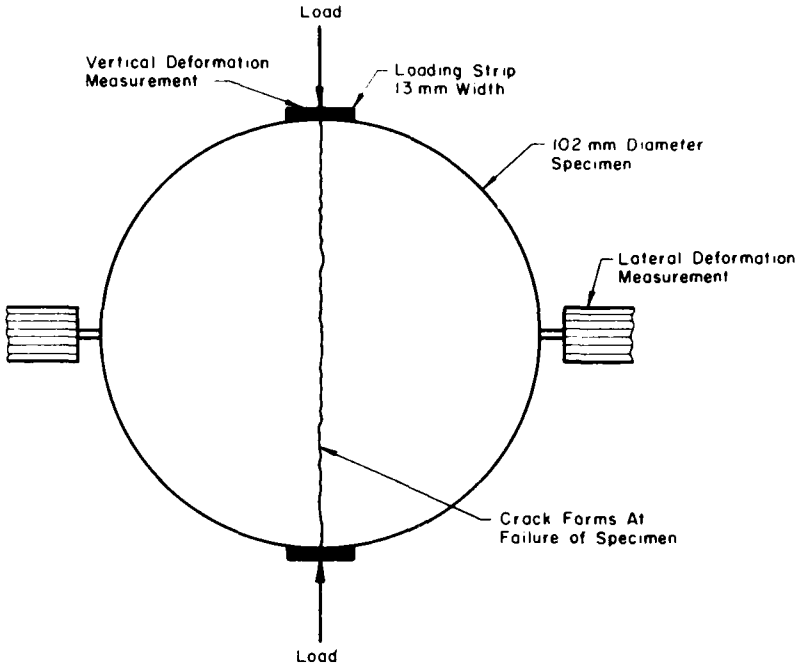

Figure 5. Diagram of Brazil test.

Marshall-sized specimen was loaded across its diameter by two curved loading strips (Fig. 5). The vertical and horizontal deformations were measured as shown. The tensile strength, tensile strain and other parameters were computed according to equations given in Appendix B.

Resilient modulus test

The diametral repeated-load test was used to measure the resilient modulus of compacted asphalt concrete as described by Schmidt.[12] The test was conducted by use of a "Mark III Resilient Modulus Device," purchased from the Retsina Company, 1224 Contra Costa Dr., El Cerrito, California 94520. The device functions by applying a 0.1-s load pulse once every 3 s across the vertical diameter of a cylindrical specimen and sensing the resultant deformation across the horizontal diameter at either 0.05 or 0.10 s after the beginning of specimen deformation. A Marshall-sized specimen can be used; optimum diameter is 102 mm (4 in.) and thickness is 70 mm (2 3/4 in.). The vertical loads can vary from 44 to 334 N (10 to 75 lb). Specimen deformations across the horizontal diameter range from 25 nanometers to 0.050 mm (1 to 2000 u in.).

The diametral loading (i.e., the application of a load across the vertical diameter of the cylindrical specimen) results in a deformation across the horizontal diameter of the specimen. The vertical load P and the total horizontal deformation Δ are related to the resilient modulus by the following expression for a 102-mm (4-in.)-diameter specimen:

$$M_R = \frac{P(\mu+0.2734)}{t\Delta}$$

where

M_R = resilient modulus, MPa (psi)
P = vertical repeated load, N (lb)
Δ = total horizontal deformation, mm (in.)
t = thickness of specimen, mm (in.)
μ = Poisson's ratio

The resilient modulus was measured for each of the nine asphalt-aggregate mixtures over a range of temperatures.

DATA ANALYSIS–MARSHALL TESTS

Mix design data according to the Marshall method[9] are given in Appendix A. The optimum asphalt contents for the nine mixtures are compared in Figure 6. Marshall stability, flow, air voids, percentage of voids filled and unit weight (all at optimum asphalt content) are

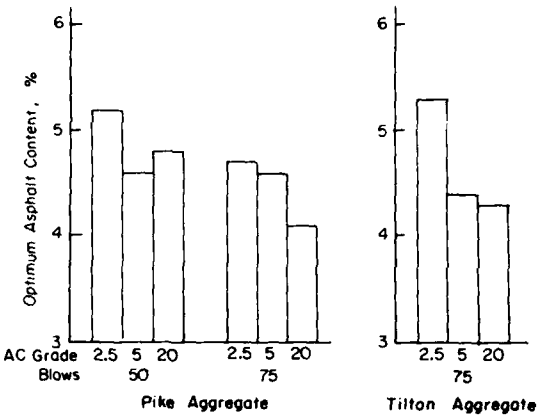

Figure 6. Comparison of optimum asphalt contents for the nine mix designs.

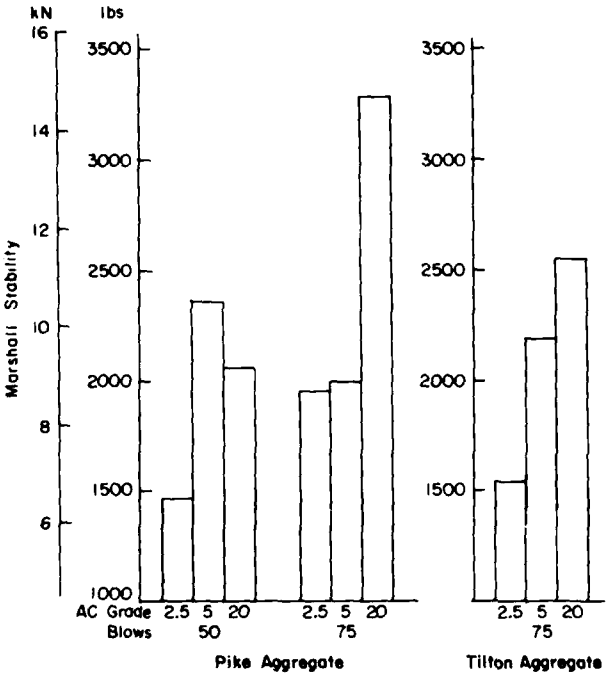

Figure 7. Comparison of Marshall stability at optimum asphalt content for the nine mix designs.

compared in Figures 7-11. The effects of asphalt grade, compactive effort and aggregate type are summarized below.

Asphalt grade

As asphalt viscosity grade increases from AC 2.5 to AC 5 to AC 20, the following generally occur, averaged over all of the data:

(1) Optimum asphalt content decreases.

AC Grade	*Mean*
AC 2.5	5.1%
AC 5	4.5%
AC 20	4.4%

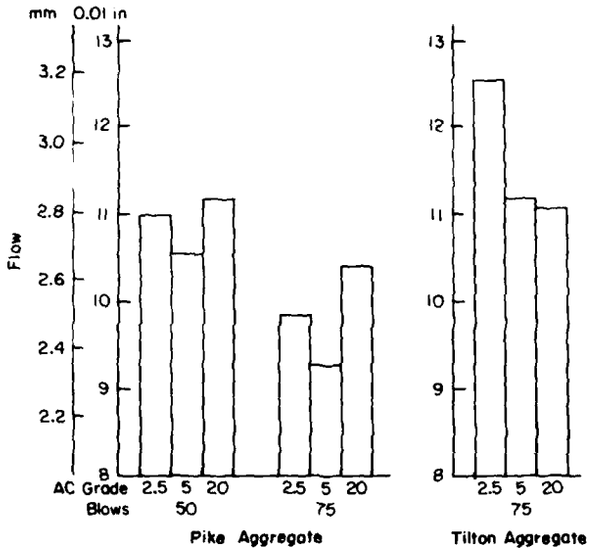

Figure 8. Comparison of flow at optimum asphalt content for the nine mix designs.

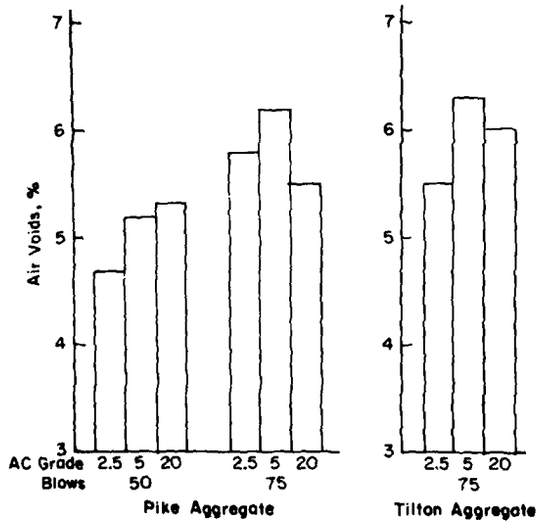

Figure 9. Comparison of air voids at optimum asphalt content for the nine mix designs.

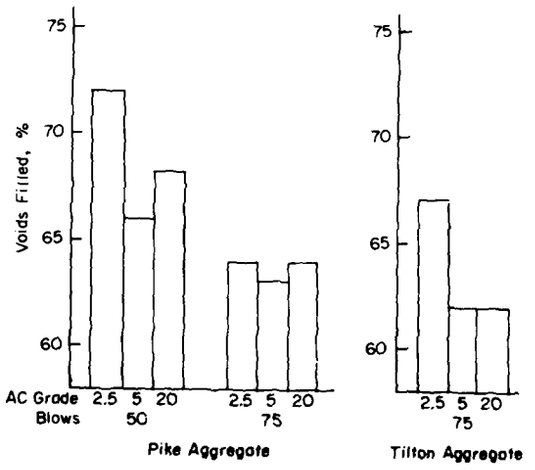

Figure 10. Comparison of voids filled at optimum asphalt content for the nine mix designs.

(2) Marshall stability increases.

AC Grade	*Mean*
AC 2.5	7.35 kN (1653 lb)
AC 5	9.82 kN (2207 lb)
AC 20	11.74 kN (2640 lb)

(3) Flow apparently decreases slightly, but the differences are scarcely significant.

AC Grade	*Mean*
AC 2.5	2.82 mm (11.1 units of 0.01 in.)
AC 5	2.64 mm (10.4 units of 0.01 in.)
AC 20	2.77 mm (10.9 units of 0.01 in.)

(4) Air voids increase.

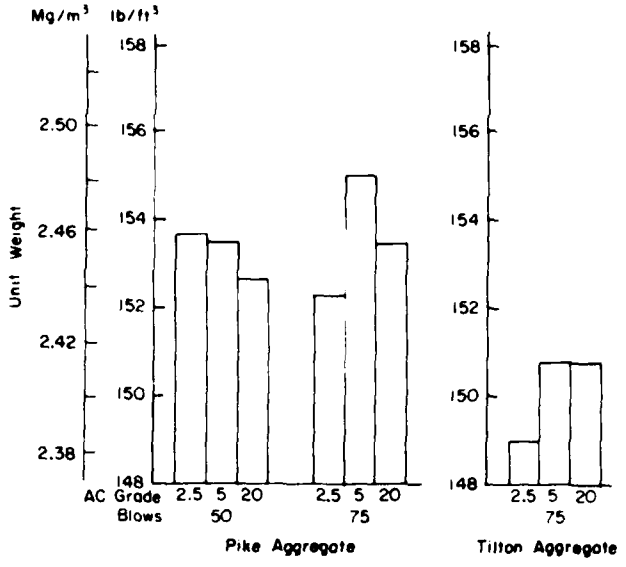

Figure 11. Comparison of unit weight at optimum asphalt content for the nine mix designs.

AC Grade	*Mean*
AC 2.5	5.3%
AC 5	5.9%
AC 20	5.6%

(5) Voids filled with asphalt decrease.

AC Grade	*Mean*
AC 2.5	67.7%
AC 5	63.7%
AC 20	64.7%

(6) Unit weight apparently increases slightly, but the differences are scarcely significant.

AC Grade	*Mean*
AC 2.5	2.43 Mg/m^3 (151.7 pcf)
AC 5	2.45 Mg/m^3 (153.1 pcf)
AC 20	2.44 Mg/m^3 (152.3 pcf)

The decrease in optimum asphalt content with increased asphalt viscosity grade results mainly from the shift (a decrease) in the asphalt content at peak stability (Table A1, App. A). Apparently the asphalt film thickness for maximum stability decreases as the asphalt viscosity increases. The decrease in optimum asphalt content results in an apparent slight increase in air voids and a decrease in percentage of voids filled with asphalt. The increase in Marshall stability, determined at 60°C (140°F), is believed to derive from the increased viscosity of the asphalt at that temperature, and from the decreased asphalt content.

Compactive effort

The effect of increased compactive effort from 50 to 75 blows for the Pike aggregate (only one compactive effort of 75 blows was used for the Tilton aggregate) is as follows:

(1) Optimum asphalt content decreases an average of 0.4%.
(2) Marshall stability increases an average of 2.10 kN (473 lb).
(3) Flow decreases 0.28 mm (1.1 units of 0.01 in.).
(4) Air voids increase 0.8%.
(5) Voids filled decrease 5.0%.
(6) Unit weight increases 0.005 Mg/m^3 (0.3 pcf).

Again, these results are expected, since greater compactive effort in a given specimen should result in higher unit weight and greater Marshall stability due to greater volume concentration of the aggregate particles. The increase in air voids at optimum asphalt content is less obvious but can be explained by the substantial decrease in asphalt content at the increased compactive effort, countered by only a slight increase in unit weight.

Aggregate type

The Pike and Tilton aggregates showed some differences in Marshall test properties. They can be compared only for the 75-blow compactive effort. By averaging results over all three asphalt grades the following differences are noted:

(1) Optimum asphalt content is approximately the same:

	Mean
Pike	4.5%
Tilton	4.7%

(2) Marshall stability is greater for Pike aggregate:

	Mean
Pike	10.84 kN (2437 lb)
Tilton	9.43 kN (2120 lb)

(3) Flow is less for Pike aggregate:

	Mean
Pike	2.49 mm (1.8 units of 0.01 in.)
Tilton	2.95 mm (11.6 units of 0.01 in.)

(4) Air voids and voids filled are approximately the same:

	Mean voids	*Mean Voids filled*
Pike	5.8%	63.7%
Tilton	5.7%	63.7%

(5) Unit weight is greater for the Pike aggregate:

	Mean
Pike	2.46 Mg/m^3 (153.6 pcf)
Tilton	2.41 Mg/m^3 (150.2 pcf)

DATA ANALYSIS–BRAZIL TESTS

Three properties of each specimen were measured from the Brazil tests: indirect tensile strength (Table 3), tensile strain at failure (Table 4), and total vertical deformation at failure (Table 5). The tabulated data are averages of the test results from three like specimens. The effects of aggregate type, asphalt grade, test temperature, and loading rate on these properties are summarized below.

Indirect tensile strength

Figure 12 shows the effects of asphalt grade, rate of loading and temperature on indirect tensile strength. As temperature decreases the tensile strength increases for all asphalt grades. The rate of change in tensile strength with temperature decreases below about -10°C; below about -20°C there is in most cases a slight decrease in tensile strength. Similar trends are reported for tests on other mixtures.[13] The higher viscosity asphalt grades have higher indirect tensile strengths at temperatures above about -10°C, but at very low temperatures (i.e., -10°C and below) the strengths for all grades tend to be very similar. The rate of loading has a very large effect on the tensile strength at +4.4°C; the higher the rate of loading, the higher the tensile strength (Fig. 13). Data were not obtained permitting direct comparison at other temperatures.

Tensile strain

As temperature increases, the tensile strain at failure increases (Fig. 14), particularly for tests at the lower loading rate (0.03 mm/s), which were run at much lower temperatures. The higher the viscosity grade of the asphalt, the lower the tensile strain at failure, particularly at the lower temperatures and loading rates. However, the rate of loading did not appear to have a large effect on tensile strain at failure, nor did the aggregate type.

Vertical deformation

As test temperature increases, the total vertical deformation at failure generally increases (Fig. 15). The mixture with AC 2.5 viscosity grade asphalt generally has a slightly higher vertical deformation than the mixtures with AC 5 or AC 20, indicating that the stiffer the asphalt binder, the less total deformation at rupture of the specimen. The data indicate that aggregate source and rate of loading did not have a large effect on total vertical deformation at failure of the specimens. The data for the Pike aggregate specimens were somewhat inconsistent and did not show well defined trends.

Summary of Brazil test results

A summary of the general trends for the effects of mix and test parameters on Brazil test results is given in Table 6. Test temperature and asphalt grade have considerable effect on all the observed stress-strain properties (strength, strain, and deformation). The rate of loading has a very significant effect on strength but not on strain

Table 3. Indirect tensile strength, MPa (psi).

Specimens prepared at optimum asphalt content and 75-blow compaction.

Rate of Loading, mm/s (in/min)	Temperature °C (°F)	Pike aggregate AC 2.5	Pike aggregate AC 5	Pike aggregate AC 20	Tilton aggregate AC 2.5	Tilton aggregate AC 5	Tilton aggregate AC 20
0.03	-40.0	3.73	3.22	3.56	3.69	3.29	3.47
(0.08)	(-40.0)	(541.0)	(467.0)	(516.3)	(535.2)	(477.2)	(503.3)
	-23.3	3.63	4.08	3.86	4.56	3.92	3.87
	(-10.0)	(526.5)	(591.8)	(559.8)	(661.4)	(568.5)	(561.3)
	-6.7	2.12	2.68	2.98	2.92	3.02	3.40
	(20.0)	(307.5)	(388.7)	(432.2)	(423.5)	(438.0)	(493.1)
	4.4	1.07	1.13		0.97	1.21	1.55
	(40.0)	(155.2)	(163.9)		(140.7)	(175.5)	(224.8)
0.83	4.4	2.19	2.54		2.45	2.70	2.55
(1.97)	(40.0)	(317.6)	(368.4)		(355.3)	(391.6)	(369.8)
	21.1	0.50	0.65	1.14	0.49	0.69	1.08
	(70.0)	(72.5)	(94.3)	(165.3)	(71.1)	(100.1)	(156.6)
	32.2	0.21	0.27	--	0.12	--	0.32
	(90.0)	(30.4)	(39.2)		(17.4)		(46.4)

Table 4. Tensile strain at failure, mm/mm (= in/in)

Specimens prepared at optimum asphalt content and 75-blow compaction.

Rate of Loading mm/s (in/min)	Temperature, °C (°F)	Pike aggregate AC 2.5	Pike aggregate AC 5	Pike aggregate AC 20	Tilton aggregate AC 2.5	Tilton aggregate AC 5	Tilton aggregate AC 20
0.03	-40.0	0.12	0.09	0.08	0.21	0.12	0.15
(0.08)	(-40.0)						
	-23.3	0.08	0.11	0.11	0.13	0.16	0.13
	(-10.0)						
	-6.7	0.20	0.17	0.11	0.23	0.19	0.17
	(20.0)						
	4.4	0.24	0.29	--	0.29	0.29	0.23
	(40.0)						
0.83	4.4	0.27	0.25	--	0.29	0.23	0.19
(1.97)	(40.0)						
	21.1	0.27	0.31	0.29	0.25	0.28	0.29
	(70.0)						
	32.2	0.26	0.26	--	0.33	--	0.29
	(90.0)						

or deformation, and aggregate source did not have an effect on any of these properties.

DATA ANALYSIS--RESILIENT MODULUS

The resilient modulus of asphalt-aggregate mixtures was measured at two loading times for a range of temperatures, asphalt viscosity grades, compactive efforts, and aggregate sources (Table 7). The effects of these variables on the resilient moduli of the mixtures are summarized below.

The general effect of temperature is shown in Figure 16 for mixes with Pike and Tilton aggregate for two different loading times, measured from start of deformation. These results show that as temperature decreased from about 20°C to -20°C, the resilient modulus increased as much as two orders of magnitude.

The effects of asphalt grade and compactive effort for mixtures with Pike aggregate are shown in Figure 17, and the effects of asphalt grade at a single compactive effort are shown for Tilton aggregate in Figure 18. The resilient modulus generally increased with increasing asphalt viscosity grade, particularly at the higher temperature (i.e., 21.1°C or 23.9°C). At lower temperatures, the resilient modulus was not always higher for the higher viscosity asphalt (Fig. 17). Loading time (from start of deformation) showed a pronounced effect on

Table 5. Total vertical deformation at failure, mm (in)

Specimens prepared at optimum asphalt content and 75-blow compaction.

Rate of Loading, mm/s (in/min)	Temperature, °C (°F)	Pike aggregate			Tilton aggregate		
		AC 2.5	AC 5	AC 20	AC 2.5	AC 5	AC 20
0.03	-40.0	1.50	1.58	1.80	1.52	1.07	0.97
(0.08)	(-40.0)	(0.060)	(0.062)	(0.071)	(0.060)	(0.042)	(0.038)
	-23.3	1.40	1.68	1.50	1.35	1.37	1.27
	(-10.0)	(0.055)	(0.066)	(0.059)	(0.053)	(0.054)	(0.050)
	-6.7	2.08	1.98	1.50	1.83	1.52	1.45
	(20.0)	(0.082)	(0.078)	(0.059)	(0.072)	(0.060)	(0.057)
	4.4	1.70	1.78	--	2.02	1.93	1.63
	(40.0)	(0.067)	(0.070)		(0.079)	(0.076)	(0.064)
0.83	4.4	2.26	2.01	--	2.01	1.88	1.50
(1.97)	(40.0)	(0.089)	(0.079)		(0.079)	(0.074)	(0.059)
	21.1	2.82	3.05	3.07	3.30	3.18	3.43
	(70.0)	(0.111)	(0.120)	(0.121)	(0.130)	(0.125)	(0.135)
	32.2	2.68	2.54	--	2.64	--	2.90
	(90.0)	(0.106)	(0.100)		(0.104)		(0.114)

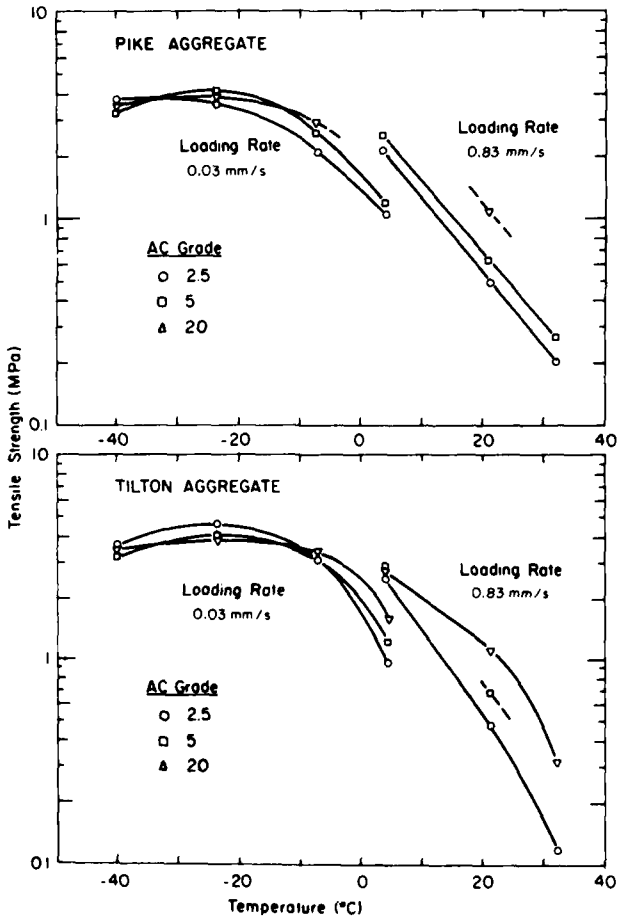

Figure 12. Effects of asphalt grade, rate of loading, and temperature on indirect tensile strength (75-blow compaction).

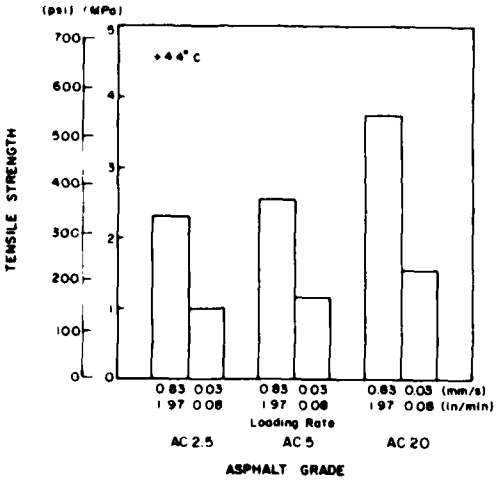

Figure 13. Comparison of tensile strengths at two rates of loading (75-blow compaction).

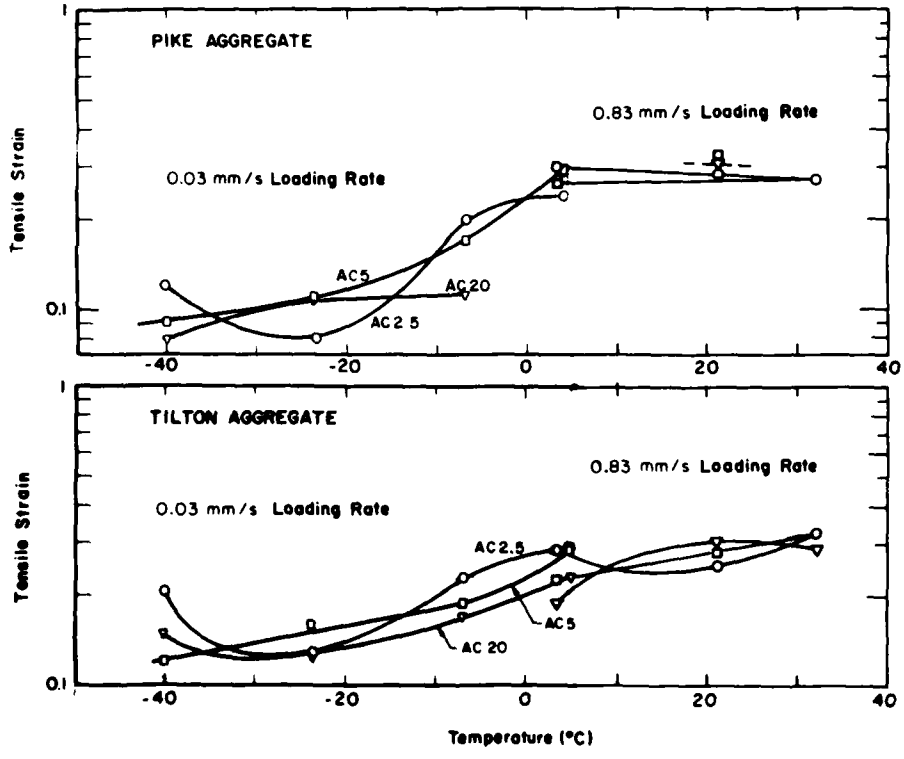

Figure 14. Effects of asphalt grade, rate of loading, and temperature on tensile strain at failure (75-blow compaction).

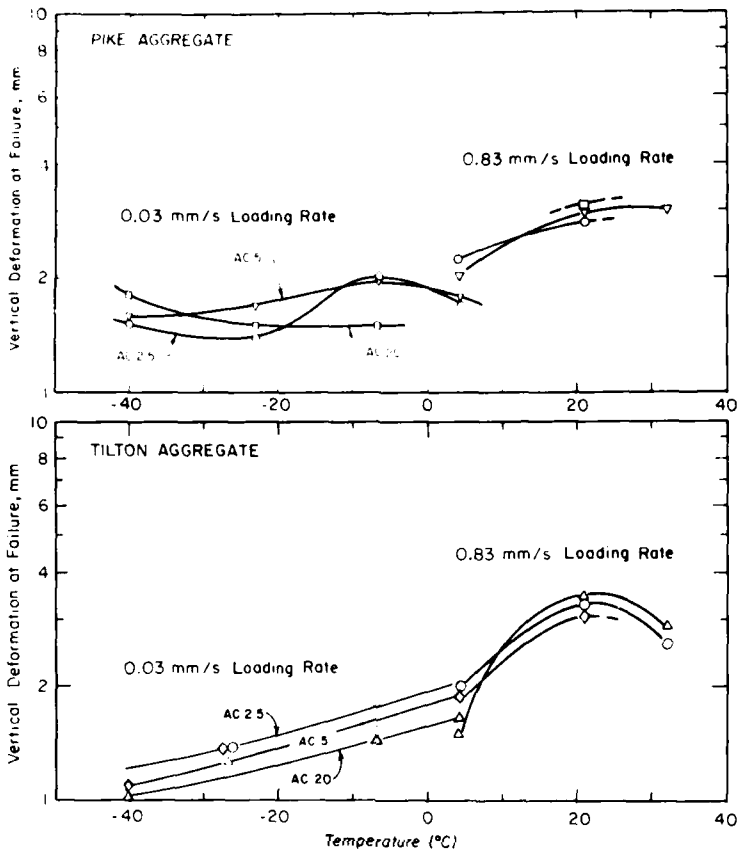

Figure 15. Effects of asphalt grade, rate of loading and temperature on total vertical deformation at failure (75-blow compaction).

Table 6. Summary of effects of mix and test parameters on Brazil test results.

Factor	*Tensile strength*	*Tensile strain at failure*	*Vertical deformation at failure*
Increase temperature	Decrease	Increase	Increase
Increase rate of load	Increase	No effect	No effect
Aggregate source	No effect	No effect	No effect
Increase AC viscosity grade	Increase	Decrease	Decrease

the resilient modulus; in general, the modulus increased by a factor of 1.5 to 2 as the time was decreased from 0.10 to 0.05 s, an exception being at the lowest temperatures, where the increase was smaller. The influence of compactive effort for the Pike aggregate also should be noted. The higher compactive effort (75 blows as opposed to 50 blows) resulted in a resilient modulus that averaged about 15% higher. Aggregate type appears to have a very significant influence on resilient modulus (Fig. 19). The Tilton aggregate shows a much higher modulus at higher temperatures (approximately 45% higher for temperatures greater than 0°C) than the Pike aggregate. At lower temperatures mixtures made from the two aggregates have approximately the same moduli, except that the AC 5 mixture shows a higher modulus with Pike aggregate than with Tilton aggregate.

These results are in general agreement with previous research findings.[12, 14, 15] They show that the resilient

Table 7. Resilient modulus, MPa (10^3 kg/cm^2).

Asphalt Grade	Temperature, °C (°F)	Pike Aggregate 50-blow compaction Time from start of deformation, s 0.05	0.10	Pike Aggregate 75-blow compaction Time from start of deformation, s 0.05	0.10	Tilton Aggregate 75-blow compaction Time from start of deformation, s 0.05	0.10
AC 2.5	22.2 (72.0)	–	–	–	–	2.15 (21.9)	0.94 (9.6)
	21.1 (70.0)	0.71 (7.2)	0.39 (4.0)	0.80 (8.2)	0.39 (4.0)	–	–
	4.4 (40.0)	12.1 (123)	7.26 (74)	14.5 (148)	8.92 (91)	20.4 (208)	19.7 (201)
	-6.7 (20.0)	–	–	–	–	26.6 (271)	26.1 (266)
	-17.8 (0.0)	51.6 (526)	31.9 (325)	32.1 (327)	45.8 (467)	31.4 (320)	33.4 (341)
	-28.9 (-20.0)	–	54.2 (553)	–	76.8 (783)	38.4 (392)	38.1 (389)
AC 5	23.9 (75.0)	–	–	–	–	1.86 (19.0)	1.12 (11.4)
	21.1 (70.0)	0.80 (8.2)	0.43 (4.4)	1.18 (12.0)	0.66 (6.7)	–	–
	4.4 (40.0)	13.9 (142)	8.53 (87)	13.1 (134)	8.14 (83)	18.7 (191)	15.7 (160)
	-6.7 (20.0)	–	–	–	–	31.3 (319)	31.4 (320)
	-17.8 (0.0)	37.3 (380)	26.9 (274)	60.5 (617)	41.8 (426)	43.5 (444)	46.2 (471)
	-28.9 (-20.0)	–	78.6 (801)	–	51.6 (526)	74.7 (762)	51.8 (528)
AC 20	23.9 (75.0)	–	–	–	–	4.47 (45.6)	2.93 (29.9)
	21.1 (70.0)	2.45 (25.0)	1.50 (15.3)	2.81 (28.7)	1.83 (18.1)	–	–
	4.4 (40.0)	(161)	(128)	(181)	(132)	(201)	(176)
	-6.7 (20.0)	–	–	–	–	31.8 (324)	29.8 (304)
	-17.8 (0.0)	39.3 (401)	30.5 (311)	45.7 (466)	34.6 (353)	45.5 (464)	39.3 (401)
	-28.9 (-20.0)	–	71.1 (725)		74.4 (759)	119.2 (1216)	69.6 (710)

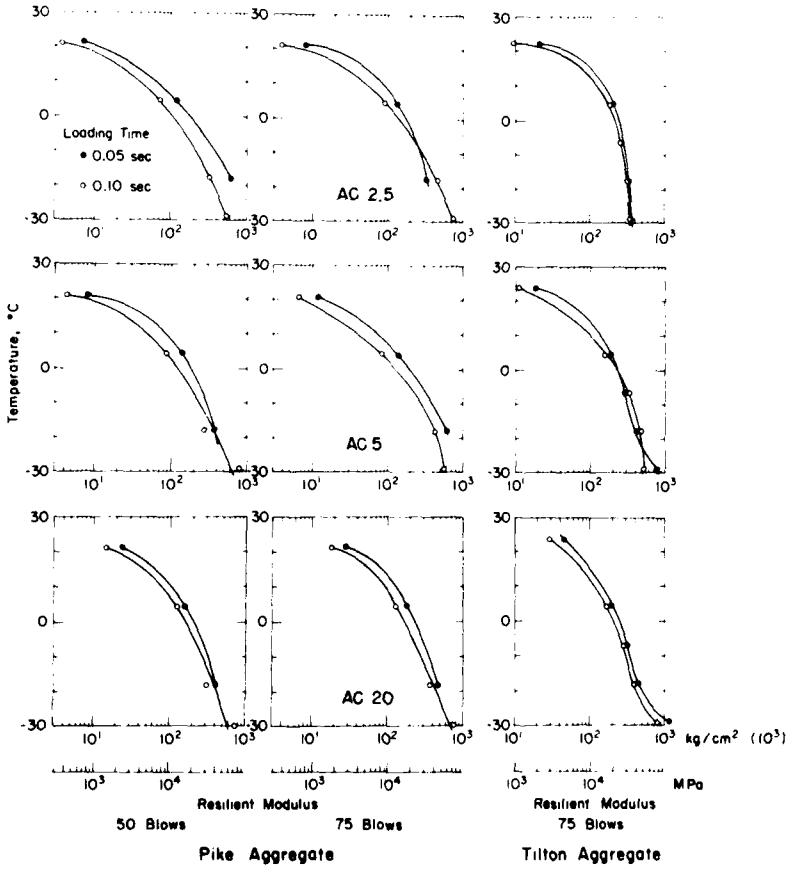

Figure 16. Effect of temperature on resilient modulus measured at 0.05 and 0.10 s from start of deformation.

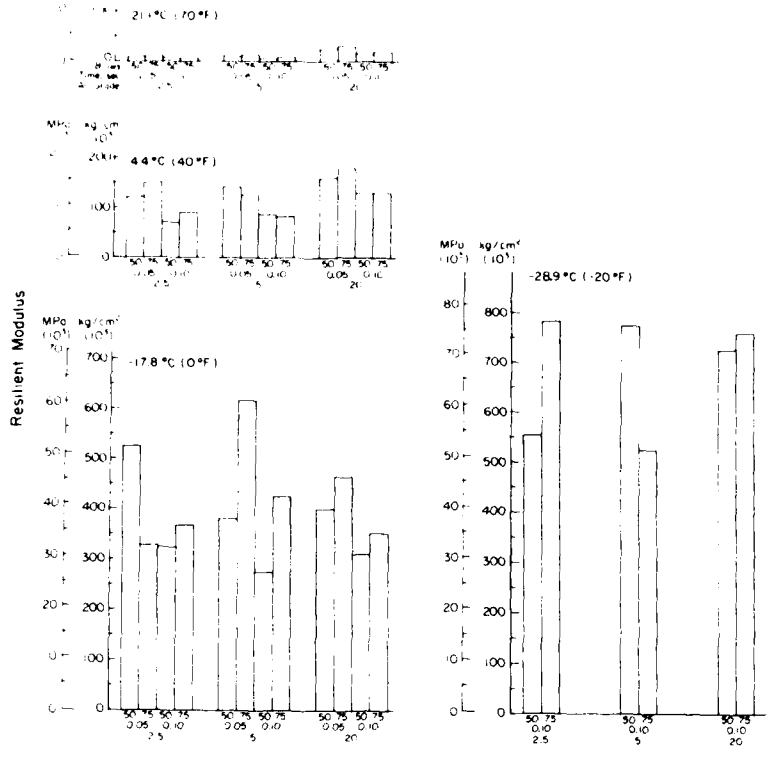

Figure 17. Effects of asphalt grade, loading time from start of deformation, and compactive effort on resilient modulus of mixes with Pike aggregate.

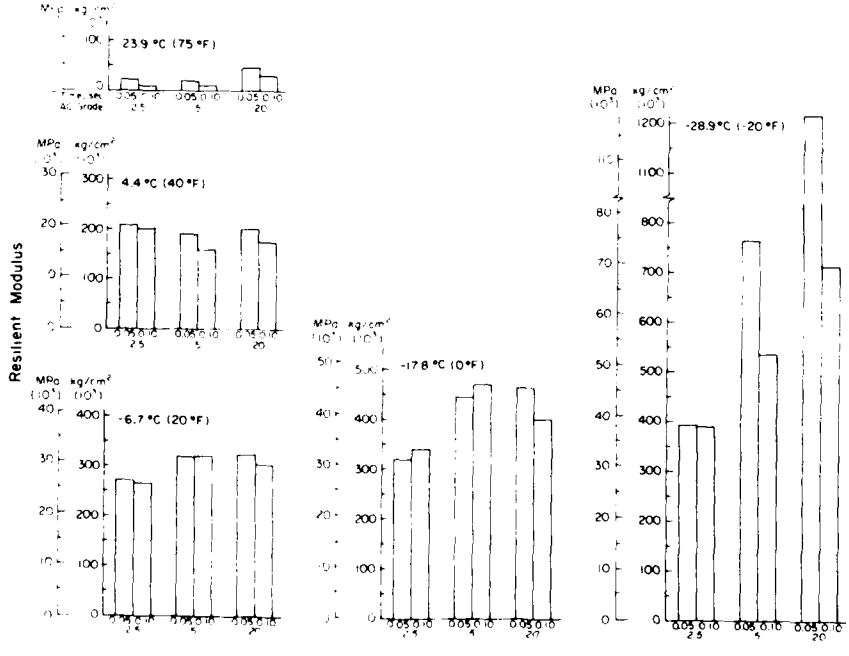

Figure 18. Effects of asphalt grade and loading time from start of deformation on resilient modulus of mixes with Tilton aggregate at 75-blow compaction.

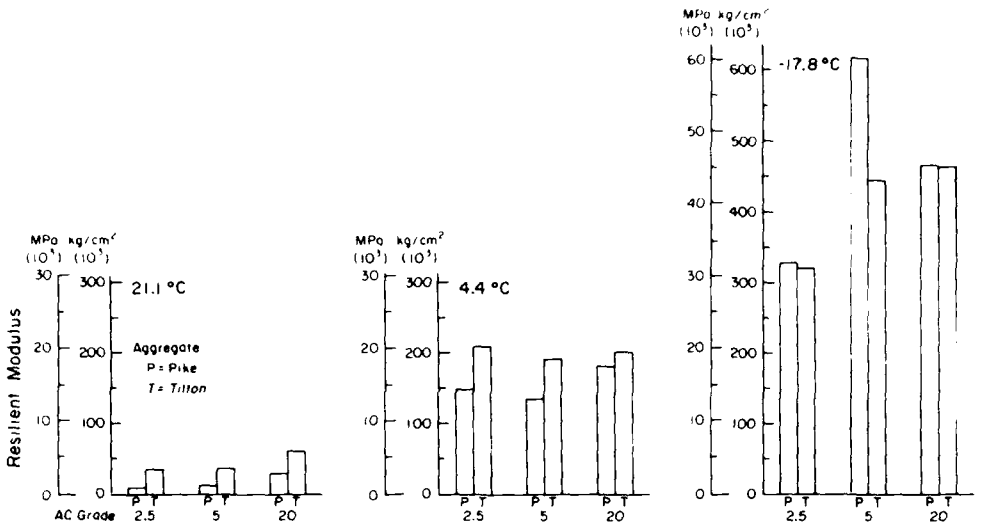

Figure 19. Effects of asphalt grade and aggregate type on resilient modulus measured at 0.05 s from start of deformation (mixes compacted at 75 blows).

modulus for asphalt concrete varies widely with mix temperature, loading time, asphalt viscosity grade, aggregate type, and compactive effort. The most significant factor by far is the temperature of the mix.

COMPARISON OF MIXTURE SUSCEPTIBILITY TO TEMPERATURE CRACKING

General

The primary purpose of this phase of the study was to analyze the temperature cracking expected to develop in the various mixtures. Both stiffness variation with time and thermal cracking were determined over a 10-year period for the six different mix designs compacted at 75 blows, by using the thermal computer program developed by Shahin.[5]

In the program the models and submodels forming the system provide for simulation of pavement temperatures, estimation of asphalt concrete stiffness, prediction of in-service aging of asphalts, and consideration of stochastic variations and thermal fatigue distresses. Temperature cracking is predicted by the developed system as the appropriate addition of two forms of cracking, which are briefly defined below:

(1) low-temperature cracking, which occurs when the thermal tensile stress exceeds the asphalt concrete tensile strength, and

(2) thermal-fatigue cracking, which occurs when the thermal fatigue distress, due to daily temperature cycling, exceeds the asphalt concrete fatigue resistance.

The stiffness and temperature cracking were predicted for the low temperatures and thermal cycles expected in a 127-mm (5-in.) asphalt concrete pavement at depths of 0, 50.8, and 127 mm (0, 2, and 5 in.) for a cold climate (Fairbanks, Alaska), and a moderate climate (Springfield, Illinois), and a warm climate (Houston, Texas). Table 8 shows the input data for the three climatic conditions.

Asphalt concrete stiffness

Figure 20 shows the influence of climatic region and age on the annual maximum stiffness (stiffness on the coldest day of an average year) of the asphalt concrete mixes assuming a loading time of one hour. The stiffness was calculated by a computer program developed by Shahin,[5] for which the inputs are air temperature, solar radiation, wind velocity, asphalt-aggregate mixture thermal properties, asphalt penetration and softening point, and volume concentration of aggregate in the mixture; inputs for analysis of aging include penetration, softening point (ring and ball), and percentage of original penetration after the thin-film oven test. In Figure 20 only the stiffness at the pavement surface and for a compactive effort of 75 blows is shown. As expected, the calculated stiffnesses of the asphalt mixes with both the Pike and Tilton aggregates were found to increase not only with age and with asphalt viscosity but also with the climate becoming colder. The calculated stiffnesses of the Pike mixtures containing a given asphalt are slightly greater than those for the Tilton mixtures at the same temperature. Figure

Table 8. Climatic input data for stiffness and thermal cracking analysis.

Input data	Cold climate (Fairbanks, Alaska)	Moderate climate (Springfield, Ill.)	Warm climate (Houston, Texas)
Average annual solar radiation, J/m²-s (langleys per day)	108 (224)	174 (360)	203 (420)
Average July solar radiation, J/m²-s (langleys per day)	210 (434)	266 (550)	281 (580)
Average annual wind velocity, m/s (mph)	2.4 (5.3)	5.1 (11.4)	3.4 (7.6)
Average annual air temp., C (F)	-3.5 (25.7)	11.5 (52.7)	20.5 (68.9)
Average annual range of air temp., C (F)	40.3 (72.6)	27.4 (49.4)	17.4 (31.3)
Average daily range of air temp., C (F)	11.8 (21.3)	11.0 (19.8)	12.1 (21.8)

20 also shows that the calculated rate of increase of asphalt mix stiffness with age is greater for the warmer climates than for the cold climates.

Thermal cracking

The progression of total calculated thermal cracking as the pavement ages is shown (Fig. 21) for the various asphalt concrete mixes designed at 75-blow compaction for cold, moderate and warm climates, respectively. The total thermal cracking developed by the end of each year was determined over a 10-year period based on the low temperatures and temperature cycles expected at pavement depths of 0, 50.8, and 125 mm (0, 2, and 5 in.). A thermal loading time of one hour as recommended by Shahin[5] was used in the analysis. The calculated thermal cracking includes both low-temperature cracking and thermal fatigue cracking.

The analysis shows that, in most cases, thermal cracking will occur only at the temperatures projected to prevail at the pavement surface. Figure 22 shows a summary of the total thermal cracking predicted to develop by the end of the 10-year period after construction, for the different mixes and climatic conditions. For depths of 0 and 50.8 mm (2 in.), respectively, the mixes with the AC 20 asphalt cement will experience the most thermal cracking for all the climatic conditions, while the least cracking is expected in the mixes using AC 2.5. There is no consistent pattern showing greater or lesser cracking in mixes using Tilton aggregate compared with mixes using Pike aggregate. Shahin[5] has indicated that cracking of 200 m/305 m² (200 ft/1000 ft²) can be considered severe. Accordingly, it can be interpreted that the mixes using both the AC 5 and AC 20 develop moderately severe to severe thermal cracking at the pavement surface under cold climatic conditions, and that mixes with AC 20 have substantial cracking potential at the pavement surface in the moderate climate also.

The results of this analysis show that, considering only thermal cracking, mixes containing either AC 2.5, AC 5, or AC 20 would perform well in the warm climate that was studied. Only AC 2.5 and AC 5 mixes would perform well in the moderate climate, and only AC 2.5 mixes would perform well in the cold climate. The suitability of each of these mixes for adequate performance under traffic in a particular climatic zone will depend also upon its resistance to rutting and fatigue distress. Traffic-load-associated distress is discussed below.

Influence of asphalt cement properties

The influence of asphalt cement properties on thermal cracking can often be evaluated in terms of the pen-vis number (PVN) (Table 1). However, since comparisons in this report are being made between mixes with asphalt cements of different viscosity grades the effect of PVN cannot be effectively evaluated.

Figure 23 and 24 show the influence of asphalt cement viscosity and penetration, respectively, on thermal cracking at the pavement surface. As expected, the calculated total thermal cracking increases with an increase in asphalt viscosity and decreases with an increase in penetration.

The influence of climate on the amount of thermal cracking is also readily apparent in these figures. It appears that asphalt cements with viscosities (135°C) less than about 300 mm²/s (300 centistokes) and penetrations greater than about 120 would not experience large amounts of thermal cracking in the moderate climate that was studied. Viscosity less than about 160 mm²/s (160 centistokes) and penetration greater than about 260 are needed to restrict cracking to an acceptable degree in the cold climate. In both cases the predicted cracking after 10 years would then be in the range of 40-60 m/305 m² (40-60 ft/1000 ft²).

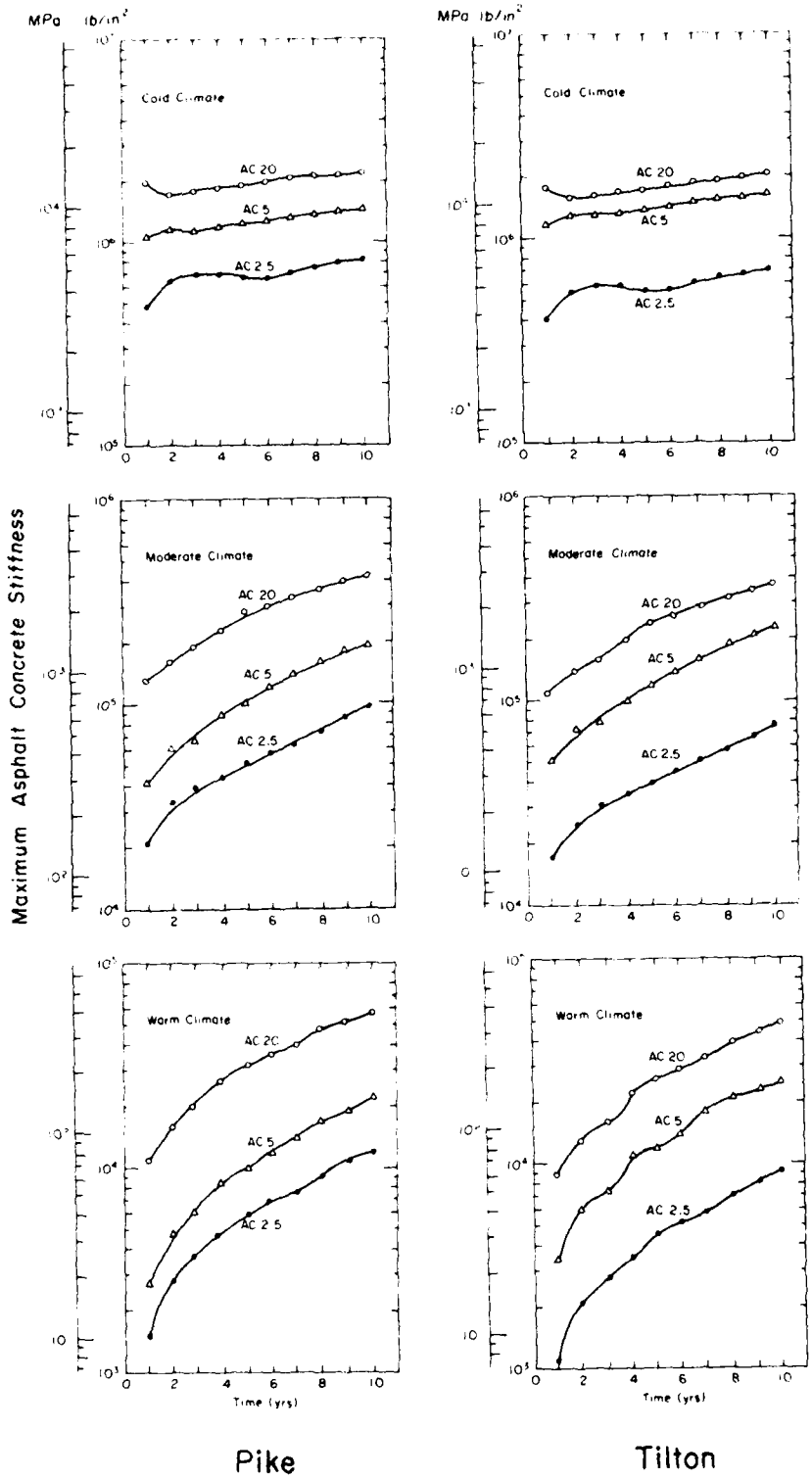

Figure 20. Effects of age and asphalt grade on stiffness of pavement surface of mixture compacted at 75 blows.

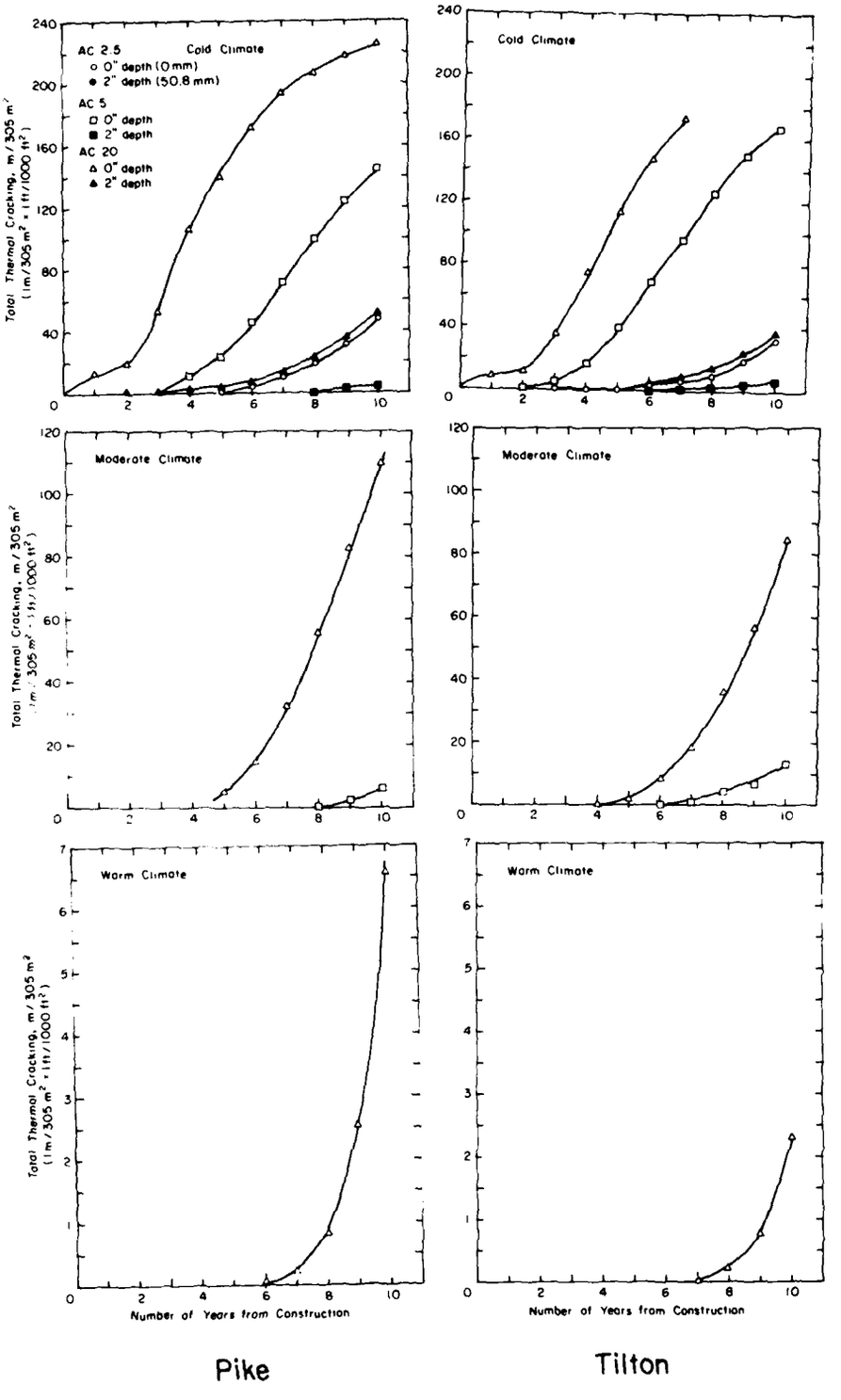

Figure 21. Projected development of total thermal cracking over 10-year period in various mixtures compacted at 75 blows (no cracking predicted except where shown, and in no case is cracking predicted at the 127-mm (5-in.) depth).

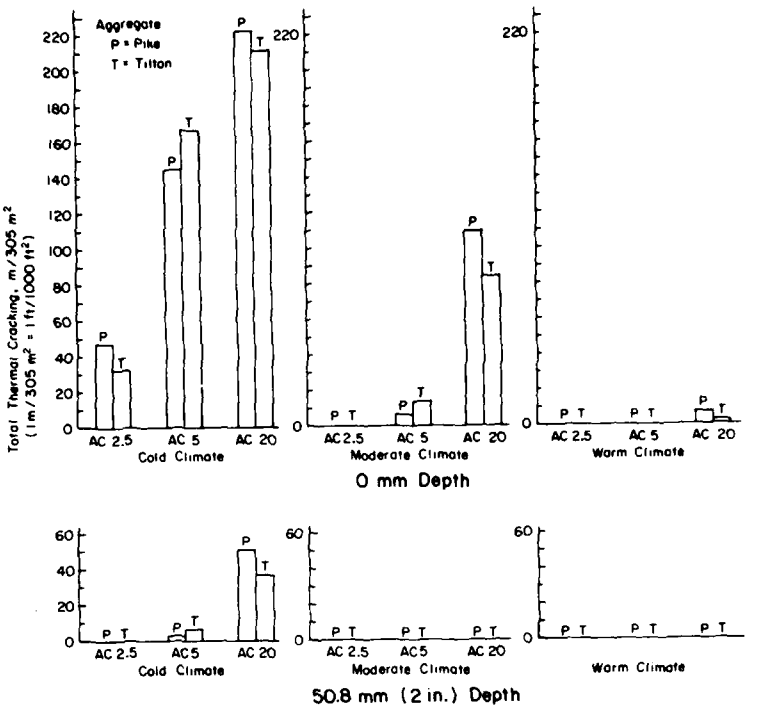

Figure 22. Total thermal cracking projected at 10 years after construction, for mixes with two aggregate types and three asphalt grades.

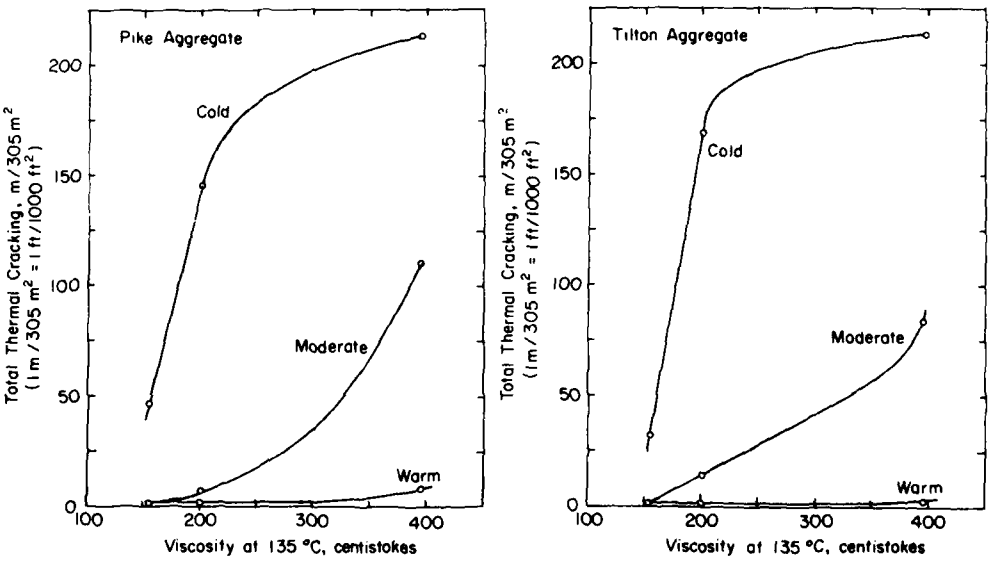

Figure 23. Effect of asphalt cement viscosity on projected total thermal cracking at pavement surface 10 years after construction.

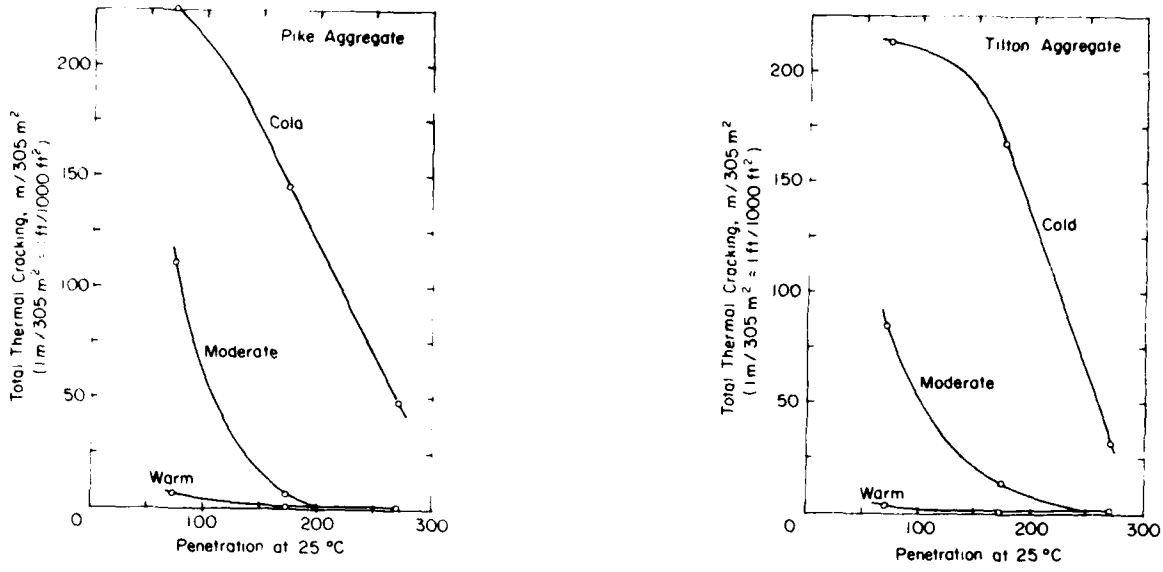

Figure 24. Effect of asphalt penetration on projected total thermal cracking at pavement surface 10 years after construction.

It is clear from the figures that asphalt cement properties such as viscosity and penetration are important in the design of asphalt concrete pavements that will resist thermal cracking and that asphalt grades must be selected with consideration of climatic conditions.

Summary

Mixes using AC 2.5 asphalt cement and either Pike or Tilton aggregate show excellent resistance to thermal cracking in the cold, moderate and warm climates that were studied. Mixes with AC 5 also should perform well in the moderate and warm climates, but show significant thermal cracking in the cold climate. Mixes with AC 20 show severe cracking in the cold climate, considerable cracking in the moderate climate, and negligible cracking in the warm climate. Asphalt viscosity and penetration, accordingly, have a substantial effect on thermal cracking of the mix. But the choice of grade of asphalt cement should also account for mixture resistance to traffic-induced distress (see below).

COMPARISON OF MIXTURE SUSCEPTIBILITY TO TRAFFIC-LOAD-ASSOCIATED DISTRESS

Stress/strain analysis

An analysis of the behavior of the various asphalt concrete mixtures under aircraft loading is presented. The analysis was conducted using a typical airfield flexible pavement cross section for F-104 fighter aircraft loading (Fig. 25), and a computer program[16] for linear elastic layered systems. The pavement structure shown in Figure 25 meets the U.S. Army Corps of Engineers criteria[17] as to layer thickness and CBR values. The resilient moduli of asphalt concrete used in the analysis were taken from relationships between temperature and resilient modulus determined by laboratory tests. These values are summarized in Table 9 for three temperatures. Table 9 also shows aircraft loads as well as resilient moduli and Poisson's ratios assumed for the other layers of the pavement structure. The resilient moduli for the base and subbases were typical values as measured by Allen and Thompson[18] in repeated-load triaxial testing. The subgrade was assumed to be clay, with a modulus of 41 MPa (6000 psi). To simplify the analysis and comparison of the asphalt concrete mixtures, the moduli of the subgrade, subbases and base were assumed to be constant throughout the loading periods at various temperatures. Significant seasonal variation of these moduli would be expected in actual service, especially in frost areas.

The model for elastic layered systems was used to compute stresses, strains, and displacements at critical locations in the pavement structures when loaded with one wheel of the fully loaded F-104 aircraft. The displacements, strains and stresses directly beneath the center of the wheel load at various depths below the pavement surface are tabulated in Appendix C. The same parameters, which are widely used as indicators

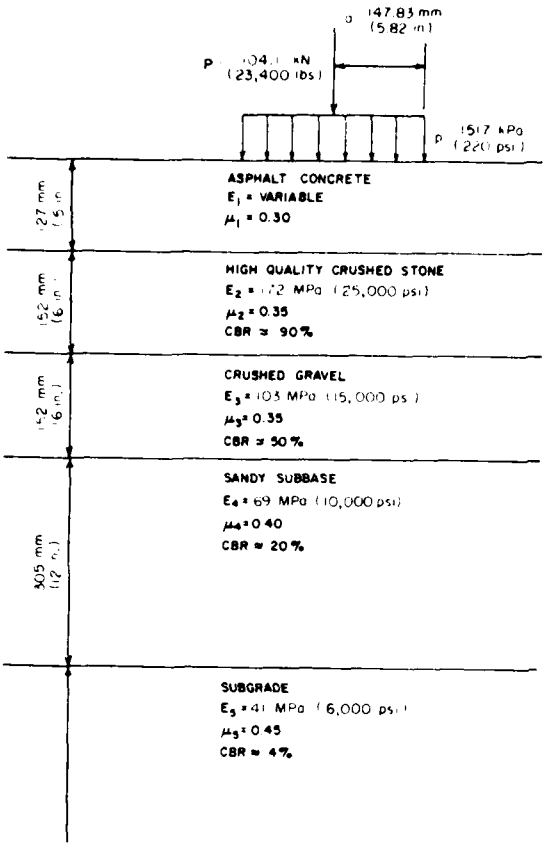

Figure 25. Aircraft loading and pavement/subgrade structure analyzed for fatigue and rutting. E = *Resilient modulus,* μ = *Poisson's ratio, and* CBR = *California bearing ratio.*

of expected pavement performance, are plotted in Figures 26 to 30 to illustrate the effects of asphalt viscosity grade, aggregate type, compactive effort, and temperature.

Vertical displacement (or deflection) of the pavement surface (Fig. 26) increased with increased temperature. Deflection decreased with increased asphalt viscosity grade, particularly at higher temperatures. The Pike aggregate in the mix resulted in higher deflection than the Tilton aggregate. A higher deflection is generally indicative of relatively fewer load applications to pavement distress occurrence.[19]

The temperature of the asphalt concrete has a very large effect on radial strain at the bottom of the asphalt concrete layer (Fig. 27). The higher the temperature, the higher the strain, because of the decrease in resilient modulus. As the asphalt viscosity grade increases, the tensile strain decreases, particularly at the highest temperature. Asphalt concrete containing the Pike aggregate has greater tensile strains than the mix containing the Tilton aggregate. Data from Table C2 (App. C) show that compactive effort has only minimal effect on radial tensile strains.

Radial tensile strain has generally been used as an indicator of a pavement's susceptibility to fatigue damage. As a rule, a higher strain, whether caused by a higher wheel load or by lower subgrade or base course stiffness, is associated with a higher potential for fatigue damage.[20, 21, 22] In the present comparison, however, both the wheel load and the subgrade and base course stiffness are assumed to be constant. Consequently, any difference in radial tensile strain found in this comparative study results only from a difference in the resilient modulus of the asphalt concrete itself, and therefore is associated also with a difference in the tensile stress. The variation of the calculated radial tensile stresses at the bottom of the asphalt concrete layer (Fig. 28) confirms this principle. Hence, no special conclusions can be drawn at this point regarding the significance of the variations in the calculated radial stresses and strains. An analysis of fatigue damage is required for their interpretation (see below).

Vertical subgrade compressive strain is plotted in Figure 29. As the temperature increases, the resilient modulus of the asphalt concrete decreases and the subgrade vertical compressive strain beneath the wheel load increases very significantly. The higher the asphalt viscosity grade, the less the vertical subgrade strain, especially at the highest temperature. The subgrade strain was higher in the mix with Pike aggregate than in the mix with Tilton aggregate. Greater vertical subgrade strain has generally been associated with increased load-associated deformation (rutting) of the pavement.[23, 24, 25]

The vertical stress at the top of the granular base course increases rapidly as the temperature increases (Fig. 30). At the highest temperature the vertical stress decreases as the asphalt viscosity grade increases. The Pike aggregate in the mix results in a much higher vertical stress on the base course at higher temperatures. The higher the vertical stress on the base course, the higher the potential for permanent deformation in the base course, and consequent rutting of the surface.[24]

Fatigue damage analysis

The result of fatigue damage from repeated aircraft loadings is alligator cracking of the asphalt concrete surface as described and illustrated by Shahin et al.[26] The radial strain in the asphalt concrete surface is the major load parameter that has been associated with fatigue damage in flexible pavements.[27, 28, 29] With asphalt concrete at a given temperature, and having a certain resilient modulus, higher radial tensile strains

Table 9. Material properties and aircraft loads used in stress-strain analysis.

a. Material Properties

Layer	Resilient modulus, MPa	(psi)	Poisson's ratio	Thickness, mm	(in.)
1	variable (see below)		0.30	127.0	(5.0)
2	172	(25,000)	0.35	152.4	(6.0)
3	103	(15,000)	0.35	152.4	(6.0)
4	69	(10,000)	0.40	304.8	(12.0)
5	41	(6,000)	0.45	semi-infinite	

b. Aircraft Loading

Aircraft wheel load kN	(lb)	Pressure kPa	(psi)	Radius mm	(in.)
104.1	(23,400)	1517	(220)	147.83	(5.82)

c. Resilient modulus in GPa (psi) of asphalt concrete made with different grades of asphalt cement.

Surface temp °C (°F)	Compaction (blows)	Pike aggregate AC 2.5	AC 5	AC 20	Tilton aggregate AC 2.5	AC 5	AC 20
-6.7 (20)	50	16.66 (2,416,000)	19.59 (2,842,000)	22.53 (3,268,000)			
	75	21.56 (3,128,000)	23.51 (3,410,000)	23.52 (3,411,000)	26.47 (3,839,000)	30.39 (4,408,000)	29.41 (4,266,000)
-7.2 (45)	50	5.68 (824,000)	6.66 (966,000)	10.78 (1,563,000)			
	75	6.86 (995,000)	6.37 (924,000	10.29 (1,492,000)	15.68 (2,275,000)	12.75 (1,849,000)	14.71 (2,133,000)
21.1 (70)	50	0.38 (55,000)	0.43 (63,000)	3.23 (469,000)			
	75	0.39 (57,000)	0.65 (94,000)	1.76 (256,000)	1.57 (228,000)	2.25 (327,000)	4.21 (611,000)

in the bottom of the layer, caused by either greater wheel loads or reduced infrastructure support, can be interpreted to signify reduced number of load applications to cause fatigue cracking (decreased fatigue life). In the present case the variation in radial tensile strains has been calculated under an unchanging wheel load at an assumed constant substructure support, and results only from differences in asphalt concrete mixture resilient modulus, caused by varying temperatures or by different mixtures. Accordingly, as mentioned above, to interpret the variation in radial strains it is necessary to examine available fatigue failure relationships.

Fatigue failure has been observed in repeated-load laboratory flexural testing of asphalt concrete beams, as evidenced by the development of cracks in the beams; and in pavements subjected to traffic loads, by alligator cracking visible at the pavement surface. For both classes of fatigue failure, the fatigue life has been expressed as a function of tensile strain. In the absence of data relating fatigue life to tensile strain for the asphalt concrete mixes that are the subject of this report,

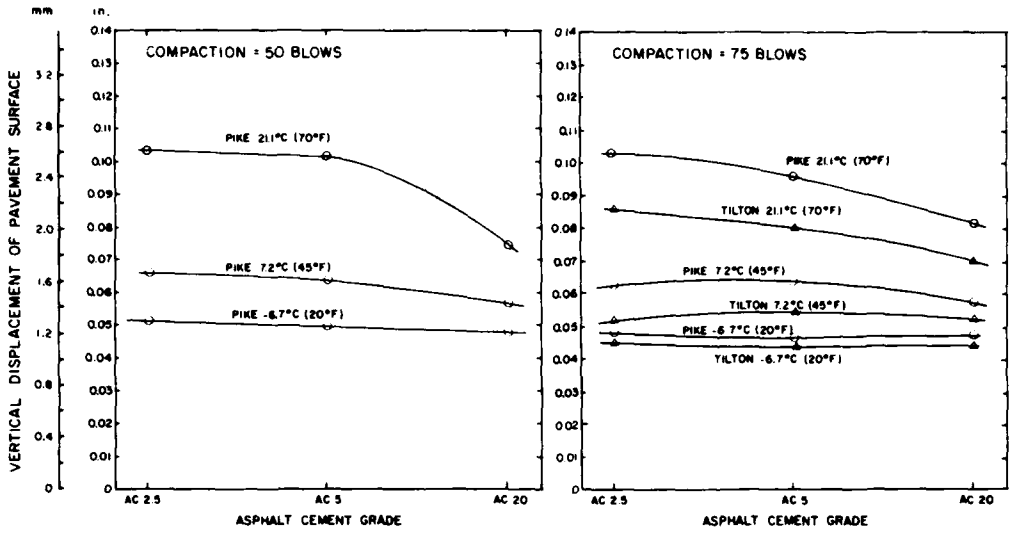

Figure 26. Effects of asphalt grade, aggregate type, and temperature on vertical displacement on pavement surface.

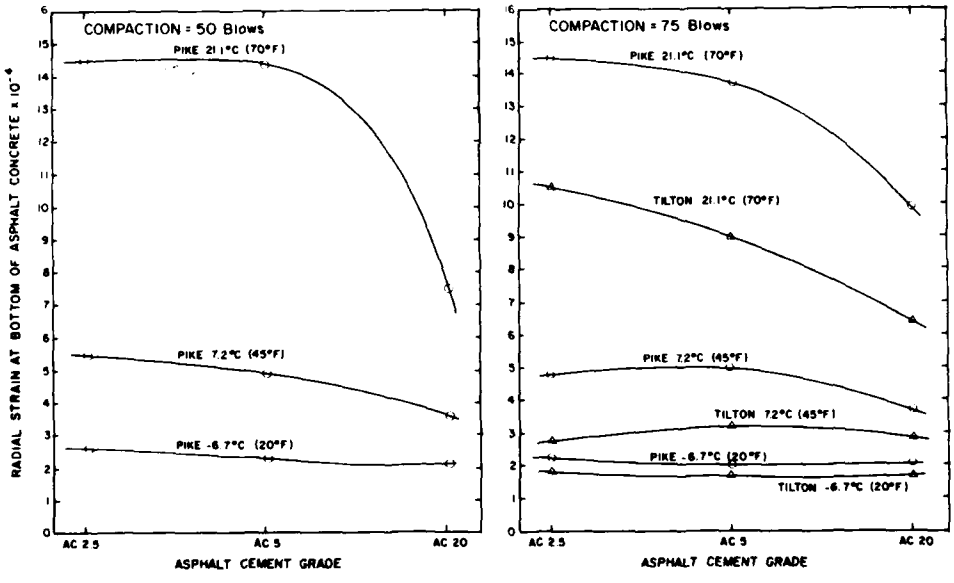

Figure 27. Effects of asphalt grade, aggregate type, and temperature on radial strain in asphalt concrete.

published fatigue data on other asphalt concrete mixes were used. Hence, the present fatigue analyses will not yield absolute values of fatigue life, but will be useful only for purposes of comparative analyses of the asphalt concrete mixtures.

Two sets of laboratory fatigue curves are shown in Figure 31;[30, 31] the first, after Heukelom and Klomp,[30] is termed by the author "provisional laboratory fatigue data," and attributed to Nijboer,[32] while the second, after Monismith and Finn,[31] is based upon laboratory controlled-stress testing of a dense-graded asphalt concrete mixture with about 5% voids. Two sets of field fatigue curves derived by Kingham[33] from the AASHO Road Test are shown in Figure 32. The first is based

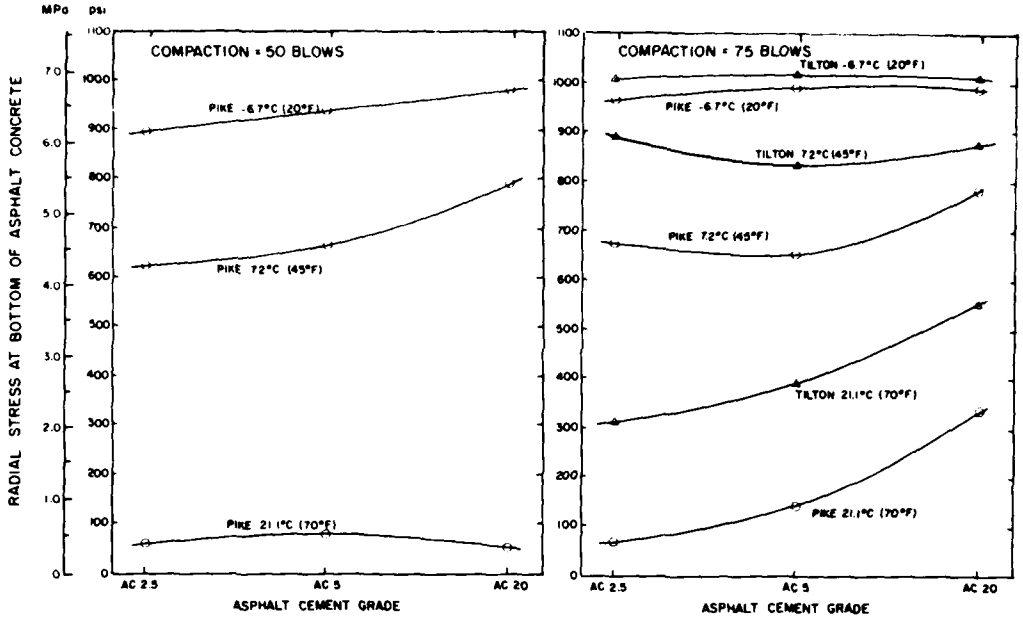

Figure 28. Effects of asphalt grade, aggregate type, and temperature on radial stress in asphalt concrete.

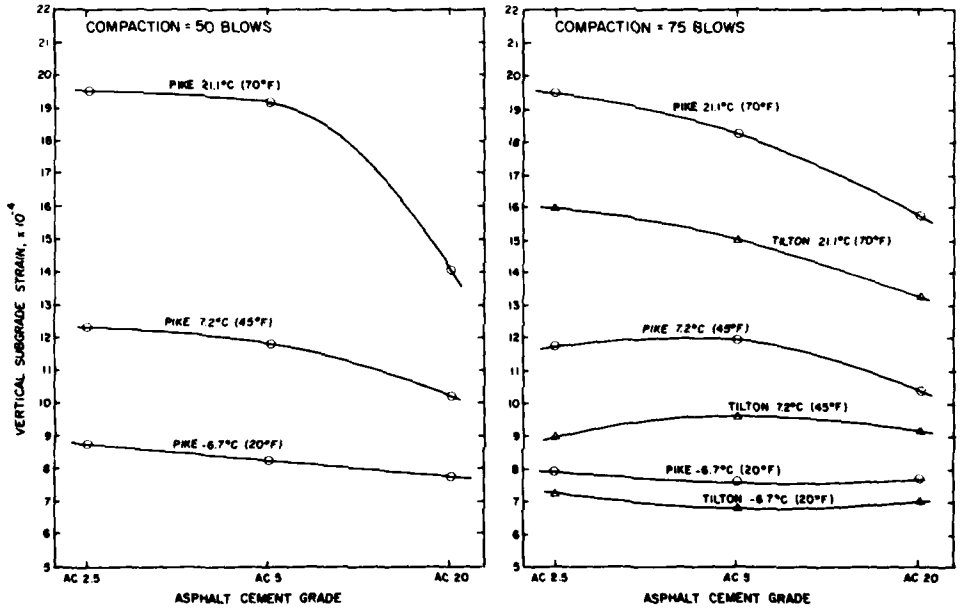

Figure 29. Effects of asphalt grade, aggregate type, and temperature on vertical subgrade strain.

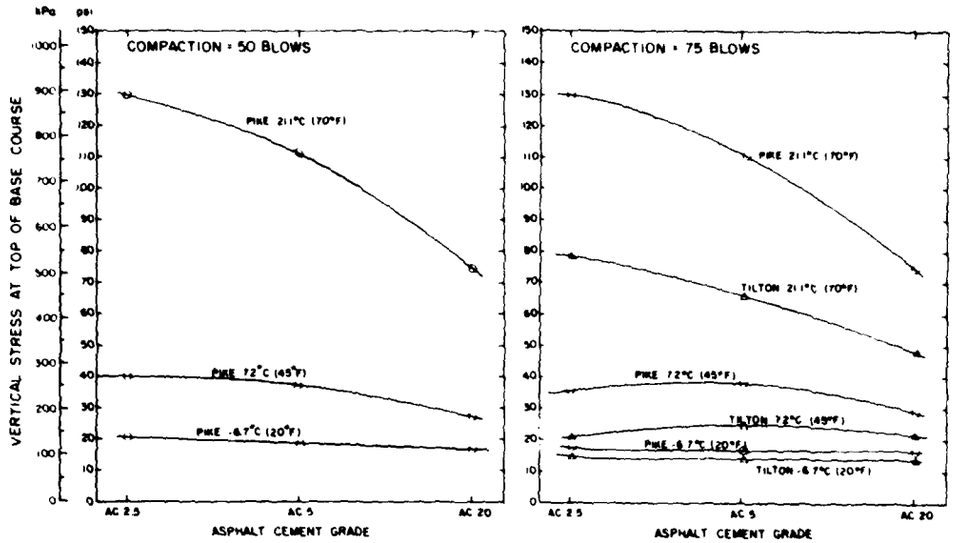

Figure 30. Effects of asphalt grade, aggregate type, and temperature on vertical stress at top of base course.

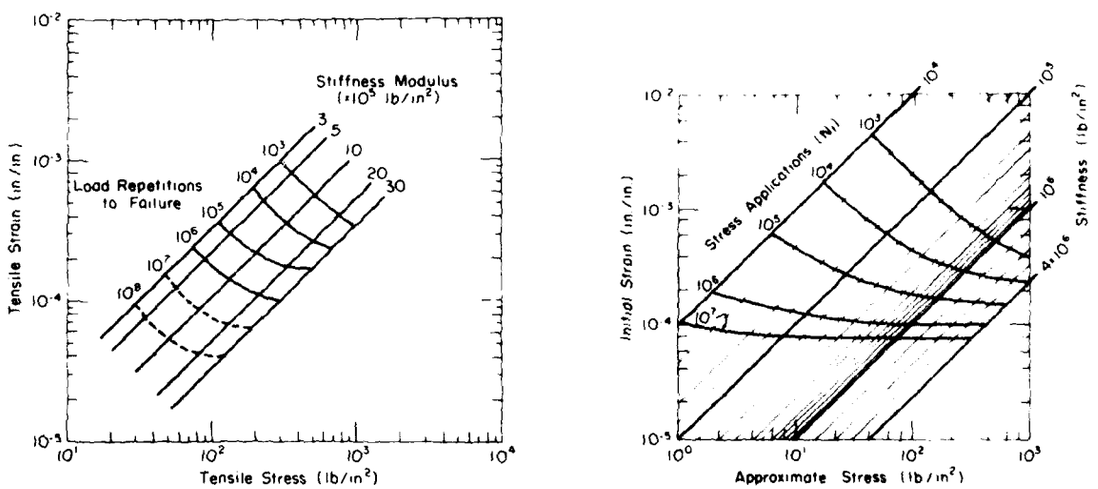

a. Provisional laboratory fatigue data, after Heukelom and Klomp[30].

b. Data from controlled-stress testing, after Monismith and Finn[31]

Figure 31. Laboratory fatigue data.

on analysis of all strain data and load repetitions throughout the period of the Road Test, including times when the subgrade was frozen. The second is based on an analysis of data that exclude the period when the subgrades were frozen.

The resilient moduli of the asphalt concrete and the radial tensile strains previously computed with the elastic layered system program were used with the four sets of fatigue curves to compute the numbers of load applications of the F-104 aircraft expected to cause 1) crack initiation of laboratory beam specimens and 2) field fatigue failure conditions. In some cases the strains and resilient moduli fell outside the limits of

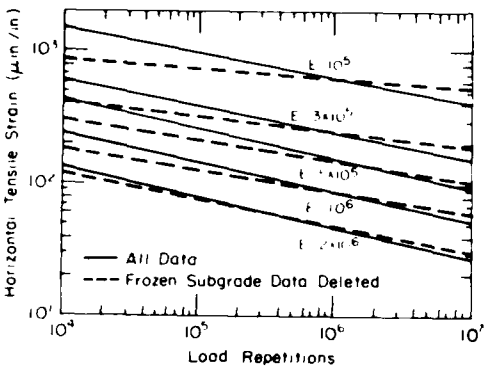

Figure 32. Field fatigue failure curves with and without data from frozen periods, after Kingham.[33]

the curves. In those cases no laboratory fatigue lives were estimated, but field fatigue lives were estimated with the equations representing the respective curves, and rounded to the nearest 100 load applications. Consequently, some of the field fatigue lives contain an element of uncertainty regarding the validity of the extrapolations beyond the limits of the curves. The calculated fatigue lives, listed in Table 10 and plotted in Figures 33 and 34, show the following results:

(1) The two sets of laboratory fatigue curves, which are derived from tests on different asphalt concrete mixes, give fatigue lives (numbers of load applications) that generally are of similar orders of magnitude for a given mix at a particular temperature.

(2) According to the laboratory fatigue curves, the fatigue life decreases with increasing temperature. There is no consistent pattern of significant change in fatigue life with asphalt viscosity grade, especially for mixes with the Tilton aggregate. For mixes with Pike aggregate at -6.7 and 7.2°C the fatigue curves of Figure 31b project higher fatigue life for mixes with AC 5 and AC 20 asphalt cements, while at 21.1°C the fatigue life is higher for mixes with AC 2.5. The fatigue life in most cases is higher for mixes with Tilton aggregate than for mixes with Pike aggregate. There is little change in fatigue life with the compactive effort used in the mixes.

(3) The two sets of field fatigue failure curves, which are based on complete or partial data sets from the AASHO Road Test, show little difference in fatigue life at -6.7°C. At higher temperatures the curves based on all data give much higher fatigue lives, ranging up to one order of magnitude higher at 7.2°C and to more than two orders of magnitude higher at 21.1°C.

(4) From both sets of field fatigue failure curves the highest fatigue life was obtained for the mix with AC 2.5 at 21.1°C. For other mixes and temperatures the curves based on all data give fatigue lives that increase with increasing temperature, while the curves based on data that omit frozen subgrades give fatigue lives that decrease with increasing temperature. There is little variation in fatigue life with asphalt viscosity grade, except that at 21.1°C the fatigue life decreases sharply with increasing viscosity grade. There is little variation in fatigue life with aggregate type at -6.7 and 7.2°C, but at 21.1°C the Pike aggregate gives much higher fatigue lives than the Tilton aggregate. There is little change in fatigue life with the compactive effort used in the mixes.

(5) For either aggregate the fatigue lives given by any of the four sets of fatigue curves show little variation with asphalt viscosity grade at -6.7 and 7.2°C. At 21.1°C the fatigue life is either about the same for different asphalt grades, as given by both sets of laboratory fatigue curves, or is much higher for softer grades, as given by the field fatigue failure curves.

The large discrepancies evident in the results given by the various sets of fatigue curves lead to some uncertainty in interpreting the results, and emphasize the importance of developing specific criteria of radial strain vs fatigue life for the particular asphalt concrete mix in question. In the present case one must choose among the various fatigue curves available from the work of others, and there is reason to give more credence to the pattern of variation of fatigue life given by the field fatigue failure curves. They are based on observed numbers of load applications to failure in relation to tensile stresses and strains developed in the asphalt concrete under actual traffic conditions. Also, the set of field fatigue failure curves based on the complete data set from the AASHO Road Test may be the more reasonable choice, among the two field fatigue curves, for application to loads applied throughout the year. According to Kingham,[33] this set of curves was selected by Witczak[34] in his development of a design procedure for airfield pavements.

Accordingly, if the fatigue lives of the various mixes given by Kingham's[33] fatigue curves for the complete data set are judged to give the most valid comparison of the mixes, one concludes that the fatigue life either is essentially equal for the three asphalt grades or is highest for AC 2.5 asphalt. Also, the portion of the total fatigue life that is expended by one load application is much higher at low and moderate temperatures (-6.7 and 7.2°C) than at higher temperature (21.1°C). This finding is reasonable in the light of the conclusion reached by Freeme and Marais[35] that, for pavements

Table 10. Estimated load applications to laboratory fatigue initiation and field fatigue failure condition.

Surface Temperature °C (°F)	Compaction (blows)	Pike aggregate AC 2.5	Pike aggregate AC 5	Pike aggregate AC 20	Tilton aggregate AC 2.5	Tilton aggregate AC 5	Tilton aggregate AC 20
-6.1 (20)	50	9000	15000	30000			
	75	30000	30000	30000	50000	100000	100000
7.2 (45)	50	3000	3000	6000			
	75	4000	3000	6000	8000	7000	8000
21.1 (70)	50	*	*	3000			
	75	*	*	1000	*	1500	3000

*Outside limit of chart.

a) Laboratory, after Heukelom and Klomp.[30]

Surface Temperature °C (°F)	Compaction (blows)	Pike aggregate AC 2.5	Pike aggregate AC 5	Pike aggregate AC 20	Tilton aggregate AC 2.5	Tilton aggregate AC 5	Tilton aggregate AC 20
-6.1 (20)	50	9000	10000	10000			
	75	11000	20000	20000	50000	80000	70000
7.2 (45)	50	1000	1100	4000			
	75	1100	1000	4000	7000	7000	7000
21.1 (70)	50	3000	3000	900			
	75	3000	2000	900	900	800	900

b) Laboratory, after Monismith and Finn.[31]

Surface Temperature, °C (°F)	Compaction (blows)	Pike aggregate AC 2.5	Pike aggregate AC 5	Pike aggregate AC 20	Tilton aggregate AC 2.5	Tilton aggregate AC 5	Tilton aggregate AC 20
-6.1 (20)	50	200	200	200			
	75	200	200	200	200	200	200
7.2 (45)	50	400	300	300			
	75	300	300	300	200	200	200
21.1 (70)	50	215,000	113,000	600			
	75	80,000	22,000	1,500	1800	1000	500

c) Field, all data, after Kingham.[33]

Surface Temperature, °C (°F)	Compaction (blows)	Pike aggregate AC 2.5	Pike aggregate AC 5	Pike aggregate AC 20	Tilton aggregate AC 2.5	Tilton aggregate AC 5	Tilton aggregate AC 20
-6.1 (20)	50	100	100	200			
	75	200	200	200	200	200	200
7.2 (45)	50	< 100	< 100	< 100			
	75	< 100	< 100	< 100	100	100	100
21.1 (70)	50	1200	300	< 100			
	75	800	< 100	< 100	< 100	< 100	< 100

d) Field, omitting frozen subgrades, after Kingham.[33]

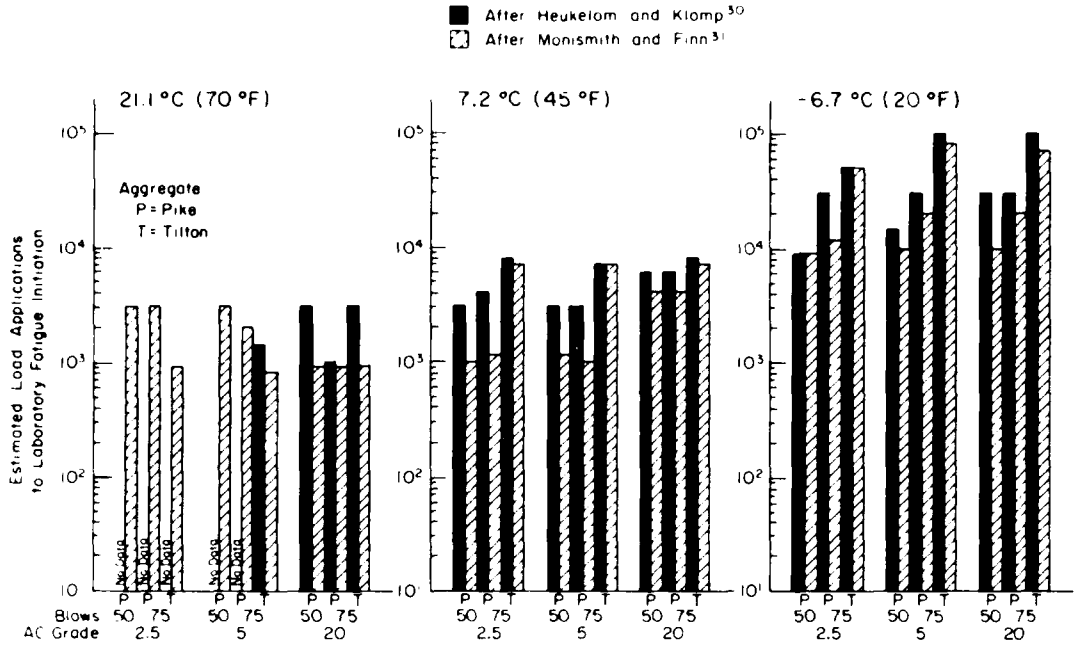

Figure 33. Estimated load applications to fatigue crack initiation in laboratory beams.

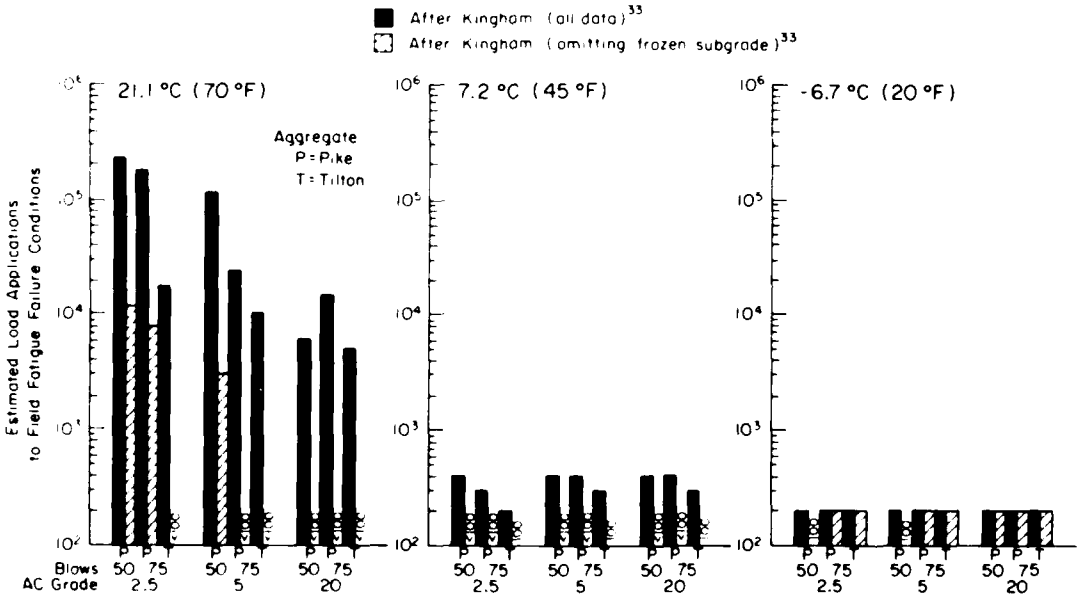

Figure 34. Estimated load applications to field fatigue failure.

with thin asphalt concrete surfaces, the fatigue life is lowest at low temperatures. But the comparative data on which it is based are perhaps exaggerated by the fact that all the radial strains were calculated from assumed constant values of resilient modulus of the base and subgrade soils. In seasonal frost areas, if the temperature of the asphalt concrete were -6.7°C, at least part of the base and subgrade would be frozen, and the much higher modulus would result in much lower radial tensile strain in the asphalt concrete. Consequently, the fatigue lives at -6.7°C would be higher than those tabulated. In spring and early summer, when the subgrade would be first thawing and then recovering from its softened condition, the moduli would be much lower and the strains much higher. Consequently, the fatigue lives for load applications during this period would be lower than those tabulated. For these reasons, the numbers of load applications to fatigue failure shown in Table 10 do not represent absolute or even realistic values of fatigue life, but are useful only for comparison of the various asphalt concrete mixes.

Rutting analysis

The rutting of airfield pavements from repeated loads results from permanent deformation of the various pavement layers and the subgrade. The vertical compressive strain at the top of the subgrade has been considered a prime factor affecting rutting. Dorman and Metcalf[36] developed strain criteria based upon elastic layered system analysis and data from the AASHO Road Test. A plot of vertical compressive strain at the top of the subgrade versus the number of load applications associated with ultimate rut depths of about 19 mm (3/4 in.)[23, 36] is shown in Figure 35.

Other researchers have developed criteria for lesser amounts of rutting.[24, 37, 38] However, the criteria of Dorman and Metcalf[36] are used herein to show the relative difference in rutting potential between the mixes.

Table 11 summarizes the estimated number of load applications to rutting failure [i.e., about 19 mm (3/4 in.)], computed with the equation given in Figure 35, based on the calculated vertical subgrade strain summarized in Table C4 (App. C). The results are plotted in Figure 36 and can be summarized as follows:

(1) Temperature of the asphalt concrete surface course has a very significant effect on the vertical compressive subgrade strain and consequently on the load applications to significant rutting. The higher the temperature, the fewer the load applications to significant rutting; this confirms a long-standing concern for the risk of rutting in pavements constructed in warmer climates. In frost areas, the vertical compressive subgrade strain would be much increased during the spring when deformability of the supporting layers for the pavement is increased. In such areas it is likely that the period of greatest rutting potential would include also the period of moderate temperatures in the spring. Data from the AASHO Road Test show that most rutting occurred during the spring and summer and none during the winter.

(2) Asphalt viscosity grade had a significant effect on rutting at the highest temperature that was analyzed. The higher the viscosity grade, the more load applications were required to cause significant rutting, indicating a need for asphalt of higher viscosity grades to be used in warmer climates.

(3) The mix with Tilton aggregate allowed more load applications to significant rutting than did the mix with Pike aggregate.

A mix parameter that has been considered to be related to rutting or permanent deformation originating in the asphalt concrete itself is the Marshall stability. This test is conducted at a temperature of 60°C (140°F), which is about the highest temperature of in-service pavements in moderate and warm climates. Some field data show that in mixes having moderate Marshall stability lower viscosity asphalt results in greater rutting. The following data were taken from the Utah experimental road test:[39]

Asphalt cement used in mix	*Mean rutting (12 mos.)*	*Marshall stability*, 60°C*
AC 6	3.5 mm (0.14 in.)	4.45 kN (1000 lb)
AC 12	2.1 mm (0.08 in.)	5.34 kN (1200 lb)

*Stability of cores at 12 months.

In view of data such as these, the Marshall stabilities of the various mixes analyzed in this report were examined in relation to possible rutting. The Marshall stability for each of the mixes is shown in Figure 7. These data show that the higher the asphalt viscosity grade, the higher the Marshall stability, with the one exception that AC 5 asphalt cement gives higher stability than AC 20 with Pike aggregate at 50 blows. For 75-blow compaction, and including both Pike and Tilton aggregates, the following mean stabilities are obtained:

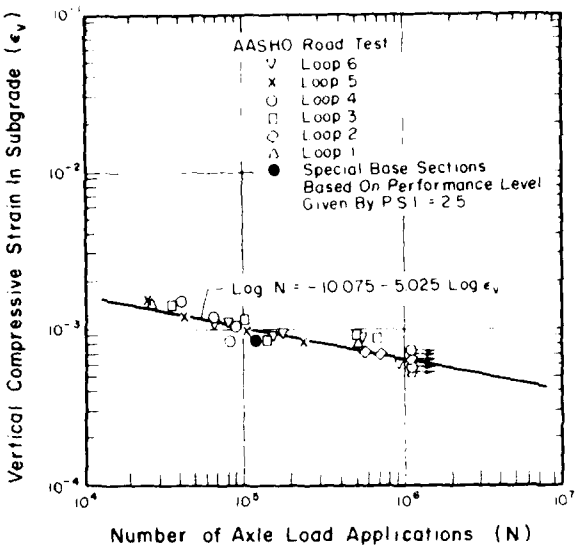

Figure 35. Relation between vertical subgrade strain and number of load applications to rutting failure, from Dorman and Metcalf.[36]

Table 11. Estimated load applications to rutting failure [Rut depth = 19 mm (3/4 in.)]

Surface Temperature, °C (°F)	Compaction (blows)	Pike Aggregate AC 2.5	Pike Aggregate AC 5	Pike Aggregate AC 20	Tilton Aggregate AC 2.5	Tilton Aggregate AC 5	Tilton Aggregate AC 20
-6.7 (20)	50	195,618	269,417	362,307			
	75	331,097	397,110	397,110	513,867	704,808	654,814
7.2 (45)	50	34,623	43,162	89,202			
	75	44,852	40,342	82,510	174,618	118,984	154,559
21.1 (70)	50	3,452	3,741	18,046			
	75	3,056	4,920	10,300	9,396	12,734	24,222

Log N = -10.075-5.025 log ϵ_v.
N = Load Applications.
ϵ_v = Vertical Compressive Strain on Subgrade (from Table C4, App. C).

Asphalt cement grade	Marshall stability	Ratio to AC 2.5
AC 2.5	7.78 kN (1750 lb)	1.00
AC 5	9.34 kN (2100 lb)	1.20
AC 20	13.03 kN (2930 lb)	1.67

Although the AC 20 grade, giving the highest stability, would be expected to have less rutting potential than the AC 2.5 or AC 5, the stabilities given by all three grades are so high as to eliminate rutting originating in the asphalt concrete as a significant consideration.

STRENGTH CORRELATIONS

A study was completed to determine if there was a correlation between Marshall stability, indirect tensile strength, and modulus of resilience for the various mixes. F tests were performed to determine whether correlations existed at a significance level of 5 percent ($\alpha = 0.05$). It was found that there was no significant correlation ($\alpha = 0.05$) between Marshall stability and modulus of resilience. However, there was significant correlation ($\alpha = 0.05$) between Marshall stability and indirect tensile strength at moderate and higher temperatures. Significant linear correlation was found

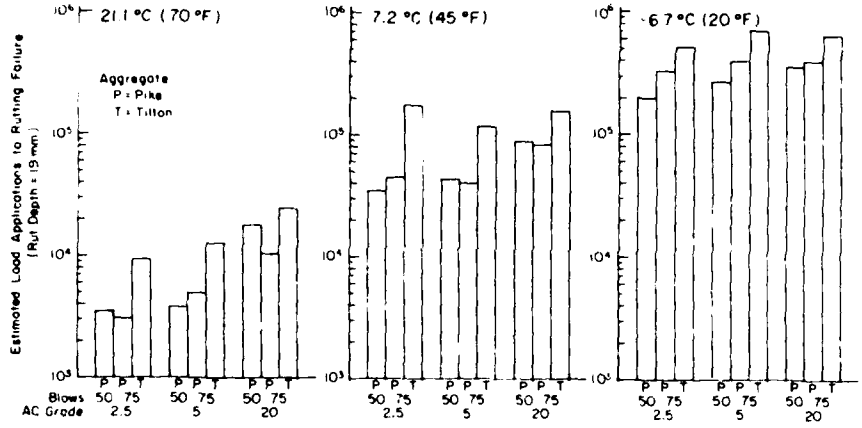

Figure 36. Estimated load applications to rutting failure.

between indirect tensile strength and resilient modulus, but the correlation is not considered useful because of excessive scatter in the data.

Marshall stability and indirect tensile strength

Figure 37 shows the linear regression correlations between Marshall stability and indirect tensile strength for asphalt mixes using Pike and Tilton aggregates. The correlation was influenced by test temperature and by the loading rate used in the indirect tensile strength determination. A significant correlation ($\alpha \leq 0.05$) was found between Marshall stability and indirect tensile strength at 4.4°C and 21.1°C. But the correlation with indirect tensile strength at -23.3°C was not significant ($\alpha > 0.05$).

Indirect tensile strength and resilient modulus

There was no significant linear correlation ($\alpha > 0.05$) between indirect tensile strength and resilient modulus at a specified temperature and rate of loading. While there was significant linear correlation ($\alpha \leq 0.05$) when comparing all data regardless of test temperature and loading rates (Fig. 38), the correlation is not considered useful because of excessive scatter in the data.

Summary

In summary, there would generally appear to be significant correlation ($\alpha \leq 0.05$) between Marshall stability and indirect tensile strength. Acceptable linear correlation was not found between either of these properties and resilient modulus.

SUMMARY AND CONCLUSIONS

Recapitulation of investigations

A comprehensive analysis was conducted to predict and compare the thermal cracking and aircraft-load-associated distress in pavements with surface courses consisting of one of several asphalt concrete mixtures. Marshall, Brazil, and modulus of resilience test data were analyzed and correlations were determined.

Asphalt mix design behavior at low temperatures was analyzed over a 10-year period. Stiffness history and projected thermal cracking were determined at various depths for the different mixes.

The behavior of the mixes in a typical pavement system was analyzed using the layered elastic system program. Both fatigue damage and rutting analyses were conducted for the various asphalt concrete mixes.

Summary of results

Temperature was found to have considerable influence on the properties of the asphalt concrete mixes studied. The Marshall stability of the mixes increased as the asphalt viscosity grade increased from AC 2.5 to AC 20, but the stability of all the mixes was so high as to preclude concern for pavement distress dependent upon this test property. The optimum asphalt content of the mixes decreased with viscosity increase. For a given asphalt viscosity and compactive effort, the mean Marshall stabilities of the mixes with Pike aggregate were higher than those of mixes with Tilton aggregate. Mixes compacted at 75 blows generally displayed higher stability than those compacted at 50 blows.

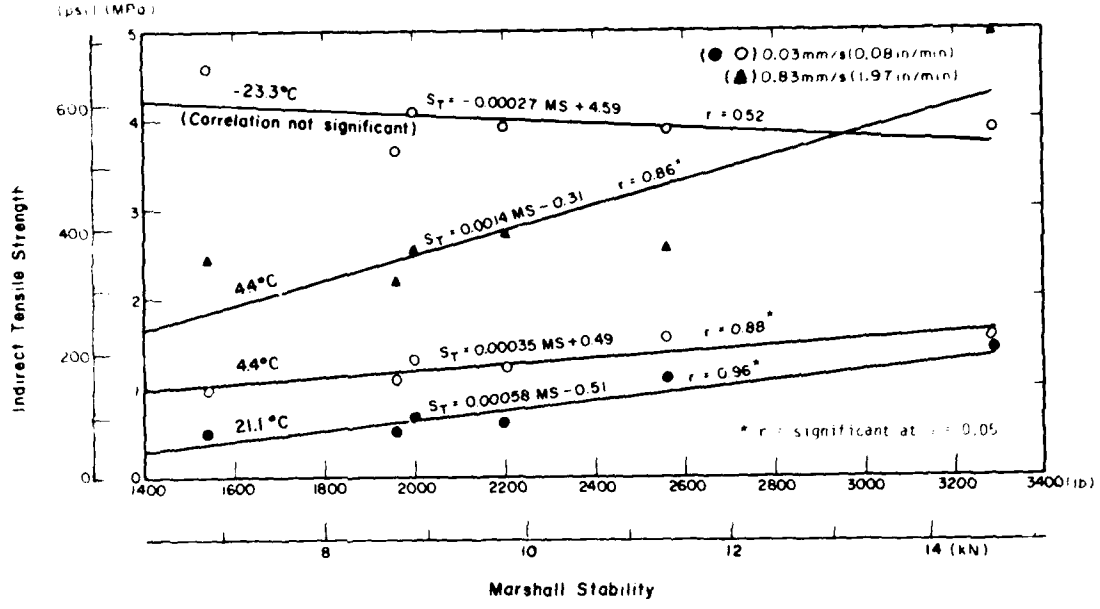

Figure 37. Correlation between Marshall stability and indirect tensile strength. Note: Regression equations refer to tensile strength (S_T) in MPa and Marshall stability (MS) in lb.

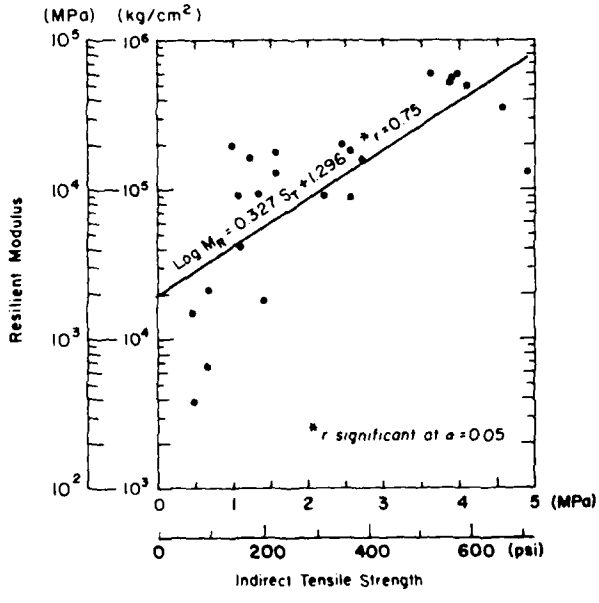

Figure 38. Correlation between indirect tensile strength and resilient modulus. Note: Regression equation refers to resilient modulus (M_r) in kg/cm² and tensile strength (S_T) in MPa.

The tensile strength of the mixes increased as the asphalt viscosity increased, except that at temperatures below about -10°C the strengths of all the mixes tended to be similar. However, both the tensile strain and vertical deformation at failure were less for the higher viscosity grades than for the lower viscosity grades. Temperatures had substantial influence on the strength parameters. The tensile strength decreased and the tensile strain and vertical deformation increased as temperature increased. Aggregate source did not have a substantial influence on the strength parameters. At the one test temperature at which pertinent data were obtained, there was evidence that loading rate influenced the tensile strength of the asphalt mixes; the higher tensile strengths were obtained at the faster rates of loading.

The resilient modulus of the mixes generally increased as the viscosity grade increased, particularly at the highest test temperatures. At lower temperatures (below 0°C), the resilient modulus was not always higher for the mixture containing the more viscous asphalt. The higher compactive effort (75 blows as compared with 50 blows) resulted in about a 15% increase in resilient modulus for mixes with Pike aggregate. Mixes with Tilton aggregate displayed a higher resilient modulus than those with Pike aggregate at the higher temperatures (greater than 0°C). The resilient moduli of mixes with the two aggregates differed less at temperatures below 0°C.

The susceptibility of the various mix designs to thermal cracking was studied in detail. Studies were conducted for climatic zones defined as cold, moderate and warm. The most severe thermal cracking was predicted for the cold climate represented by central Alaska. In this climatic zone the average annual air temperature is low and the average annual range of air temperature is very broad. A study of asphalt mix stiffness estimated in relation to temperature, asphalt penetration and softening point, volume concentration of aggregate, and thin-film oven tests indicated that the mixture stiffness generally increases with age and with increase in asphalt viscosity grade. Stiffness changes with age and asphalt viscosity were not greatly influenced by the aggregate type used in the mix. The total thermal cracking predicted to develop after a 10-year period was generally greatest for the mixes with AC 20 asphalt cement at both the surface and at the 50.8-mm (2-in.) depth. Mixes with the AC 2.5 asphalt cement displayed the least amount of thermal cracking. Mixes using the AC 5 asphalt cement displayed thermal cracking intermediate between the mixes using AC 2.5 and AC 20.

Analysis of fatigue damage that would be experienced in each of the mixtures when incorporated in a pavement subjected to aircraft traffic, based on field fatigue failure criteria developed for the asphalt concrete pavement at the AASHO Road Test, showed that fatigue damage under each load application would be most severe at low temperatures. The analysis also showed that the fatigue damage would be essentially equal for the three asphalt grades, except at the highest test temperature (21.1°C), which shows far better performance for the mixes with the softer grades of asphalt. The fatigue performance of the mixes with Pike aggregate is about the same as that of mixes with Tilton aggregate at -6.7°C and 7.2°C, and far better than that of mixes with Tilton aggregate at 21.1°C. Mixes compacted at 50 blows displayed better fatigue performance, at high temperature, than mixes compacted at 75 blows, while performance of mixes designed at the two levels of compaction was about the same at low temperature.

It is again emphasized that no fatigue testing was performed, and that the analyses of fatigue performance are based upon relationships among tensile strain, stiffness modulus, and fatigue life developed for other asphalt-aggregate mixtures. Hence a high degree of confidence in the results is not justified. Fatigue testing of the actual mixtures that were analyzed would be needed to reach definitive conclusions regarding the projected fatigue life of each mix for each climatic zone. The large seasonal variations in subgrade resilient modulus also should be included in a more definitive analysis.

It was found that rutting damage would be most severe in warmer climates for the mixes analyzed. The number of load applications to cause significant rutting generally increased somewhat as the asphalt grade used in the mix increased from AC 2.5 to AC 20, and the increase became more significant as the temperature increased. Compared with mixes containing Pike aggregate, the higher resilient modulus of mixes using the Tilton aggregate resulted in lower vertical strain on the subgrade and hence better performance in relation to rutting potential. Also, mixes compacted at 75 blows displayed less rutting potential than mixes compacted at 50 blows.

Correlation studies indicated that Marshall stability was significantly related ($\alpha \leq 0.05$) to indirect tensile strength at moderate and higher temperatures. Acceptable linear correlations between Marshall stability and resilient modulus, and between indirect tensile strength and resilient modulus, were not evident.

Conclusions

Conclusions concerning the asphalt concrete mixes that were analyzed are as follows.

1. Well designed asphalt concrete mixes using AC 2.5 asphalt similar to that tested and described here should perform satisfactorily in cold climates.

2. Mixes using AC 5 asphalt similar to that described here showed little susceptibility to thermal cracking in the moderate climate, while mixes using the AC 20 asphalt showed negligible thermal cracking in the warm climate that was studied.

3. Although the Marshall stabilities of mixtures with AC 2.5 and AC 5 asphalts are excellent, their lower resilient moduli at moderately high temperatures could lead to unacceptable rutting originating in the subgrades of pavements constructed in warm climate. Use of the harder AC 20 asphalt would give better rutting performance, but it is subject to moderate to severe thermal cracking. As rutting is considered to be the more detrimental of these two distress modes, it is believed the compromise choice of asphalt for use in warm climate would have to favor the harder grade.

4. Asphalt concrete mixes using the Tilton aggregates may be expected to exhibit less rutting potential than mixes using the Pike aggregates.

5. Mixes compacted at 75 blows generally displayed higher Marshall stabilities and resilient moduli than mixes compacted at 50 blows, but there was little difference in the projected susceptibility to fatigue and rutting distress.

6. Marshall stability may be significantly related to indirect tensile strength at $\alpha = 0.05$.

LITERATURE CITED

1. Johnson, T.C., R.L. Berg, K.L. Carey, and C.W. Kaplar (1975) Roadway design in seasonal frost areas. U.S. Army Cold Regions Research and Engineering Laboratory Translation 259; and Transportation Research Board Synthesis of Highway Practice No. 26.
2. Vedros, P.J. (1973) Condition survey, Minot Air Force Base, North Dakota. U.S. Army Engineer Waterways Experiment station, Miscellaneous Paper S-73-23.
3. Jackson, R.D. (1973) Condition survey, Loring Air Force Base, Maine. USAE WES, Miscellaneous Paper 3-73-51.
4. Vedros, P.J. and H.J. Thornton (1973) Condition survey, Grand Forks Air Force Base, North Dakato. USAE WES, MP S-73-42.
5. Shahin, M.Y. (1972) Prediction of low temperature and thermal fatigue cracking in flexible pavements. Thesis, University of Texas.
6. Haas, R.C.G. (1973) A method for designing asphalt pavements to minimize low-temperature shrinkage cracking. The Asphalt Institute, Research Report RR-73-1.
7. Department of the Army, Office of the Chief of Engineers (1976) Selecting and specifying asphalt cements. Engineer Technical Letter ETL 1110-1-83.
8. McLeod, N.W. (1976) Asphalt cements: Pen-Vis number and its application to moduli of stiffness. *ASTM Journal of Testing and Evaluation*, vol. 4, no. 4.
9. Headquarters, Department of the Army (1971) Technical Manual, Bituminuous Pavements Standard Practice. TM 5-822-8.
10. Gonzalez, G., T.W. Kennedy, and J.N. Anagnos (1975) Evaluation of the resilient elastic characteristics of asphalt mixtures using the indirect tensile test. University of Texas, Research Report 183-6.
11. Christison, J.T., D.W. Murray and K.D. Anderson (1972) Stress prediction and low temperature fracture susceptibility of asphaltic concrete pavments. *Proceedings, Association of Asphalt Paving Technologists*, vol. 41.
12. Schmidt, R.J. (1972) A practical method for measuring the resilient modulus of asphalt-treated mixes. Highway Research Board, Highway Research Record no. 404.
13. Darter, M.I., R. Vokac, J.E. Fitzgerald and T.I. Lai (1969) Use of synthetic rubber-in-asphalt pavement to determine mixture behavior, pavement performance and thermorheologic properties. Utah Department of Transportation, Interim Report.
14. Schmidt, R.J. and P.E. Graft (1972) The effect of water on the resilient modulus of asphalt treated mixes. *Proceedings Association of Asphalt Paving Technologists*, vol. 41, p. 118-162.
15. Hadley, W.O., W.J. Hudson, and T.W. Kennedy (1971) Evaluation and prediction of the tensile properties of asphalt-treated materials. University of Texas, Research Report No. 98-9.
16. Pavement and Materials Group, Department of Civil Engineering, University of Illinois. Layered elastic system program for pavement analysis and design. (Undated)
17. Headquarters, Department of the Army (1969) Technical Manual, Airfield Flexible Pavements. TM 5-824-2; AFM 88-6, Chapter 2.
18. Allen, J.J. and M.R. Thompson (1974) Resilient response of granular materials subjected to time-dependent lateral stress. Transportation Research Board, Transportation Research Record No. 510.
19. Witczak, M.W. (1974) Structural evaluation and overlay design methodology of airfield pavements: State of the art. Federal Highway Administration, Report No. FHWA-RD-74-60.
20. Deacon, J.A. (1973) Fatigue life prediction. Highway Research Board, Special Report 140.
21. Witczak, M.W. (1973) Fatigue subsystem solution for asphalt concrete airfield pavements. Highway Research Board, Special Report 140.
22. Darter, M.I. and E.J. Barenberg (1976) Zero maintenance pavement: Results of field studies on the performance requirements and capabilities of conventional pavement systems. Federal Highway Administration, Report No. FHWA-RD-105.
23. Monismith, C.L. (1976) Rutting prediction in asphalt concrete pavements. Transportation Research Board, Transportation Research Board, Report No. 616.
24. Saraf, C.L., W.S. Smith, and F.N. Finn (1976) Rut depth prediction. Transportation Research Board, Transportation Research Board, Report No. 616.
25. Chan, Y.T. (1976) Analysis of subgrade rutting in flexible airfield pavements. Transportation Research Board, Transportation Research Board, Report No. 616.

26. Shahin, M.Y., M.I. Darter, and S.D. Kohn (1976) Development of a pavement maintenance management system. Vol. II - Airfield Pavement Distress Identification Manual. U.S. Air Force C.E.C., Technical Report No. AFCEC-TR-76-27.
27. Deacon, J.A. (1973) Fatigue life prediction. Highway Research Board, Special Report 140.
28. Witczak, M.W. (1973) Fatigue subsystem solution for asphalt concrete airfield pavements. Highway Research Board, Special Report 140.
29. Darter, M.I. and E.J. Barenberg (1976) Zero maintenance pavement: Results of field studies on the performance requirements and capabilities of conventional pavement systems. Federal Highway Administration, Report No. FHWA-RD-105.
30. Heukelom, W. and A.J.G. Klomp (1962) Dynamic testing as a means of controlling pavements during and after construction. *Proceedings, International Conference on the Structural Design of Asphalt Pavements*, University of Michigan.
31. Monismith, C.L. and F.N. Finn (1975) Flexible pavement design: A state of the art–1975. *Proceedings ASCE Specialty Conference on Pavement Design for Practicing Engineers*, Georgia Inst. of Tech., Atlanta Georgia.
32. Nijboer, L.W. (1960) *Strasse und Verkehr*. vol. 46, p. 515.
33. Kingham, R.I. (1972) Failure criteria developed from AASHO Road Test data. *Proceedings, Third International Conference on the Structural Design of Asphalt Pavements*, University of Michigan.
34. Witczak, M.W. (1972) Design of full-depth asphalt airfield pavements. *Proceedings, Third International Conference on the Structural Design of Asphalt Pavements*, University of Michigan.
35. Freeme, C.R. and C.P. Marais (1973) Thin bituminous surfaces: Their fatigue behavior and prediction. Transportation Research Board, Special Report 140.
36. Dorman, G.M. and C.T. Metcalf (1965) Design curves for flexible pavements based on a layered system theory. Highway Research Board, Highway Research Report No. 71.
37. Monismith, C.L., D.B. McLean, and N. Ogawa (1973) Design considerations for asphalt pavements. Department of Civil Engineering, University of California, Report 73-5.
38. Hicks, R.G. and F.N. Finn (1974) Prediction of pavement performance from calculated stresses and strains at the San Diego Test Road. *Proceedings AAPT*.
39. Lai, J.R., M.I. Darter, and R. Volcoe (1971) Trends of pavement characteristics during 12 months of a designed experiment. Highway Research Board, Special Report 116.

APPENDIX A: ASPHALT-AGGREGATE MIXTURE PROPERTIES BY MARSHALL METHOD

Table A1. Percentage of asphalt* obtained at peak stability, and by established criteria for air voids, and voids filled.

Asphalt grade/ Compaction		*Peak stability*	*5% Air voids*	*75 blows 60% voids filled*	*50 blows 70% voids filled*	*Average*
			Pike aggregate			
AC 2.5	50 blows	5.5	5.1		5.0	5.2
	75 blows	4.9	5.0	4.2		4.7
AC 5	50 blows	4.5	4.6	--	4.8	4.6
	75 blows	4.5	5.0	4.4		4.6
AC 20	50 blows	4.5	4.8		5.0	4.8
	75 blows	4.1	4.3	3.9	--	4.1
			Tilton aggregate			
AC 2.5	75 blows	5.7	5.6	4.7	--	5.3
AC 5	75 blows	4.2	4.9	4.2	--	4.4
AC 20	75 blows	4.0	4.7	4.2	--	4.3

*Percent asphalt by weight of dry aggregate.

BITUMINOUS MIX CURVES — Pike Aggregate — DATE: June 1976

PROJECT: Stiffness and Fracture of Asphalt Concrete — JOB: AC-2.5 50-blow — Replotted 9/77

RECAP OF MARSHALL TEST RESULTS

PERCENT BITUMEN CONTENT By wt of agg	3.5	4.0	4.5	5.0	5.5 / 6.0
UNIT WEIGHT AGGREGATE ONLY					
UNIT WEIGHT TOTAL MIX	148.7	150.1	152.3	152.0	154.0 / 153.8
STABILITY	1022	1091	1282	1378	1800 / 1434
FLOW	10.3	8.0	9.5	9.0	10.8 / 13.4
PERCENT VOIDS AGGREGATE ONLY					
PERCENT VOIDS TOTAL MIX	9.7	8.1	6.0	5.6	3.7 / 3.1
PERCENT OF TOTAL VOIDS FILLED WITH BITUMEN	43.7	52.4	62.8	66.7	77.1 / 81.1

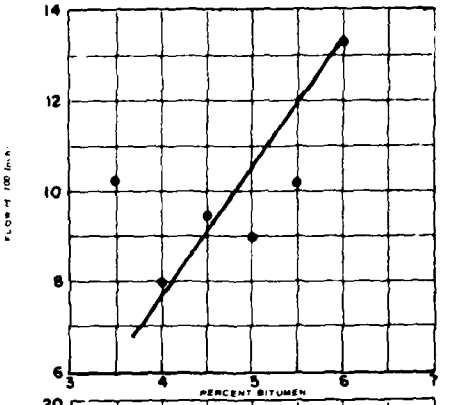

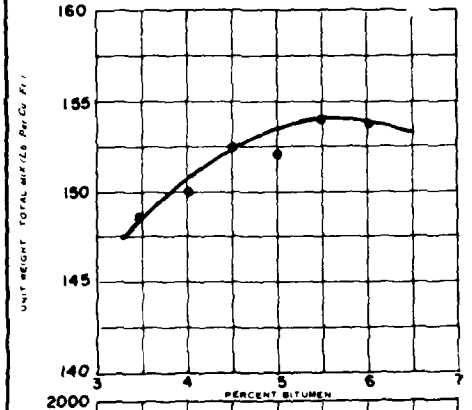

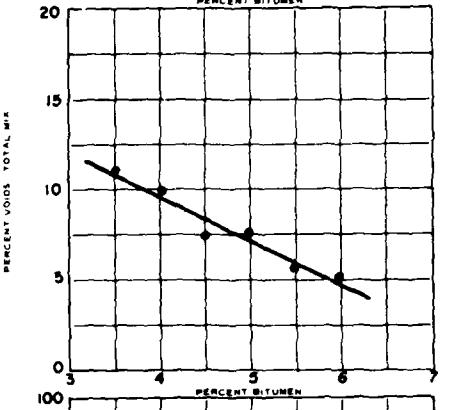

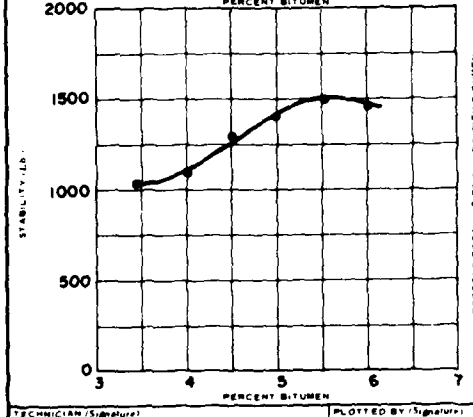

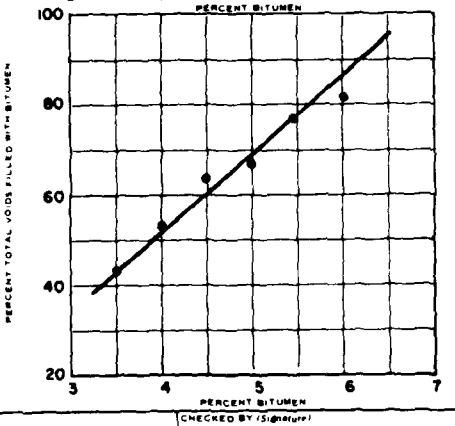

TECHNICIAN (Signature) | PLOTTED BY (Signature) | CHECKED BY (Signature)

DD FORM 1 DEC 68 1219 — PREVIOUS EDITION OF THIS FORM IS OBSOLETE

BITUMINOUS MIX CURVES Tilton Aggregate

DATE: 19 April 1977

PROJECT: Stiffness and Fracture of Asphalt Concrete

JOB: AC-2.5 75-blow

Replotted 9/77

RECAP OF MARSHALL TEST RESULTS

PERCENT BITUMEN CONTENT by wt of agg	3.6	4.2	4.7	5.3	5.8 / 6.4
UNIT WEIGHT AGGREGATE ONLY					
UNIT WEIGHT TOTAL MIX	146.2	147.1	147.6	149.1	149.6 / 150.6
STABILITY	1322	1124	1399	1383	1396 / 1477
FLOW	11.5	11.8	12.3	12.8	11.4 / 12.8
PERCENT VOIDS AGGREGATE ONLY					
PERCENT VOIDS TOTAL MIX	9.6	8.3	7.3	5.6	4.6 / 3.2
PERCENT OF TOTAL VOIDS FILLED WITH BITUMEN	45.2	52.7	58.5	67.6	73.3 / 81.4

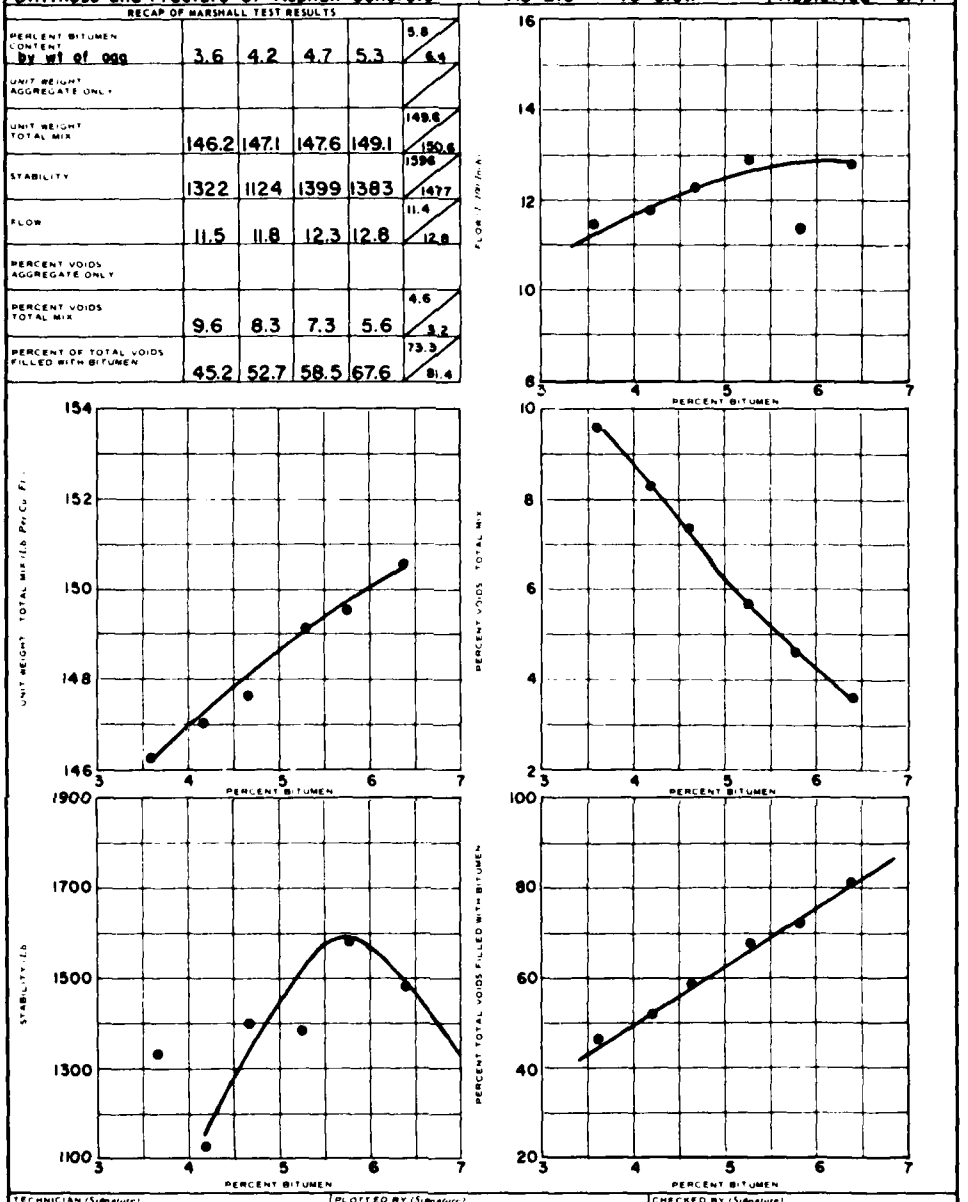

TECHNICIAN (Signature) | PLOTTED BY (Signature) | CHECKED BY (Signature)

DD FORM 1219 PREVIOUS EDITION OF THIS FORM IS OBSOLETE

BITUMINOUS MIX CURVES Pike Aggregate — June 1976

Stiffness and Fracture of Asphalt Concrete — AC-5 50-blow — Replotted 9/77

RECAP OF MARSHALL TEST RESULTS

PERCENT BITUMEN by wt of agg	3.5	4.0	4.5	5.0	5.5 / 6.0
	151.2	153.2	153.6	154.1	154.6 / 154.2
	1345	1914	2374	2211	1990 / 1493
	9.3	9.2	10.3	12.0	14.0 / 18.0
PERCENT VOIDS TOTAL MIX	8.3	6.4	5.5	4.5	3.1 / 3.2
PERCENT OF TOTAL VOIDS FILLED WITH BITUMEN	48.3	58.2	64.7	71.2	80.3 / 80.7

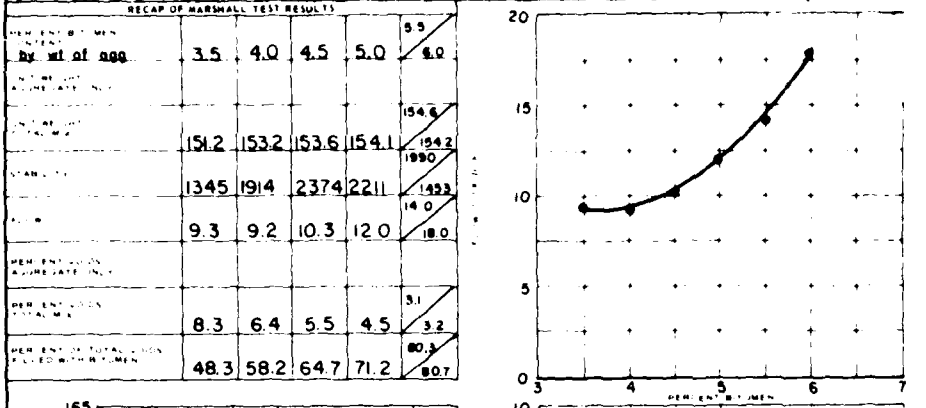

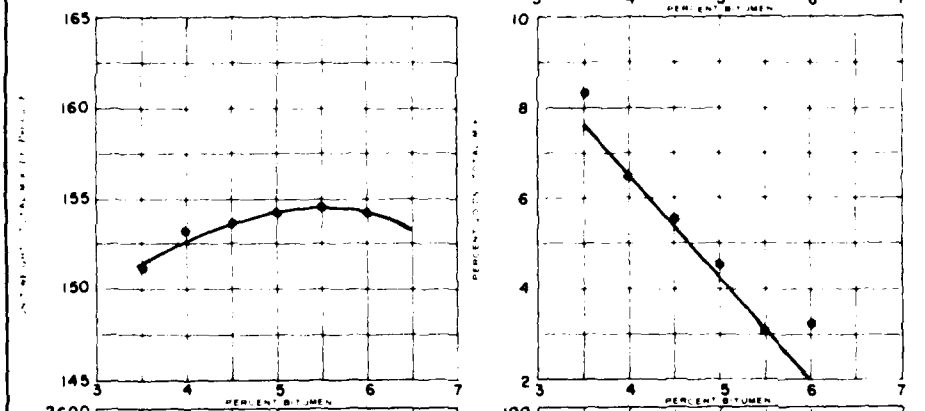

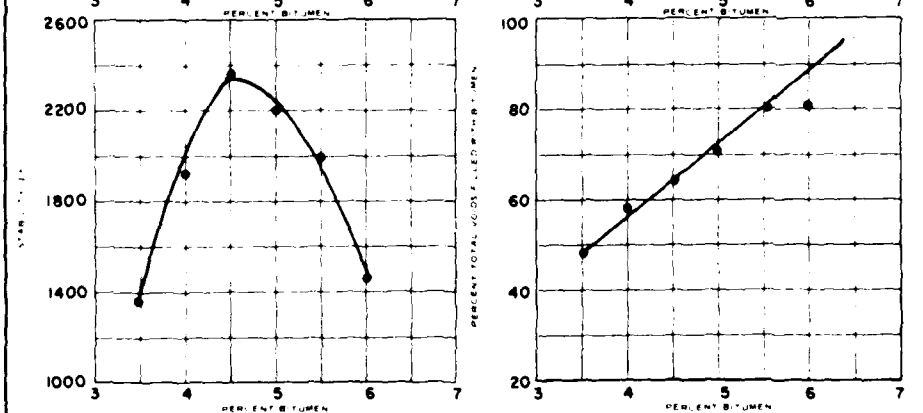

PLOTTED BY — CHECKED BY

DD FORM 1219 PREVIOUS EDITION OF THIS FORM IS OBSOLETE

BITUMINOUS MIX CURVES — Pike Aggregate — June 1976

Stiffness and Fracture of Asphalt Concrete — AC-2.5 75-blow — Replotted 9/77

RECAP OF MARSHALL TEST RESULTS

Percent Bitumen by wt of agg	3.5	4.0	4.5	5.0	5.5
Unit Wt Aggregate Only					
Unit Wt Total Mix	151.1	151.4	152.4	152.4	152.8
Stability	1391	1394	1930	1962	1592
Flow	7.8	9.3	8.3	9.5	11.3
Percent Voids Aggregate Only					
Percent Voids Total Mix	8.3	7.4	6.0	5.4	4.5
Percent of Total Voids Filled with Bitumen	48.9	55.0	62.8	67.7	73.5

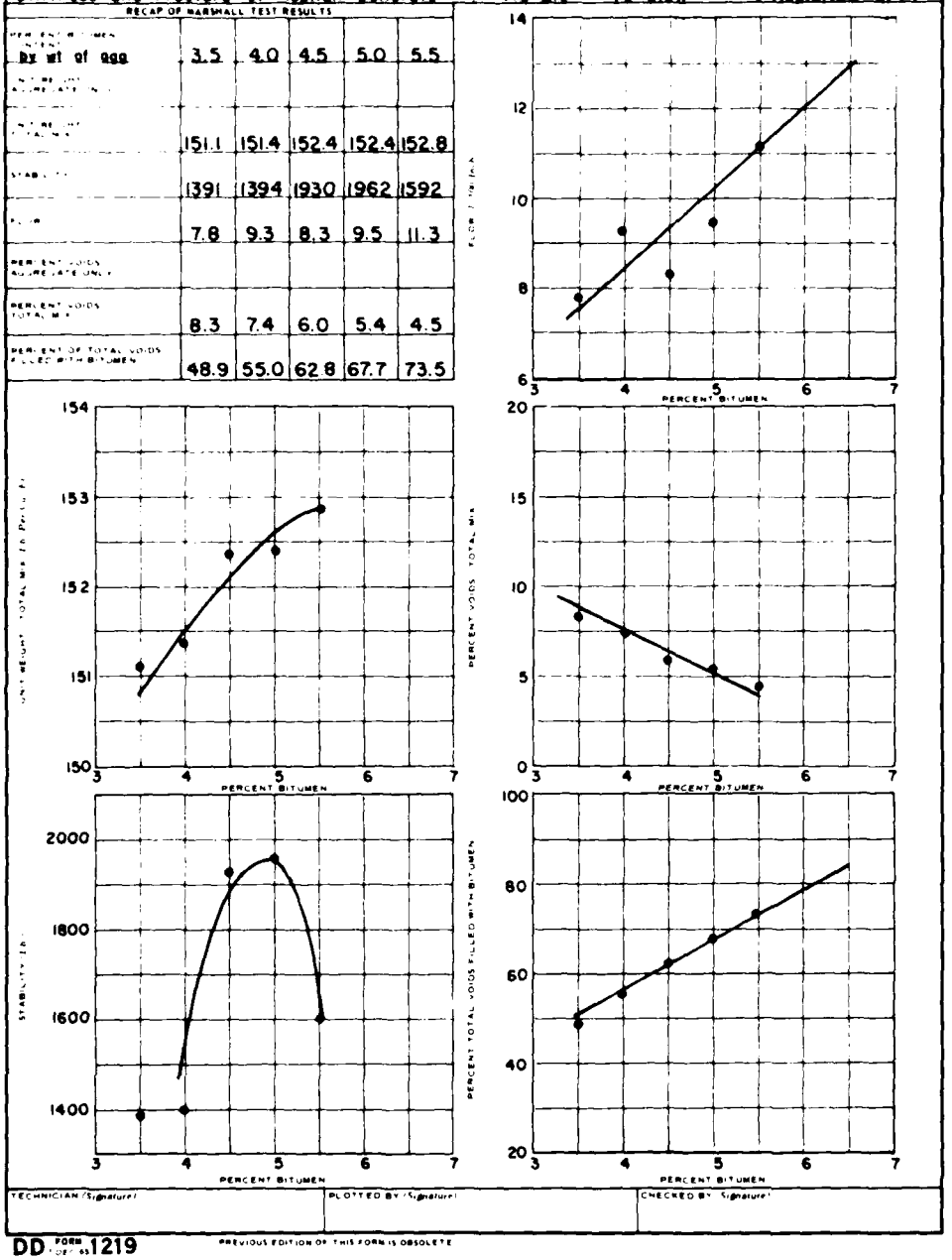

TECHNICIAN (Signature) | PLOTTED BY (Signature) | CHECKED BY (Signature)

DD FORM 1219 — PREVIOUS EDITION OF THIS FORM IS OBSOLETE

BITUMINOUS MIX CURVES Pike Aggregate June 1976

Stiffness and Fracture of Asphalt Concrete AC-5 75-blow Replotted 9/77

RECAP OF MARSHALL TEST RESULTS

PERCENT BITUMEN CONTENT By wt of Agg	3.5	4.0	4.5	5.0	5.5
UNIT WEIGHT AGGREGATE ONLY					
UNIT WEIGHT TOTAL MIX	151.1	149.2	154.9	151.0	153.7
STABILITY	1726	1329	2012	1588	1961
FLOW	9.3	9.0	9.0	6.8	11
PERCENT VOIDS AGGREGATE ONLY					
PERCENT VOIDS TOTAL MIX	8.4	8.9	4.7	6.5	4.0
PERCENT OF TOTAL VOIDS FILLED WITH BITUMEN	47.8	49.6	68.3	62.9	75.6

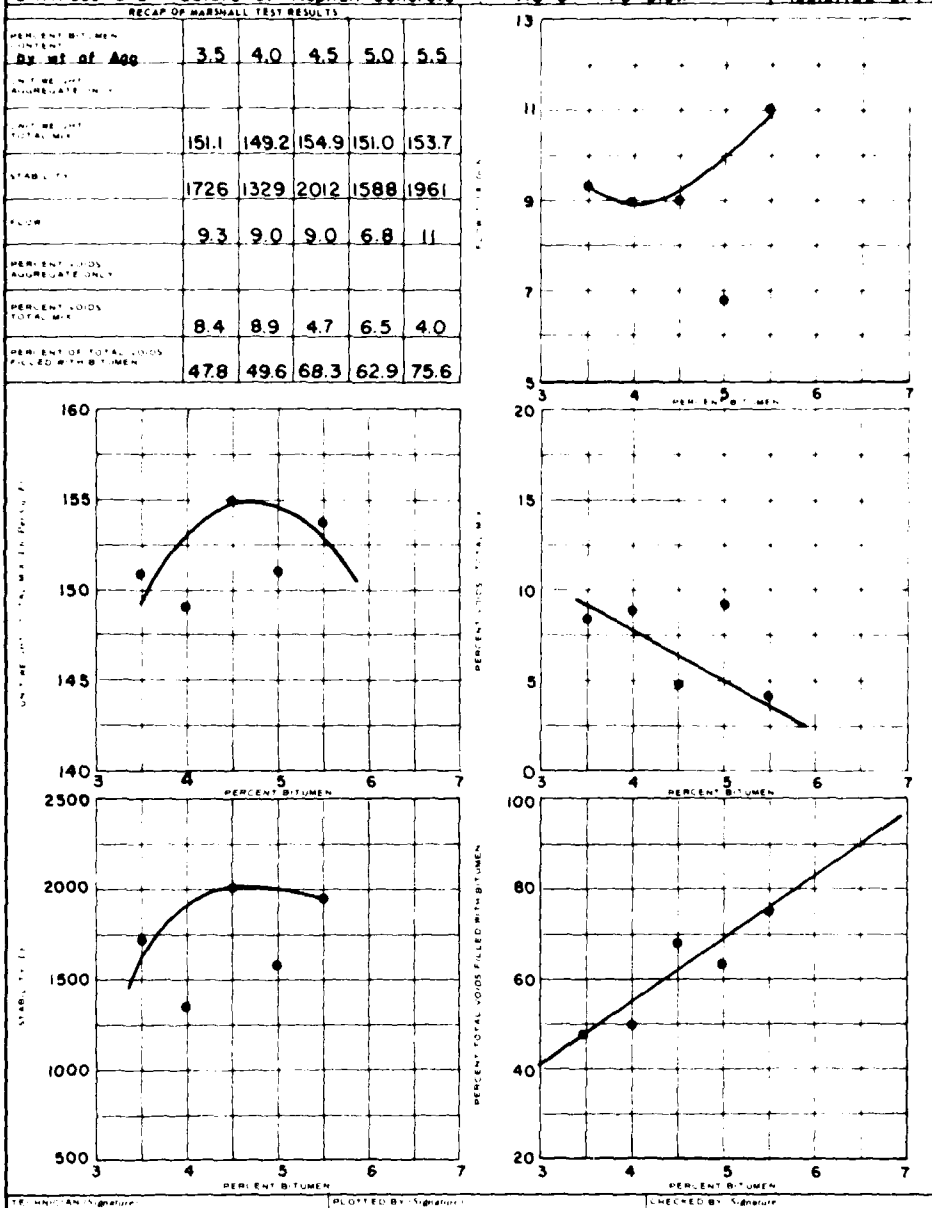

TECHNICIAN Signature PLOTTED BY Signature CHECKED BY Signature

DD FORM 1219 PREVIOUS EDITION OF THIS FORM IS OBSOLETE

BITUMINOUS MIX CURVES Pike Aggregate | June 1976

Stiffness and Fracture of Asphalt Concrete | AC-20 50-blow | Replotted 9/77

RECAP OF MARSHALL TEST RESULTS

by wt of agg.	3.5	4.0	4.5	5.0	6.0
	150.3	146.7	151.7	153.1	154.0
	1530	1507	2258	1921	1846
	7	10	11	10	18
	8.6	10.1	6.4	4.8	2.9
	48.0	46.6	61.6	70.4	82.7

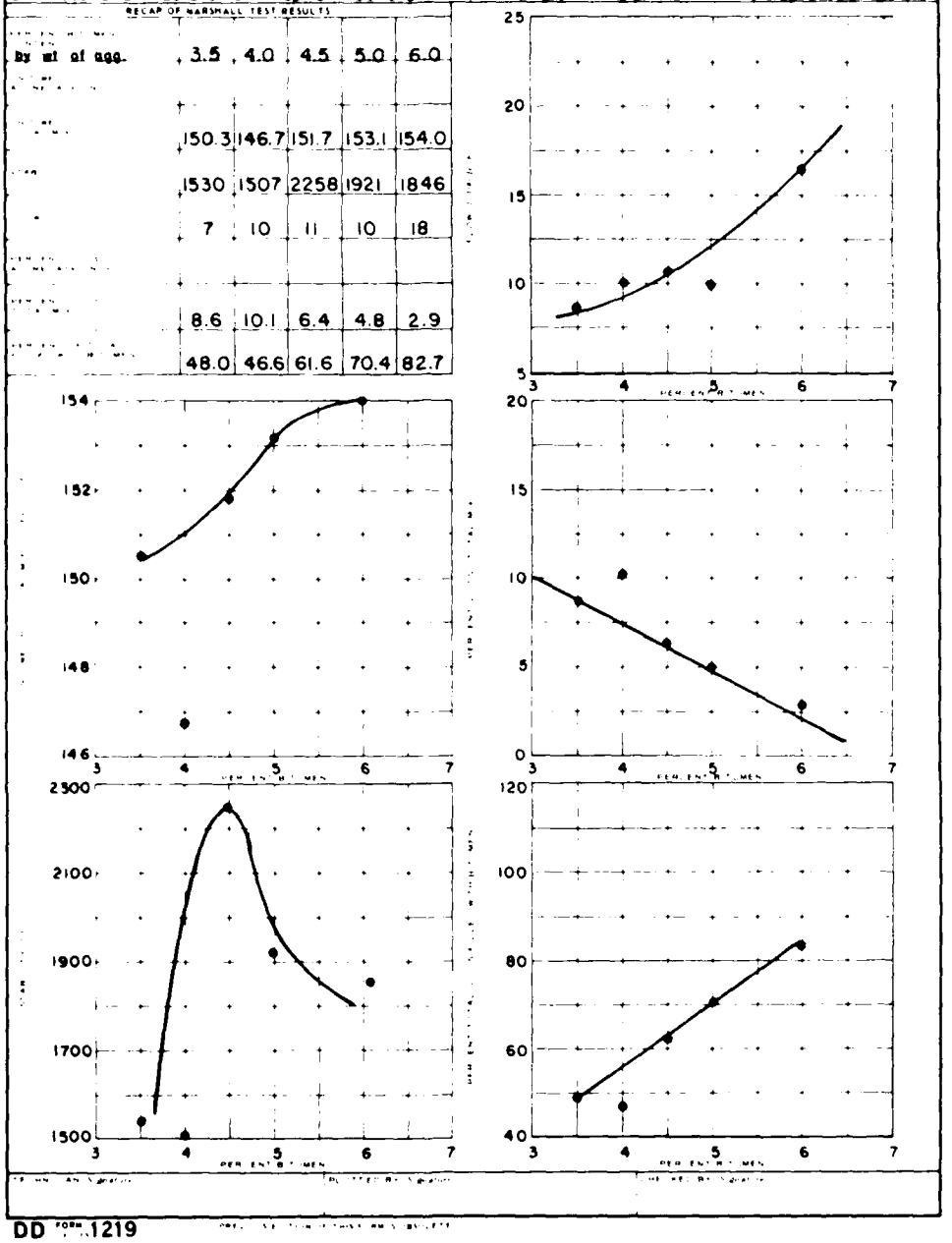

DD FORM 1219

BITUMINOUS MIX CURVES — Pike Aggregate — June 1976

Stiffness and Fracture of Asphalt Concrete — AC-20 — 75-blow — Replotted 9/77

RECAP OF MARSHALL TEST RESULTS

PERCENT BITUMEN by wt of agg	3.5	4.0	4.5	5.0	5.5
	150.1	154.4	154.3	154.1	153.5
	1286	3312	3223	2615	2082
	9	10	11.5	13.8	14
	8.8	5.4	4.8	4.2	3.9
	47.6	63.2	68.6	73.3	76.2

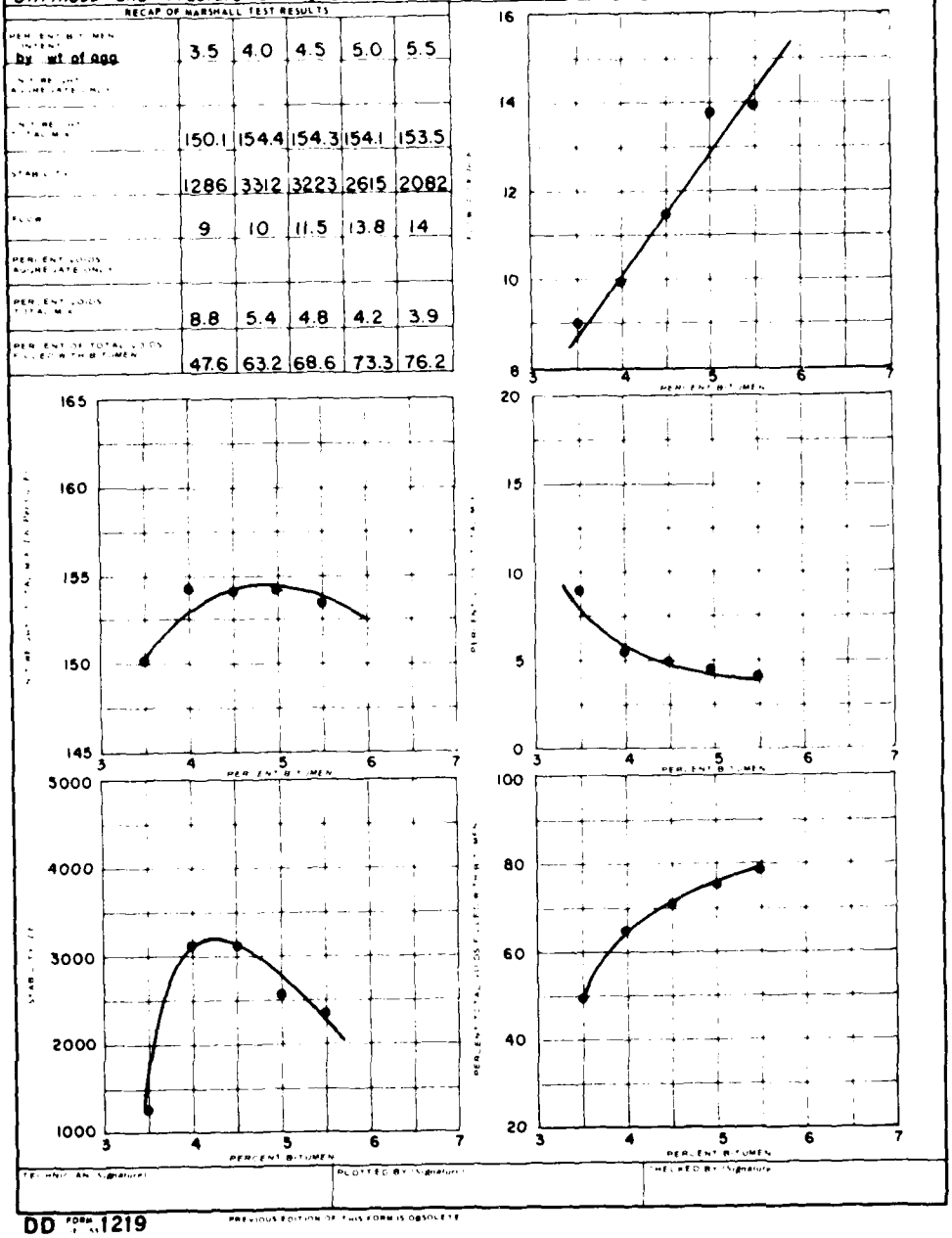

DD FORM 1219 PREVIOUS EDITION OF THIS FORM IS OBSOLETE

BITUMINOUS MIX CURVES — Tilton Aggregate — 15 Feb 1977

Stiffness and Fracture of Asphalt Concrete — AC-5 — 75-blow — Replotted 9/77

RECAP OF MARSHALL TEST RESULTS

By wt of agg	3.6	4.2	4.7	5.3	5.8
	149.1	150.6	150.9	150.6	152.7
	1743	2217	2145	2217	2175
	10	11	12.2	12.2	13
	8.0	6.3	5.6	4.9	2.9
	49.5	59.4	64.8	70.4	81.7

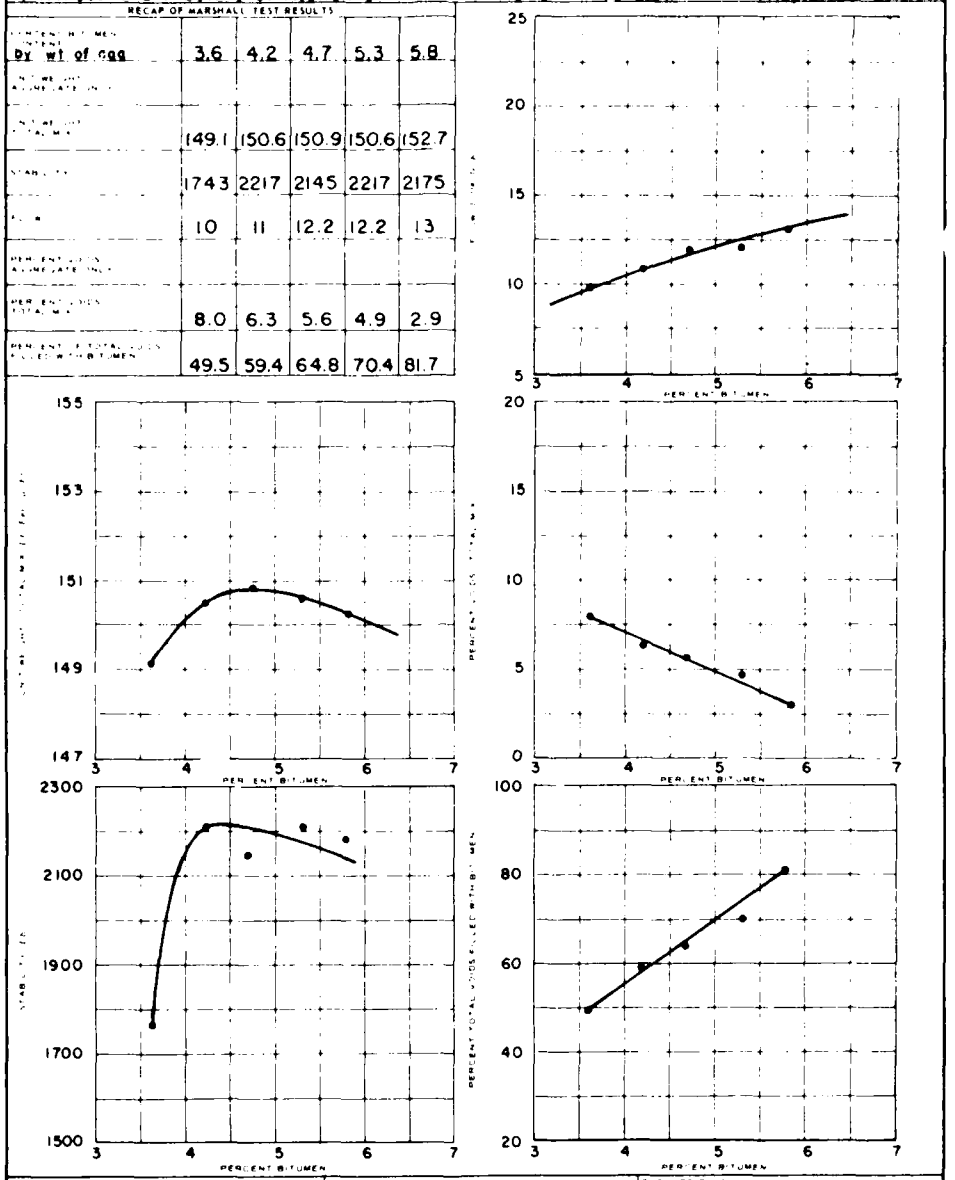

TECHNICIAN (Signature) | PLOTTED BY (Signature) | CHECKED BY (Signature)

DD FORM 1219 PREVIOUS EDITION OF THIS FORM IS OBSOLETE

BITUMINOUS MIX CURVES Tilton Aggregate

DATE 4 Feb 1977

PROJECT Stiffness and Fracture of Asphalt Concrete

JOB AC-20 75-blow

Replotted 9/77

RECAP OF MARSHALL TEST RESULTS

PERCENT BITUMEN CONTENT by wt of agg	3.5	4.0	4.5	5.0	5.5
UNIT WEIGHT AGGREGATE ONLY					
UNIT WEIGHT TOTAL MIX	1488	150.2	150.7	151.9	152.1
STABILITY	1895	2624	2402	2415	2217
FLOW	11	11	11.7	11.3	14
PERCENT VOIDS AGGREGATE ONLY					
PERCENT VOIDS TOTAL MIX	8.5	6.5	5.5	4.1	3.3
PERCENT OF TOTAL VOIDS FILLED WITH BITUMEN	46.4	58.2	64.8	73.6	79.3

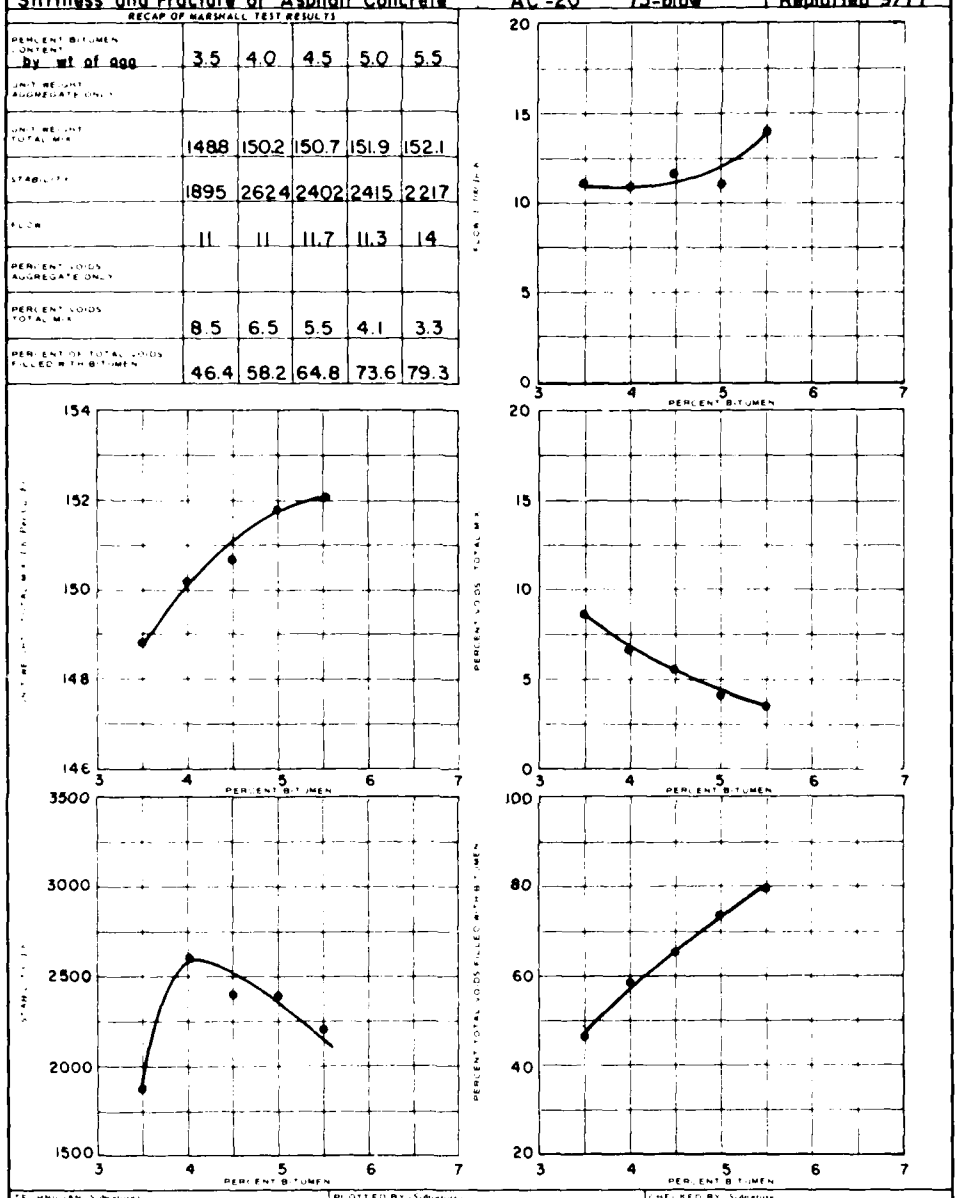

TECHNICIAN Signature | PLOTTED BY Signature | CHECKED BY Signature

DD FORM 1219 PREVIOUS EDITION OF THIS FORM IS OBSOLETE

APPENDIX B: EQUATIONS FOR CALCULATING SPECIMEN PROPERTIES FROM BRAZIL TESTS

Table B1. Equations for Calculating Tensile Properties[25] from Brazil Tests.

Static Properties		
(1)	Tensile strength S_T, psi	$= \frac{P_{Fail}}{h} \cdot A_0$
(2)	Poisson's ratio ν	$= \frac{DR \cdot A_1 + B_1}{DR \cdot A_2 + B_2}$
(3)	Modulus of elasticity E, psi	$= \frac{S_H}{h} (A_3 - \nu \cdot A_4)$
(4)	Tensile strain ϵ_T	$= X_T \left[\frac{A_5 - \nu \cdot A_6}{A_1 - \nu \cdot A_2}\right]$
(5)	Compressive strain ϵ_C	$= Y_T \left[\frac{B_3 - \nu \cdot B_4}{B_1 - \nu \cdot B_2}\right]$
Repeated-Load Properties		
(6)	Instantaneous resilient Poisson's ratio ν_{RI}	$= \frac{\frac{V_{RI}}{H_{RI}} A_1 + B_1}{\frac{V_{RI}}{H_{RI}} A_2 + B_2}$
(7)	Instantaneous resilient modulus of elasticity E_{RI}, psi	$= \frac{P}{H_{RI} h} (A_3 - \nu_{RI} \cdot A_4)$

P_{Fail} = total load at failure (maximum load P_{max} or load at first inflection point), pounds

P = applied load or repeated load, pounds

h = height of specimen, inches

DR = deformation ratio $\frac{Y_T}{X_T}$ (the slope of line of best fit* between vertical deformation Y_T and the corresponding horizontal deformation X_T up to failure load)

X_T = total horizontal deformation, inches

Y_T = total vertical deformation, inches

S_H = horizontal tangent modulus $\frac{P}{X_T}$ (the slope of the line of best fit* between load P and horizontal deformation X_T for loads up to failure load)

H_{RI}, V_{RI} = instantaneous resilient horizontal and vertical deformations, respectively

A_0, A_1, A_2, A_3, A_4, A_5, A_6, B_1, B_2, B_3, B_4 = constants (see Table B2).

*It is recommended that the line of best fit be determined by the method of least squares.

Table B2. Constants for Equations for Calculating Tensile Properties[10] from Brazil Tests.

Diameter, inches	A_0	A_1	A_2	A_3	A_4	A_5	A_6	B_1	B_2	B_3	B_4
3.5	.177	.0766	-.2847	.2680	-.9966	.05056	-.1545	-.9765	-.0204	-.1545	.05056
3.6	.172	.0745	-.2769	.2683	-.9968	.04786	-.1461	-.9590	-.0193	-.1461	.04786
3.7	.168	.0726	-.2694	.2685	-.9970	.04537	-.1384	-.9422	-.0183	-.1384	.04537
3.8	.164	.0707	-.2624	.2688	-.9971	.04307	-.1312	-.9260	-.0173	-.1312	.04307
3.9	.160	.0690	-.2557	.2690	-.9973	.04094	-.1246	-.9104	-.0165	-.1247	.04094
4.0	.156	.0673	-.2494	.2692	-.9974	.03896	-.1185	-.8954	-.0156	-.1185	.03896
4.1	.152	.0657	-.2433	.2694	-.9975	.03712	-.1129	-.8810	-.0149	-.1129	.03712
4.2	.149	.0642	-.2375	.2696	-.9976	.03541	-.1076	-.8671	-.0142	-.1076	.03541
4.3	.145	.0627	-.2320	.2698	-.9977	.03381	-.1027	-.8537	-.0136	-.1027	.03381
4.4	.142	.0613	-.2268	.2699	-.9978	.03232	-.0981	-.8407	-.0130	-.0981	.03232
4.5	.139	.0600	-.2218	.2701	-.9979	.03092	-.0938	-.8282	-.0124	-.0938	.03092
4.6	.136	.0587	-.2170	.2702	-.9980	.02961	-.0898	-.8161	-.0118	-.0898	.02961
4.7	.133	.0575	-.2124	.2703	-.9981	.02838	-.0860	-.8043	-.0114	-.0860	.02839
4.8	.131	.0563	-.2080	.2704	-.9982	.02723	-.0825	-.7930	-.0109	-.0825	.02723
4.9	.128	.0552	-.2037	.2706	-.9983	.02615	-.0792	-.7820	-.0105	-.0792	.02615
5.0	.126	.0541	-.1997	.2707	-.9983	.02512	-.0760	-.7714	-.0100	-.0761	.02513
5.1	.123	.0531	-.1958	.2708	-.9984	.02416	-.0731	-.7610	-.0097	-.0731	.02416
5.2	.121	.0521	-.1920	.2709	-.9985	.02325	-.0703	-.7510	-.0093	-.0703	.02325
5.3	.119	.0511	-.1884	.2709	-.9985	.02239	-.0677	-.7413	-.0090	-.0677	.02240
5.4	.116	.0502	-.1849	.2710	-.9986	.02158	-.0652	-.7319	-.0086	-.0652	.02158
5.5	.114	.0493	-.1816	.2711	-.9986	.02081	-.0629	-.7227	-.0083	-.0629	.02081
5.6	.112	.0484	-.1783	.2712	-.9987	.02008	-.0607	-.7138	-.0080	-.0607	.02008
5.7	.110	.0476	-.1752	.2713	-.9987	.01939	-.0586	-.7051	-.0078	-.0586	.01939
5.8	.109	.0468	-.1722	.2713	-.9988	.01874	-.0566	-.6967	-.0075	-.0566	.01874
5.9	.107	.0460	-.1693	.2714	-.9988	.01811	-.0547	-.6884	-.0072	-.0547	.01811
6.0	.105	.0452	-.1665	.2714	-.9988	.01752	-.0529	-.6804	-.0070	-.0529	.01752
6.1	.103	.0445	-.1638	.2715	-.9989	.01695	-.0512	-.6727	-.0068	-.0512	.01696
6.2	.102	.0438	-.1611	.2716	-.9989	.01642	-.0495	-.6651	-.0066	-.0495	.01642
6.3	.100	.0431	-.1586	.2716	-.9989	.01590	-.0480	-.6577	-.0064	-.0480	.01591
6.4	.099	.0424	-.1561	.2717	-.9990	.01542	-.0465	-.6504	-.0062	-.0465	.01542
6.5	.097	.0418	-.1537	.2717	-.9990	.01495	-.0451	-.6434	-.0060	-.0451	.01495

Strip width a = 0.5 in.

APPENDIX C: CALCULATED DISPLACEMENTS, STRAINS AND STRESSES

Note: Negative sign used with stresses and strains signifies compression.

Table C1. Vertical displacement, mm (in.) at various pavement depths beneath centerline of road.

Surface temperature, °C (°F)	*Compaction (blows)*	*Depth mm (in)*	*Pike aggregate* AC 2.5	AC 5	AC 20	*Tilton aggregate* AC 2.5	AC 5	AC 20
-6.7	50	2.5 (0.1)	1.30 (0.051)	1.24 (0.049)	1.19 (0.047)	–	–	–
(20)		127 (5)	1.30 (0.051)	1.24 (0.049)	1.19 (0.047)	–	–	–
		279 (11)	1.19 (0.047)	1.14 (0.045)	1.12 (0.044)	–	–	–
		432 (17)	1.09 (0.043)	1.04 (0.041)	1.02 (0.040)	–	–	–
		737 (29)	0.91 (0.036)	0.89 (0.035)	0.86 (0.034)	–	–	–
	75	2.5 (0.1)	1.22 (0.048)	1.09 (0.047)	1.19 (0.047)	1.14 (0.045)	1.12 (0.044)	1.12 (0.044)
		127 (5)	1.22 (0.048)	1.17 (0.046)	1.17 (0.046)	1.14 (0.045)	1.12 (0.044)	1.12 (0.044)
		279 (11)	1.12 (0.044)	1.09 (0.043)	1.09 (0.043)	1.07 (0.042)	1.04 (0.041)	1.04 (0.041)
		432 (17)	1.04 (0.041)	1.02 (0.040)	1.02 (0.040)	0.84 (0.039)	0.97 (0.038)	0.97 (0.038)
		737 (29)	0.86 (0.034)	0.86 (0.034)	0.86 (0.034)	0.84 (0.033)	0.84 (0.033)	0.84 (0.033)
7.2	50	2.5 (0.1)	1.68 (0.066)	1.60 (0.063)	1.45 (0.057)	–	–	–
(45)		127 (5)	1.65 (0.065)	1.60 (0.063)	1.42 (0.056)	–	–	–
		279 (11)	1.45 (0.057)	1.42 (0.056)	1.30 (0.051)	–	–	–
		432 (17)	1.30 (0.051)	1.27 (0.050)	1.17 (0.046)	–	–	–
		737 (29)	1.02 (0.040)	1.02 (0.040)	0.97 (0.038)	–	–	–
	75	2.5 (0.1)	1.60 (0.063)	1.45 (0.064)	1.45 (0.057)	1.32 (0.052)	1.37 (0.054)	1.32 (0.052)
		127 (5)	1.57 (0.062)	1.60 (0.063)	1.45 (0.057)	1.32 (0.052)	1.37 (0.054)	1.32 (0.052)
		279 (11)	1.42 (0.056)	1.42 (0.056)	1.32 (0.052)	1.19 (0.047)	1.24 (0.049)	1.22 (0.048)
		432 (17)	1.24 (0.049)	1.27 (0.050)	1.17 (0.046)	1.09 (0.043)	1.14 (0.045)	1.12 (0.044)
		737 (29)	1.02 (0.040)	1.02 (0.040)	0.97 (0.038)	0.91 (0.036)	0.94 (0.037)	0.91 (0.036)
21.1	50	2.5 (0.1)	2.95 (0.116)	2.84 (0.112)	1.88 (0.074)	–	–	–
(70)		127 (5)	2.62 (0.103)	2.84 (0.102)	1.85 (0.073)	–	–	–
		279 (11)	2.11 (0.083)	2.08 (0.082)	1.60 (0.063)	–	–	–
		432 (17)	1.73 (0.068)	1.70 (0.067)	1.40 (0.055)	–	–	–
		737 (29)	1.27 (0.050)	1.24 (0.049)	1.07 (0.042)	–	–	–
	75	2.5 (0.1)	2.92 (0.115)	2.62 (0.103)	2.13 (0.084)	2.18 (0.086)	2.03 (0.080)	1.78 (0.070)
		127 (5)	2.62 (0.103)	2.44 (0.096)	2.08 (0.082)	2.11 (0.083)	1.98 (0.078)	1.75 (0.069)
		279 (11)	2.08 (0.082)	1.98 (0.078)	1.75 (0.069)	1.78 (0.070)	1.68 (0.066)	1.52 (0.060)
		432 (17)	1.73 (0.068)	1.65 (0.065)	1.47 (0.058)	1.50 (0.059)	1.45 (0.057)	1.35 (0.053)
		737 (29)	1.27 (0.050)	1.22 (0.048)	1.12 (0.044)	1.14 (0.045)	1.12 (0.044)	1.07 (0.042)

Table C2. Radial strains at various pavement depths beneath centerline of load.

Surface temperature, °C (°F)	Compaction (blows)	Depth mm (in)	Pike aggregate AC 2.5	Pike aggregate AC 5	Pike aggregate AC 20	Tilton aggregate AC 2.5	Tilton aggregate AC 5	Tilton aggregate AC 20
-6.7 (20)	50	2.5 (0.1)	-2.46E-04	-2.18E-04	-1.96E-04			
		127 (5)	2.62E-04	2.33E-04	2.10E-04			
		279 (11)	3.09E-04	2.80E-04	2.57E-04			
		432 (17)	3.02E-04	2.77E-04	2.56E-04			
		737 (29)	2.51E-04	2.35E-04	2.21E-04			
	75	2.5 (0.1)	-2.02E-04	-1.89E-04	-1.89E-04	-1.55E-04	-1.55E-04	-1.59E-04
		127 (5)	2.17E-04	2.03E-04	2.03E-04	1.86E-04	1.67E-04	1.71E-04
		279 (11)	2.64E-04	2.50E-04	2.50E-04	2.32E-04	2.12E-04	2.16E-04
		432 (17)	2.63E-04	2.50E-04	2.50E-04	2.34E-04	2.16E-04	2.20E-04
		737 (29)	2.25E-04	2.16E-04	2.16E-04	2.05E-04	1.92E-04	1.95E-04
7.2 (45)	50	2.5 (0.1)	-5.23E-04	-4.71E-04	-3.37E-04			
		127 (5)	5.42E-04	4.90E-04	3.57E-04			
		279 (11)	5.52E-04	5.11E-04	3.97E-04			
		432 (17)	4.49E-04	4.59E-04	3.73E-04			
		737 (29)	3.61E-04	3.45E-04	2.96E-04			
	75	2.5 (0.1)	-4.61E-04	-4.85E-04	-3.49E-04	-2.57E-04	-2.99E-04	-2.69E-04
		127 (5)	4.81E-04	5.04E-04	3.68E-04	2.74E-04	3.18E-04	2.87E-04
		279 (11)	5.03E-04	5.22E-04	4.07E-04	3.21E-04	3.62E-04	3.33E-04
		432 (17)	4.54E-04	4.68E-04	3.81E-04	3.11E-04	3.45E-04	3.21E-04
		737 (29)	3.42E-04	3.50E-04	3.01E-04	2.57E-04	2.79E-04	2.64E-04
21.1 (70)	50	2.5 (0.1)	-2.16E-03	-2.06E-03	-7.51E-04			
		121 (5)	1.45E-03	1.44E-03	7.50E-04			
		279 (11)	1.31E-03	1.28E-03	7.10E-04			
		432 (17)	9.61E-04	9.43E-04	5.96E-04			
		737 (29)	5.73E-04	5.65E-04	4.13E-04			
	75	2.5 (0.1)	-2.14E-03	-1.74E-03	-1.06E-03	-1.14E-03	-9.29E-04	-6.37E-04
		127 (5)	1.45E-03	1.37E-03	1.00E-03	1.06E-03	9.00E-04	6.47E-04
		279 (11)	1.30E-03	1.18E-03	8.92E-04	9.27E-04	8.18E-04	6.34E-04
		432 (17)	9.57E-04	8.81E-04	7.10E-04	7.32E-04	6.65E-04	5.45E-04
		737 (29)	5.72E-04	5.35E-04	4.62E-04	4.71E-04	4.43E-04	3.89E-04

Table C3. Radial stresses, kPa (psi), at various pavement depths beneath centerline of load.

Surface temperature, °C (°F)	Compaction (blows)	Depth mm (in)	Pike aggregate AC 2.5	Pike aggregate AC 5	Pike aggregate AC 20	Tilton aggregate AC 2.5	Tilton aggregate AC 5	Tilton aggregate AC 20
-6.7 (20)	50	2.5 (0.1)	-6529 (-9.47E02)	-6771 (-9.82E02)	-6964 (-1.01E03)		–	
		127 (5)	6178 (8.96E02)	6460 (9.37E02)	6702 (9.72E02)			
		279 (11)	41.8 (6.07E00)	37.6 (5.45E00)	34.2 (4.96E00)			
		432 (17)	22.4 (3.25E00)	20.4 (2.95E00)	18.6 (2.70E00)			
		737 (29)	11.8 (1.72E00)	10.8 (1.57E00)	10.0 (1.45E00)		–	
	75	2.5 (0.1)	-6895 (-1.00E03)	-7033 (-1.02E03)	-7033 (-1.02E03)	-7170 (-1.04E03)	-7377 (-1.07E03)	-7308 (-1.06E03)
		127 (5)	6626 (9.61E02)	6771 (9.82E02)	6771 (9.82E02)	6964 (1.01E03)	7171 (1.04E03)	7171 (1.04E03)
		279 (11)	35.2 (5.11E00)	33.2 (4.81E00)	33.2 (4.81E00)	30.5 (4.43E00)	27.6 (4.00E00)	28.3 (4.10E00)
		432 (17)	19.2 (2.78E00)	18.1 (2.63E00)	18.1 (2.63E00)	16.8 (2.43E00)	15.2 (2.21E00)	15.6 (2.26E00)
		737 (29)	10.3 (1.49E00)	9.7 (1.41E00)	9.7 (1.41E00)	9.0 (1.31E00)	8.2 (1.19E00)	8.4 (1.22E00)
7.2 (45)	50	2.5 (0.1)	-4930 (-7.15E02)	-5157 (-7.48E02)	-5874 (-8.52E02)		–	–
		127 (5)	4275 (6.20E02)	4557 (6.61E02)	5412 (7.85E02)		–	–
		279 (11)	77.2 (1.12E01)	71.7 (1.04E01)	54.7 (7.94E00)		–	–
		432 (17)	38.3 (5.56E00)	35.8 (5.20E00)	28.5 (4.13E00)		–	–
		737 (29)	18.5 (2.69E00)	17.6 (2.55E00)	14.6 (2.12E00)		–	–
	75	2.5 (0.1)	-5205 (-7.55E02)	-5095 (-7.39E02)	-5805 (-8.42E02)	-6440 (-9.34E02)	-6129 (-8.89E02)	-6343 (-9.20E02)
		127 (5)	4613 (6.69E02)	4475 (6.49E02)	5330 (7.73E02)	6074 (8.81E02)	5709 (8.28E02)	5957 (8.64E02)
		279 (11)	70.3 (1.02E01)	73.1 (1.06E01)	56.3 (8.16E00)	43.5 (6.31E00)	49.5 (7.18E00)	45.3 (6.57E00)
		432 (17)	35.4 (5.13E00)	36.5 (5.30E00)	29.2 (4.23E00)	23.2 (3.37E00)	26.1 (3.78E00)	24.1 (3.50E00)
		737 (29)	17.4 (2.52E00)	17.8 (2.59E00)	14.9 (2.16E00)	12.1 (1.77E00)	13.5 (1.96E00)	12.6 (1.83E00)
21.1 (70)	50	2.5 (0.1)	-1951 (-2.83E02)	-2041 (-2.96E02)	-4206 (-6.10E02)		–	–
		127 (5)	407 (5.90E01)	513 (7.44E01)	3303 (4.79E02)		–	–
		279 (11)	173 (2.51E01)	171 (2.48E01)	101 (1.46E01)		–	
		432 (17)	73.8 (1.07E01)	72.4 (1.05E01)	47.4 (6.87E00)			–
		737 (29)	29.9 (4.34E00)	29.6 (4.29E00)	21.6 (3.14E00)		–	–
	75	2.5 (0.1)	-1965 (-2.85E02)	-2386 (-3.46E02)	-3420 (-4.96E02)	-3282 (-4.76E02)	-3730 (-5.41E02)	-4571 (-6.63E02)
		127 (5)	430 (6.23E01)	938 (1.36E02)	2317 (3.36E02)	2137 (3.10E02)	2703 (3.92E02)	3758 (5.45E02)
		279 (11)	172 (2.50E01)	161 (2.34E01)	125 (1.82E01)	131 (1.90E01)	116 (1.68E01)	89.6 (1.30E01)
		432 (17)	73.1 (1.06E01)	68.9 (1.00E01)	56.6 (8.21E00)	58.3 (8.45E00)	53.0 (7.68E00)	43.1 (6.25E00)
		737 (29)	29.9 (4.33E00)	28.3 (4.10E00)	24.5 (3.56E00)	25.0 (3.63E00)	23.4 (3.40E00)	20.2 (2.93E00)

Table C4. Vertical subgrade strain beneath centerline of load.

Surface Temperature, °C (°F)	Compaction (blows)	Pike aggregate AC 2.5	Pike aggregate AC 5	Pike aggregate AC 20	Tilton aggregate AC 2.5	Tilton aggregate AC 5	Tilton aggregate AC 20
-6.7	50	-8.75E-04	-8.21E-04	-7.74E-04			
(20)	75	-7.88E-04	-7.60E-04	-7.60E-04	-7.22E-04	-6.78E-04	-6.88E-04
7.2	50	-12.35E-04	-11.82E-04	-10.23E-04			
(45)	75	-11.73E-04	-11.98E-04	-10.39E-04	-8.95E-04	-9.66E-04	-9.17E-04
21.1	50	-19.54E-04	-19.23E-04	-14.06E-04	–		
(70)	75	-19.48E-04	-18.21E-04	-15.72E-04	-16.01E-04	-15.07E-04	-13.26E-04

$$\epsilon_v = \frac{\sigma_v - 2_\mu \sigma_r}{E}$$

ϵ_v = vertical subgrade strain

σ_v = vertical subgrade stress

σ_r = radial subgrade stress

μ = Poisson's ratio

E = subgrade modulus

Table C5. Vertical stresses, kPa (psi), at various pavement depths beneath centerline of load.

Surface temperature, C (F)	Compaction (blows)	Depth mm (in)	Pike aggregate AC 2.5	Pike aggregate AC 5	Pike aggregate AC 20	Tilton aggregate AC 2.5	Tilton aggregate AC 5	Tilton aggregate AC 20
-6.7	50	2.5 (0.1)	-1593 (-2.31E02)	-1593 (-2.31E02)	-1593 (-2.31E02)			
(20)		127 (5)	-141 (-2.04E01)	-126 (-1.83E01)	-114 (-1.66E01)			
		279 (11)	-74.5 (-1.08E01)	-68.2 (-9.89E00)	-62.9 (-9.13E00)			
		432 (17)	-47.4 (-6.88E00)	-44.0 (-6.38E00)	-41.2 (-5.97E00)			
		737 (29)	-25.5 (-3.70E00)	-24.2 (-3.51E00)	-23.0 (-3.34E00)			
	75	2.5 (0.1)	-1593 (-2.31E02)	-1593 (-2.31E02)	-1593 (-2.31E02)	-1510 (-2.19E02)	-1517 (-2.20E02)	-1517 (-2.20E02)
		127 (5)	-118 (-1.71E01)	-111 (-1.61E01)	-111 (-1.61E01)	-102 (-1.48E01)	-93.1 (-1.35E01)	-95.1 (-1.38E01)
		279 (11)	-64.5 (-9.36E00)	-61.4 (-8.91E00)	-61.4 (-8.91E00)	-57.4 (-8.32E00)	-52.9 (-7.67E00)	-53.9 (-7.82E00)
		432 (17)	-42.0 (-6.09E00)	-40.3 (-5.84E00)	-40.3 (-5.84E00)	-38.1 (-5.52E00)	-35.5 (-5.15E00)	-36.1 (-5.23E00)
		737 (29)	-23.4 (-3.39E00)	-22.7 (-3.29E00)	-22.7 (-3.29E00)	-21.7 (-3.15E00)	-20.7 (-3.00E00)	-20.9 (-3.03E00)
7.2	50	2.5 (0.1)	-1593 (-2.31E02)	-1593 (-2.31E02)	-1593 (-2.31E02)			
(45)		127 (5)	-276 (-4.00E01)	-252 (-3.65E01)	-187 (-2.71E01)			
		279 (11)	-128 (-1.86E01)	-119 (-1.73E01)	-93.8 (-1.36E01)			
		432 (17)	-73.1 (-1.06E01)	-68.9 (-1.00E01)	-57.3 (-8.31E00)			
		737 (29)	-34.4 (-4.99E00)	-33.1 (-4.80E00)	-29.2 (-4.23E00)			
	75	2.5 (0.1)	-1593 (-2.31E02)	-1593 (-2.31E02)	-1593 (-2.31E02)	-1593 (-2.31E02)	-1593 (-2.31E02)	-1593 (-2.31E02)
		127 (5)	-247 (-3.58E01)	-259 (-3.75E01)	-192 (-2.79E01)	-146 (-2.12E01)	-168 (-2.43E01)	-152 (-2.21E01)
		279 (11)	-117 (-1.70E01)	-121 (-1.76E01)	-96.5 (-1.40E01)	-77.2 (-1.12E01)	-86.2 (-1.25E01)	-80.0 (-1.16E01)
		432 (17)	-68.4 (-9.92E00)	-70.3 (-1.02E01)	-58.4 (-8.47E00)	-48.7 (-7.06E00)	-53.4 (-7.74E00)	-50.1 (-7.27E00)
		737 (29)	-32.9 (-4.77E00)	-33.5 (-4.86E00)	-29.6 (-4.29E00)	-26.1 (-3.78E00)	-27.8 (-4.03E00)	-26.6 (-3.86E00)
21.1	50	2.5 (0.1)	-1799 (-2.61E02)	-1799 (-2.61E02)	-1724 (-2.50E02)			
(70)		127 (5)	-896 (-1.30E02)	-862 (-1.25E02)	-379 (-5.50E01)			
		279 (11)	-321 (-4.66E01)	-312 (-4.53E01)	-163 (-2.37E01)			
		432 (17)	-148 (-2.14E01)	-143 (-2.08E01)	-88.3 (-1.28E01)			
		737 (29)	-53.9 (-7.82E00)	-53.0 (-7.68E00)	-38.7 (-5.61E00)			
	75	2.5 (0.1)	-1799 (-2.61E02)	-1799 (-2.61E02)	-1724 (-2.50E02)	-1724 (-2.50E02)	-1724 (-2.50E02)	-1724 (-2.50E02)
		127 (5)	-889 (-1.29E02)	-765 (-1.11E02)	-513 (-7.44E01)	-541 (-7.85E01)	-456 (-6.61E01)	-328 (-4.76E01)
		279 (11)	-319 (-4.63E01)	-281 (-4.07E01)	-205 (-2.98E01)	-214 (-3.11E01)	-188 (-2.73E01)	-150 (-2.18E01)
		432 (17)	-146 (-2.12E01)	-132 (-1.92E01)	-105 (-1.52E01)	-108 (-1.56E01)	-97.9 (-1.42E01)	-81.3 (-1.18E01)
		737 (29)	-53.7 (-7.79E00)	-49.9 (-7.24E00)	-43.0 (-6.23E00)	-44.3 (-6.34E00)	-41.2 (-5.98E00)	-36.7 (-5.32E00)

A facsimile catalog card in Library of Congress MARC format is reproduced below.

Dempsey, B.J.
Asphalt concrete for cold regions, A comparative laboratory study and analysis of mixtures containing soft and hard grades of asphalt cement / by B.J. Dempsey, J. Ingersoll, T.C. Johnson and M.Y. Shahin. Hanover, N.H.: U.S. Cold Regions Research and Engineering Laboratory; Springfield, VA.: available from National Technical Information Service, 1980.
vi, 55 p., illus.; 27 cm. (CRREL Report 80-5)
Prepared for Directorate of Military Programs - Office, Chief of Engineers by Corps of Engineers, U.S. Army Cold Regions Research and Engineering Laboratory, under DA Project 4K078012AAM1.
Bibliography: p. 36.
1. Asphalt cement mixtures. 2. Asphalt concrete tests. 3. Catalytic cracking. 4. Pavements. 5. Traffic cracking and rutting. I. J. Ingersoll, co-author. II. T.C. Johnson, co-author. III. M.Y. Shahin, co-author. IV. United States. Army. Corps of Engineers. V. Army Cold Regions Research and Engineering Laboratory, Hanover, N.H. VI. Series: CRREL Report 80-5.

☆US GOVERNMENT PRINTING OFFICE: 1980 602-941/380